4 RESEARCH

CHAPTER 1

4.1 PHYSICO-CHEMICAL MODIFICATION OF KAFIRIN MICROPARTICLES FOR APPLICATION AS A BIOMATERIAL

4.1.1 Abstract

Vacuolated spherical kafirin microparticles, mean diameter 5 µm, can be formed by self-assembly from an acidic solution with water addition. Three-dimensional scaffolds for hard tissue repair require large microstructures (e.g. particle size 80–200 µm for injectable dental implants) with a high degree of interconnected porosity. Heat, transglutaminase and glutaraldehyde cross-linking treatments were investigated to modify the properties of kafirin microparticles to enhance their potential application. The microparticles treated with heat or glutaraldehyde during their formation were only slightly larger than the control, with the glutaraldehyde-formed microparticles being fairly uniform in size, whereas-the heat formed microparticles were less homogeneous. In terms of appearance, the heat- and glutaraldehyde-formed microparticles differed from the untreated control in that they had smooth surfaces and fewer internal vacuoles. Cross-linking the formed kafirin microparticles using wet heat or glutaraldehyde treatment resulted in larger microparticles (approx. 20 µm), which whilst similar in size and external morphology, were apparently formed by further assisted-assembly by two substantially different mechanisms. In addition, heat treatment increased vacuole size. In contrast, transglutaminase treatment had little effect on the size of individual microparticles but resulted in agglomeration of kafirin microparticles into large lumps. Heat treatment involved kafirin polymerization by disulphide bonding with the microparticles being formed from round, coalesced nanostructures, as shown by AFM. Kafirin polymerization of glutaraldehyde-treated microparticles was not by disulphide bonding and the nanostructures, as revealed by AFM, were spindle-shaped. Thus, kafirin microparticles, particularly modified with heat or glutaraldehyde, have potential as natural, non-animal protein scaffolds.

4.1.2 Introduction

Cereal prolamin proteins such as zein and kafirin can be self-assembled into nano- and micro-particles (Muthuselvi and Dhathathreyan, 2006; Taylor et al., 2009a). These particles have potential applications as delivery systems for drugs (Muthuselvi and Dhathathreyan, 2006), nutraceuticals (Patel, Hu, Tiwari and Velikov, 2010; Taylor et al., 2009b), antimicrobials (Xiao et al., 2011), essential oils (Parris et al., 2005), as biomaterials in tissue engineering as scaffolds (Gong et al., 2006), and as biomedical coatings for arterial/vascular prostheses (Wang et al., 2005). Zein and kafirin are natural, plant-based, non-allergenic, and slowly biodegradable therefore have some advantages over animal-based biomaterials such as silk and collagen, especially for biomedical applications. Collagen and silk have poor wet strength and bovine collagen has potential immunogenicity and has been reported to transmit diseases such as bovine spongiform encephalopathy (reviewed by Reddy and Yang, 2011).

Wang and Padua (2012) recently described a possible nanoscale mechanism for the self-assembly of zein into various mesostructures. This self-assembly appears to be driven by the amphiphilic nature of the zein protein and occurred when changes were made to the polarity of an aqueous ethanol solution of zein by evaporation. An earlier paper by the same workers indicated that, at larger scale, the zein self-assembly is by layering onto a central core (Wang and Padua, 2010). They suggested radial growth occurred by hydrophobic interactions as the solvent became more hydrophilic due to the evaporation of the ethanol.

Kafirin is very similar to zein in amino acid composition but is more hydrophobic, or more strictly speaking less hydrophilic (Belton et al., 2006) and so can be considered amphiphilic in nature. Kafirin microparticles can be made by a process that is almost opposite to that used by Wang and Padua et al. (2010, 2012). Instead of dissolving the protein in aqueous ethanol and increasing the polarity of the solution by evaporation of the ethanol, the kafirin is dissolved in a primary solvent, glacial acetic acid, water is then added resulting in the self-assembly of kafirin microparticles (Taylor et al., 2009a). In both cases, there is a change in solvent polarity, causing protein self-assembly as described by Wang and Padua (2010, 2012) for zein.

Comparison of the structure of zein and kafirin microparticles show that the kafirin microparticles are generally larger (1–10 µm, mean diameter of 5 µm) (Taylor et al., 2009a) than zein microparticles (ranges from 0.3–1.7 µm (Muthuselvi and Dhathathreyan, 2006)

when made by similar processes. Kafirin microparticles have a rough surface and internal vacuoles resulting in a large surface area, whereas, zein microparticles are generally smooth and solid (Parris et al., 2005). The vacuoles in the kafirin microparticles are thought to be the footprint of air bubbles incorporated in the very viscous protein solution, which become entrapped within the microparticles as they self-assemble (Taylor et al., 2009a).

Although there is considerable interest in nano-sized particles, some potential biomaterial applications, particularly for three dimensional scaffold type structures for hard tissue repair, require large particles with a high degree of interconnected porosity (Hou, De Bank and Shakesheff, 2004). For example, an injectable dental implant, requires a particle size 80–200 µm (Weiss, Layrolle, Clergeau, Enckel, Pilet, Amouriq, Daculsi and Giumelli, 2007). Cross-linking by physical (Zhang and Zhong, 2009), chemical (Kim, Kang, Krueger, Sen, Holcomb, Chen, Wenke and Yang, 2012) and enzymic (Zhang and Zhong, 2009) methods have been applied to water-soluble protein nano- and micro-particles, such as whey protein (Zhang and Zhong, 2009) and gelatin (Kim et al., 2012), to increase water resistance and reduce swelling. However, there has been little research on cross-linking of prolamin protein microparticles, probably because the proteins are relatively hydrophobic (Belton et al., 2006).

The main objectives of this research were to determine whether cross-linking could increase the size of kafirin microparticles to improve their potential utility as biomaterial scaffolds and to attempt to understand the underlying mechanism involved.

4.1.3 Materials and methods

4.1.3.1 *Materials*

A mixture of two similar white, tan-plant non-tannin sorghum cultivars PANNAR PEX 202 and 606, was used. Whole grain sorghum was milled using a laboratory hammer mill (Falling Number 3100, Huddinge, Sweden) fitted with a 500 µm opening screen. An analytical grade 25% glutaraldehyde solution (Saarchem, Krugersdorp, South Africa) was used. Microbial transglutaminase (Activa® WM), activity 100 U/g was kindly donated by Ajinamoto Co., Paris, France.

4.1.3.2 *Extraction of kafirin*

Kafirin was extracted from whole sorghum flour according to method of Emmambux and Taylor (2003). Briefly, milled sorghum was mixed with 70% (w/w) aqueous ethanol containing 5% sodium hydroxide (w/w) and 3.5% sodium metabisulphite (w/w) at 70^{o}C for 1 h with vigorous stirring. The clear supernatant was recovered by centrifugation and the ethanol evaporated. Kafirin was precipitated by adjusting the pH of the protein suspension to 5. The precipitated kafirin was recovered by filtration under vacuum, freeze-dried, defatted with hexane at ambient temperature and air-dried. The protein contents of defatted air-dried kafirin extracts was 84% (N × 6.25, dry matter basis) determined by Dumas nitrogen combustion method (AACC International, 2000) Method 46-30.

4.1.3.3 *Preparation of kafirin microparticles*

These were prepared essentially according to Taylor et al. (2009a), which is a simple coacervation in which microparticles are expelled from a solution of kafirin in glacial acetic acid. Some modification was made. After dissolution of the kafirin in glacial acetic acid and equilibration of the kafirin solution, distilled water was added at rate of 1.4 mL/min using a Watson-Marlow Bredel peristaltic pump (Falmouth, England) while mixing using a magnetic stirrer at 600 rpm to form kafirin microparticle suspension. The kafirin microparticle suspension contained 2% kafirin protein and 5.4% acetic acid and pH 2.0. For microparticles intended for analysis in dry form, the acetic acid was removed by washing three times with distilled water by centrifugation at 3150 *g*, then the pellets freeze-dried before storage at 10^{o}C.

4.1.3.4 *Treating kafirin microparticles*

Heat or glutaraldehyde treatment during microparticle formation

Hot distilled water (96^{o}C) or a solution of 6.85% (w/w) glutaraldehyde was added to the solution of kafirin in glacial acetic acid (24% w/w) using a peristaltic pump at the rate of 1.4 mL/h, while stirring, to give a final kafirin concentration of 2% (w/w) in 0.9 M acetic acid. The final temperature of the heat treatment was approximately 75^{o}C and the final glutaraldehyde concentration was 75% (w/w) (protein basis). Lower glutaraldehyde concentrations did not increase kafirin microparticle size (data not shown).

Wet heat treatment of kafirin microparticles

A kafirin microparticle suspension was prepared and washed free of acetic acid, as described above. The resultant pellet was re-suspended in 91% (w/w) water. Wet heat treatment was carried out by heating the kafirin microparticle suspensions at 50°C, 75°C and 96°C for 1 h. A control sample was maintained at 22°C.

Glutaraldehyde treatment of kafirin microparticles

Kafirin microparticle suspensions were prepared as described above. Glutaraldehyde was added to 4.0 g kafirin microparticle suspensions containing 2% protein (w/w) in 0.9 M acetic acid (pH 2.0), resulting in final glutaraldehyde concentrations of 0%, 10%, 20%, and 30% (w/w) on protein basis. Samples were then vortex-mixed and held at 22°C for 12 h.

Transglutaminase treatment of kafirin microparticles

Kafirin microparticle suspensions (4.0 g) were weighed in plastic centrifuge tubes. The acetic acid was washed off with distilled water as described. The supernatant was discarded while the wet kafirin microparticle pellet was retained. A working transglutaminase enzyme solution was prepared by mixing 25% Activa® WM, enzyme activity 100 U/g, in a 0.02 M Tris-HCl buffer (pH 7.0), preheated to 50°C. Transglutaminase enzyme (0.1%, 0.3% and 0.6% w/w on protein basis), was added to the wet kafirin microparticle pellets and the total mass made up to the original 4.0 g using the preheated 0.02 M Tris-HCl buffer. Pure maltodextrin (1%) solution in the buffer was used as a control. The target transglutaminase/protein (kafirin) ratio (mg/g) was 0 (control), 1, 3, and 6, which was based on work by Bruno, Giancone, Torrieri, Masi and Moresi (2008). Transglutaminase reaction was carried out at 30°C for 12 h after which the supernatants were removed and pellets washed with distilled water as described.

4.1.3.5 *SDS-PAGE*

Kafirin microparticles were characterised by SDS-PAGE under reducing and non-reducing conditions. An XCell SureLock™ Mini-Cell electrophoresis unit (Invitrogen Life Technologies, Carlsbad, CA) was used with 15-well 1 mm thick pre-prepared Invitrogen NuPAGE® 4-12% Bis-Tris gradient gels. The protein loading was ≈10 µg. Invitrogen

Mark12™ Unstained Standard was used. Proteins were stained with Coomassie® Brilliant Blue R250 overnight and then destained.

4.1.3.6 *Microscopy*

Light microscopy

Kafirin microparticle suspensions were viewed and photographed using a Nikon Optiphot light microscope (Kanagawa, Japan).

Electron microscopy

Suspensions of kafirin microparticles were prepared for SEM and TEM according Taylor et al. (2009a). Briefly, the liquid fraction of the microparticle suspension was removed and the microparticles fixed with glutaraldehyde before staining with osmium tetraoxide. Then the samples were dehydrated sequentially in different concentrations of acetone. SEM preparations were mounted on an aluminium stub using a double-sided carbon tape, sputter-coated with gold and viewed using a Jeol JSM-840 Scanning Electron Microscope (Tokyo, Japan). TEM preparations were infiltrated with Quetol resin and polymerized at 60^{o}C. Sections were cut using a microtome, stained in ural acetate and lead citrate and viewed with a Jeol JEM-2100F Field Emission Electron Microscope (Tokyo, Japan).

AFM

Freeze-dried kafirin microparticles were embedded on the surface of aluminium stubs. Then the microparticles were viewed with a Veeco Icon Dimension Atomic Force Microscope (Bruker, Cambridge, U.K.) using tapping-in-air mode. A silicon tip on nitride lever cantilever, tip size 8 nm was used. To determine the mechanical properties of the kafirin microparticles, the kafirin microparticles were embedded on a glass slide using custom-made glue. Then the mechanical properties of the microparticles were determined using Quantitative NanoMechanics (QNM) mode with the following parameter settings: Scan size 1 µm, Scan rate 0.500 Hz, Deflection sensitivity 80.2 nm/V, Deformation sensitivity 507 nm/V, and 256 scans per line. A silicon tip on nitride lever cantilever, tip size 9 nm with a spring constant 4.461 N/m was used. Force-deformation curves were generated and slopes calculated from the linear portions of these curves.

4.1.3.7 *Determination of size of the kafirin microparticles*

Microparticle size was determined by comparing their images with that of a scale bar of the same magnification. For each treatment, duplicate measurements were made each with at least 100 microparticles.

4.1.3.8 *In vitro protein digestibility (IVPD)*

An IVPD assay was performed on freeze-dried kafirin microparticles using a micro-scale pepsin digestion protocol described by Taylor and Taylor (2002), which is a modified procedure of Hamaker, Kirleis, Mertz and Axtell (1986). Accurately weighed samples (10 mg) were digested with a P7000-100G pepsin (Sigma, Johannesburg, South Africa), activity 863 units/mg protein for 2 h at 37^{o}C and the products of the digestion were pippeted off. The residue was washed with distilled water and dried at 100^{o}C overnight. The residual protein was determined by Dumas nitrogen combustion method (AACC International, 2000) method 46-30. IVPD was calculated by the difference between the total protein and the residual protein after pepsin digestion divided by the total protein and expressed as a percentage.

4.1.3.9 *FTIR spectroscopy*

FTIR spectroscopy was done as described by Taylor et al. (2009a). Freeze-dried microparticles were scanned using a Vertex 70v FT-IR spectrometer (Bruker Optik, Ettlingen, Germany), using 64 scans, 8 cm^{-1} band and an interval of 1 cm^{-1} in the Attenuated Total Reflectance (ATR) mode at wavenumber 600–4000 cm^{-1}. At least four replicates were performed for each treatment. The FTIR spectra were Fourier-deconvoluted with a resolution enhancement factor of 2 and 12 cm^{-1} bandwidth. The proportions of the α-helical conformations (≈1650 cm^{-1}) and the β-sheet structures (≈1620 cm^{-1}) were calculated by measuring the heights of the peaks assigned to these secondary structures on the FTIR spectra. The relative proportion of α-helical conformations was calculated thus:

$$\%\ \text{of α-helical conformation} = \frac{\text{Abs α-helix peak}}{\text{Abs α-helix peak} + \text{Abs β-sheet peak}} \times 100$$

Where:

Abs α-helix peak = Absorbance at ≈1650 cm^{-1} after baseline correction
Abs β-sheet peak = Absorbance at ≈1620 cm^{-1} after baseline correction

4.1.3.10 *Statistical analyses*

The IVPD and FTIR data as well as the data on mechanical properties of the kafirin microparticles were analysed by one-way analysis of variance (ANOVA). These measured parameters were the dependent variables while and heat, transglutaminase and glutaraldehyde treatments were the independent variables. All the experiments were repeated at least once. The mean differences assessed by Fischer's Least Significant Difference (LSD) test. The calculations were performed using Statistica software version 10 (StatSoft, Tulsa, OK).

4.1.4 Results and discussion

4.1.4.1 *Morphology and size distribution of treated kafirin microparticles*

Heat and glutaraldehyde treatments during microparticle preparation

Kafirin microparticles prepared at ambient temperature (22°C) were spherical, between 1 and 10 µm in diameter, with pores (vacuoles) between 0.5 and 2 µm (Figure 4.1), as reported previously (Taylor et al. 2009a). The majority of the microparticles were between 1 and 5 µm (Figure 4.2). The microparticles treated with heat or glutaraldehyde during their formation were only slightly larger than the control, with the glutaraldehyde-formed microparticles being fairly uniform in size, whereas the heat formed microparticles were less homogeneous. In terms of appearance, the heat- and glutaraldehyde-formed microparticles differed from the untreated control in that they had smooth surfaces and fewer internal vacuoles. Since the aim of the study was to substantially increase the size of the microparticles, the approach of cross-linking after the self-assembly process was investigated.

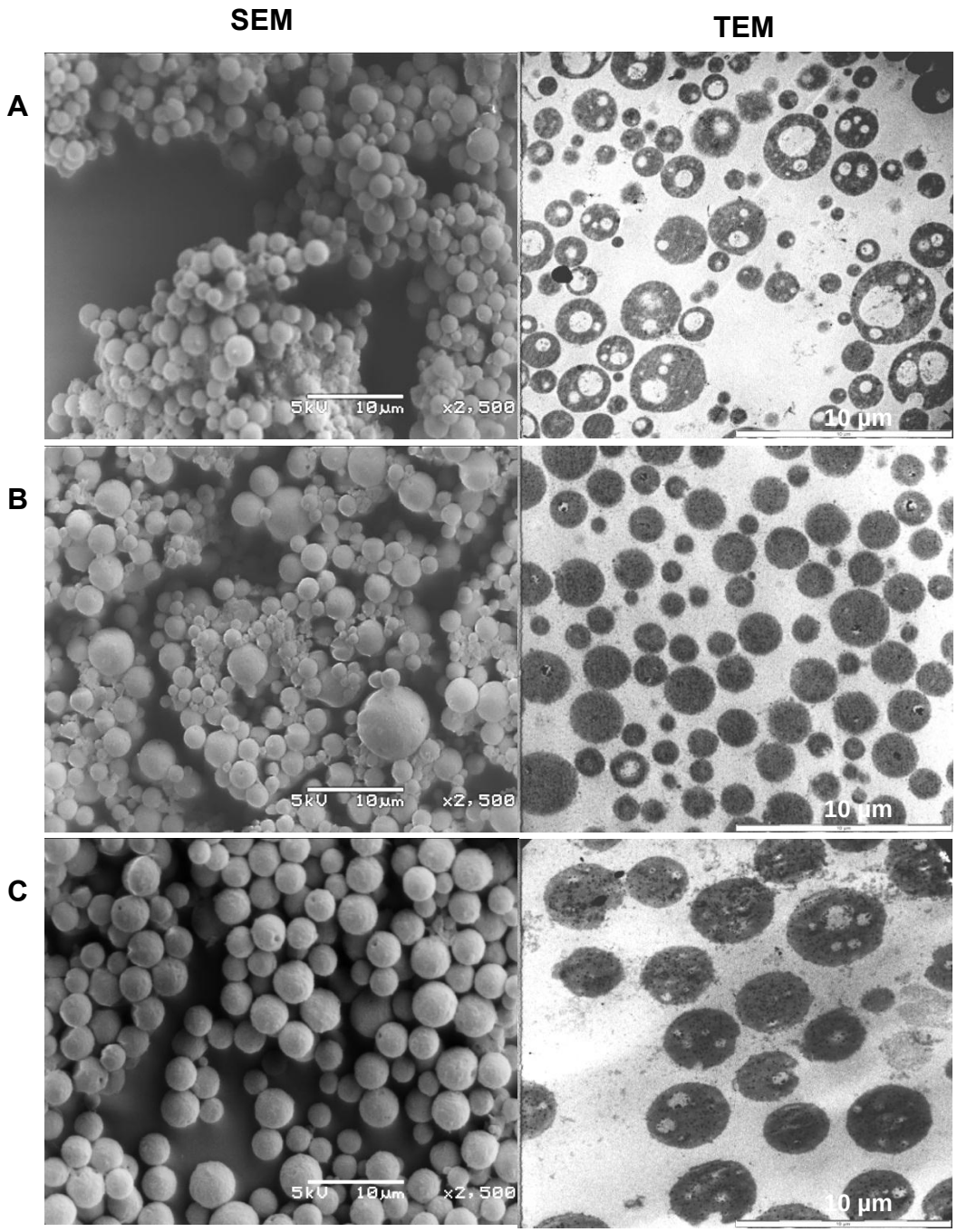

Figure 4.1 Electron microscopy of kafirin microparticles treated during preparation (formation). **A.** Control. **B.** Heat treatment. **C.** Glutaraldehyde treatment.

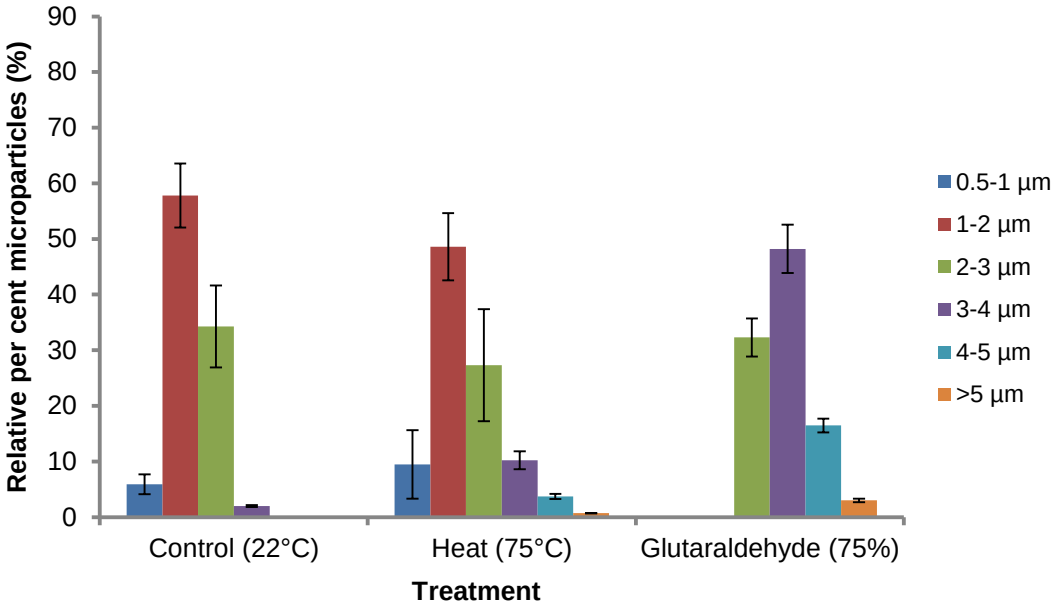

Figure 4.2 Particle size distribution of kafirin microparticles treated with heat and glutaraldehyde during microparticle formation. Error bars are standard deviations for two replicate measurements each of at least 100 particles.

Treatment following microparticle preparation

Wet heat treatment following the microparticle self-assembly changed the shape of the larger kafirin microparticles to oval and increased their average size to ≈20 µm thereby skewing the microparticle size distribution (Figure 4.3). Particle size increased with increasing severity of the heat treatment up to 75°C, after which there was no further increase in microparticle size with increased temperature. Vacuoles within the heat-treated kafirin microparticles showed a >10-fold increase in size compared to the control to a maximum of about 17 µm. The increase in vacuole size with heat treatment was probably due to greater expansion of air with higher temperature within the microparticles, since the vacuoles are probably footprints of air bubbles (Taylor et al., 2009a). The relative proportion of microparticles of size >20 µm increased by up to about 40% with increase in temperature up to 75^{o}C (Figure 4.4). Increasing the temperature to 96^{o}C did not increase further the microparticle size. The oval shape of the larger heat-treated microparticles was probably due to the rate of particle coalescence being inversely proportional to particle size, as proposed by Lehtinen and Zachariah (2001), who studied the effect of coalescence energy release on the temporal shape evolution of nanoparticles.

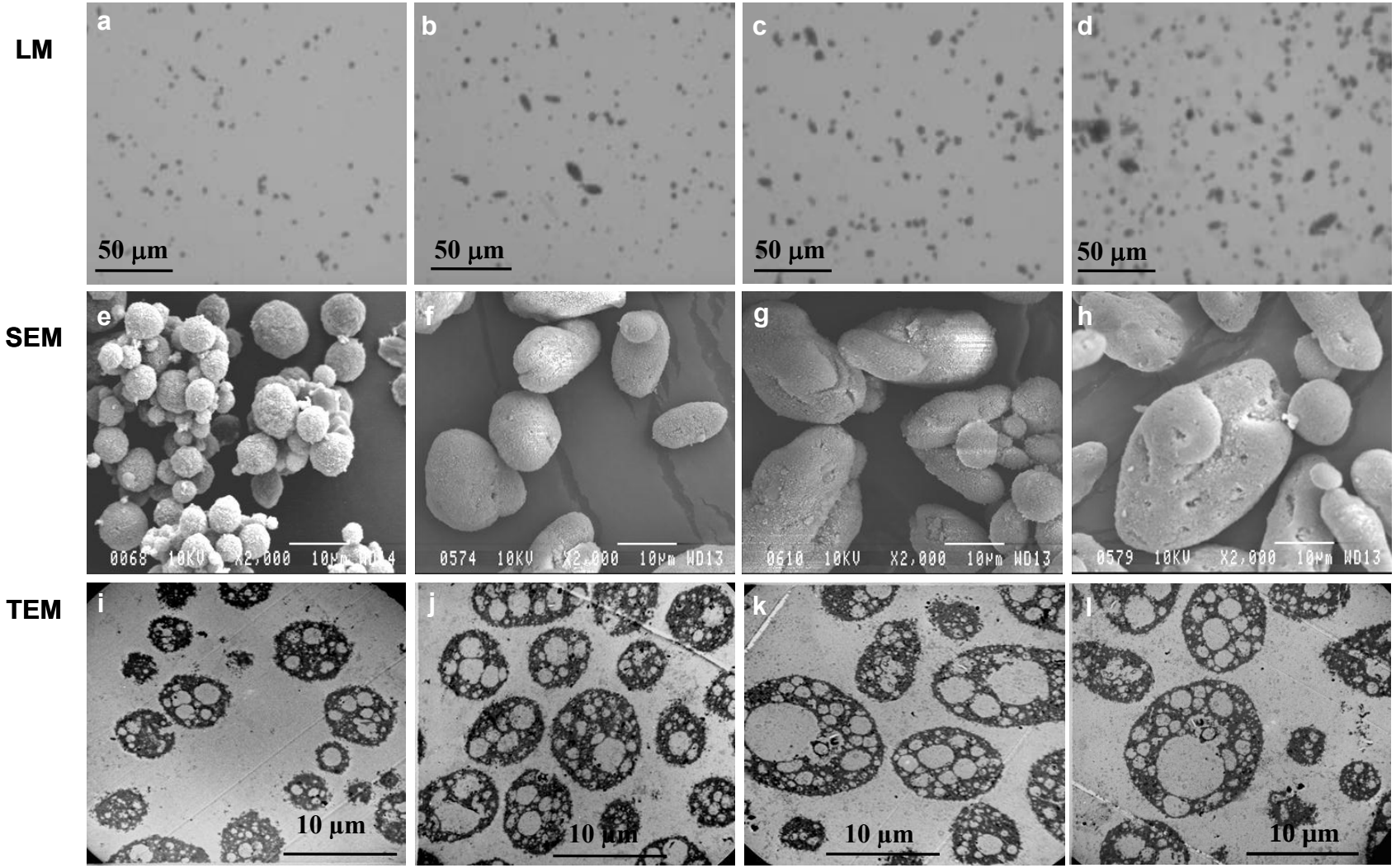

Figure 4.3 Microscopy of heat-treated kafirin microparticles. **a, e, i**- Control (22°C); **b, f, j** - 50°C; **c, g, k** - 75°C; **d, h, i**- 96°C. LM – Light microscopy; SEM – Scanning electron microscopy; TEM – Transmission electron microscopy.

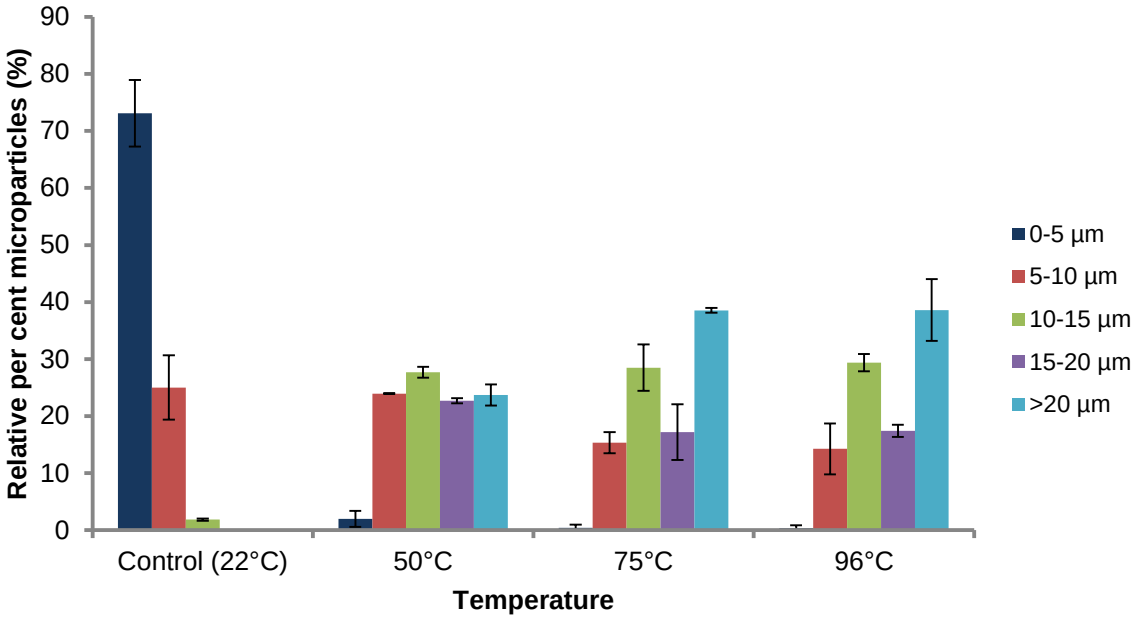

Figure 4.4 Particle size distribution of heat-treated kafirin microparticles. Error bars are standard deviations for two replicate measurements each of at least 150 particles.

Transglutaminase treatment resulted in formation of large masses (>200 µm across) of agglomerated kafirin microparticles (Figure 4.5). Evidence of kafirin microparticle agglomeration was also shown by increase in volume of kafirin microparticle sediments with transglutaminase treatment (Figure 4.6). Agglomerated particles would probably exhibit a loose packing characteristic as more interstitial spaces would not be filled, thereby resulting into particles occupying a large volume. However, individual transglutaminase-treated kafirin microparticles were round-shaped; most of them were of size 5–10 µm (Figure 4.7). Even with the higher level of transglutaminase treatment (0.6% transglutaminase), only a small proportion of microparticles (about 4%) was >20 µm in size. The fact that kafirin essentially contains no lysine (Belton et al., 2006) may have inhibited transglutaminase catalysed cross-linking through the ε-(-glutamyl)-lysine bonding mechanism (Motoki and Seguro, 1998), thereby causing the small increase in particle size. Unlike with heat treatment, the vacuole size did not change with transglutaminase treatment, probably because the reaction temperature was low (30°C), hence no air expansion. Much larger particle sizes have been reported with other proteins. For example Gan, Cheng and Easa (2008) working with SPI treated with transglutaminase at 1.0 U/g protein reported up to 280 µm microcapsule size, probably because SPI is rich in lysine.

Glutaraldehyde treatment following the self-assembly increased the microparticle size (Figure 4.8).

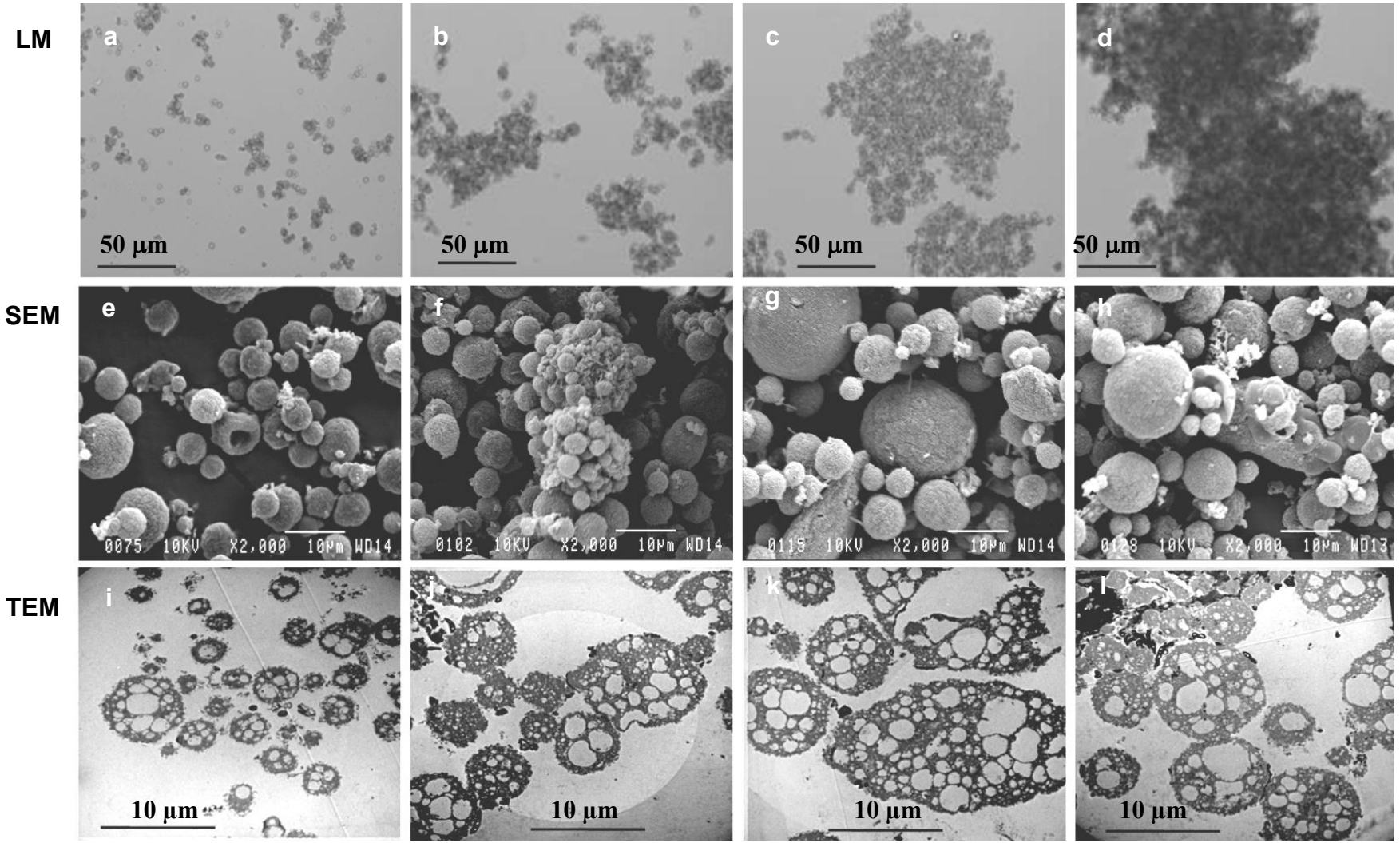

Figure 4.5 Microscopy of transglutaminase (TG)-treated kafirin microparticles. **a, e, i** - Maltodextrin (control); **b, f, j** - 0.1% TG + Maltodextrin; **c, g, k** - 0.3% TG + Maltodextrin; **d, h, i**- 0.6% TG + Maltodextrin. LM – Light microscopy; SEM – Scanning electron microscopy; TEM – Transmission electron microscopy.

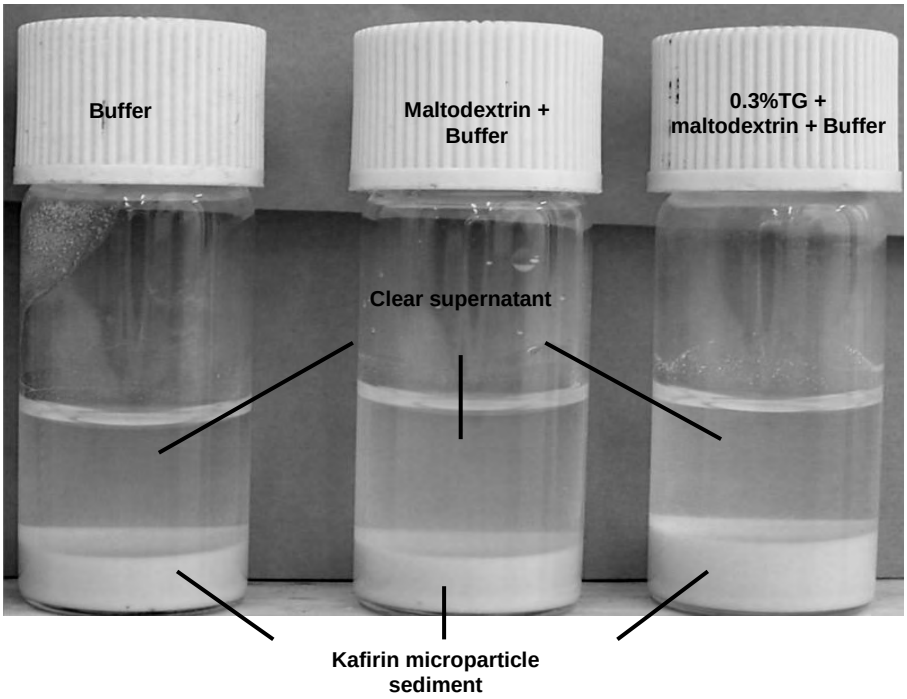

Figure 4.6 Photograph showing the volume of kafirin microparticle sediment after incubation in buffer, maltodextrin and transglutaminase (TG) for 12 h at 30°C. The same amount of microparticles was used in each treatment.

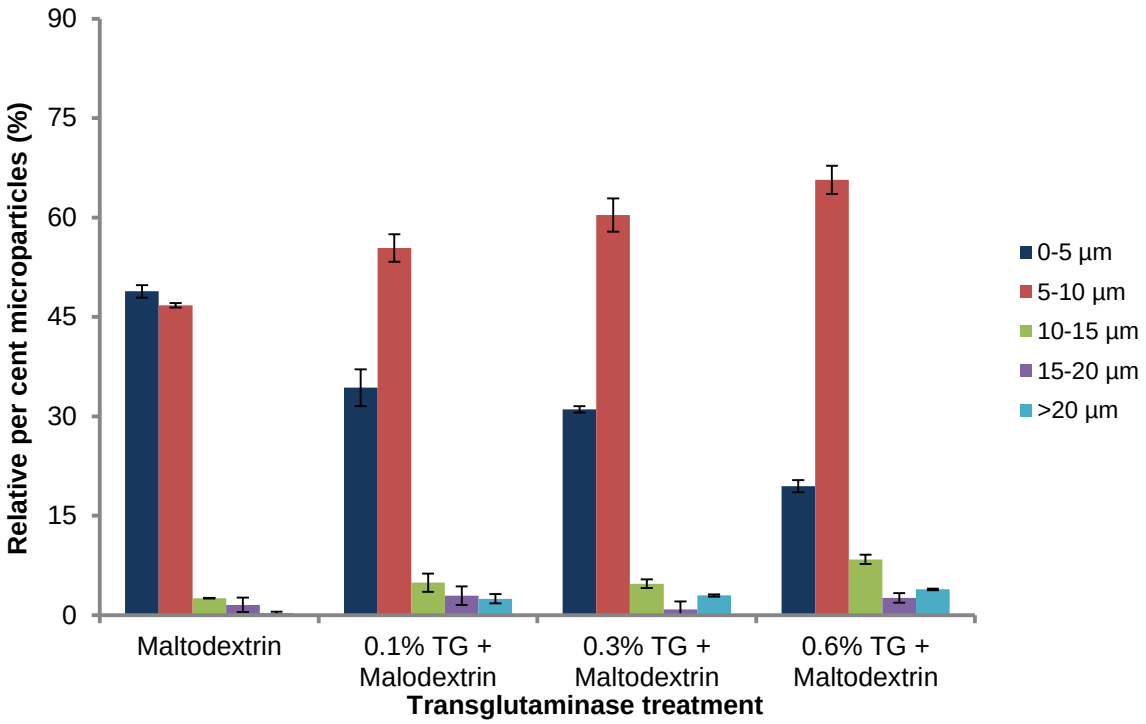

Figure 4.7 Particle size distribution of transglutaminase-treated kafirin microparticles. Error bars are standard deviations for two replicate measurements each of at least 100 particles.

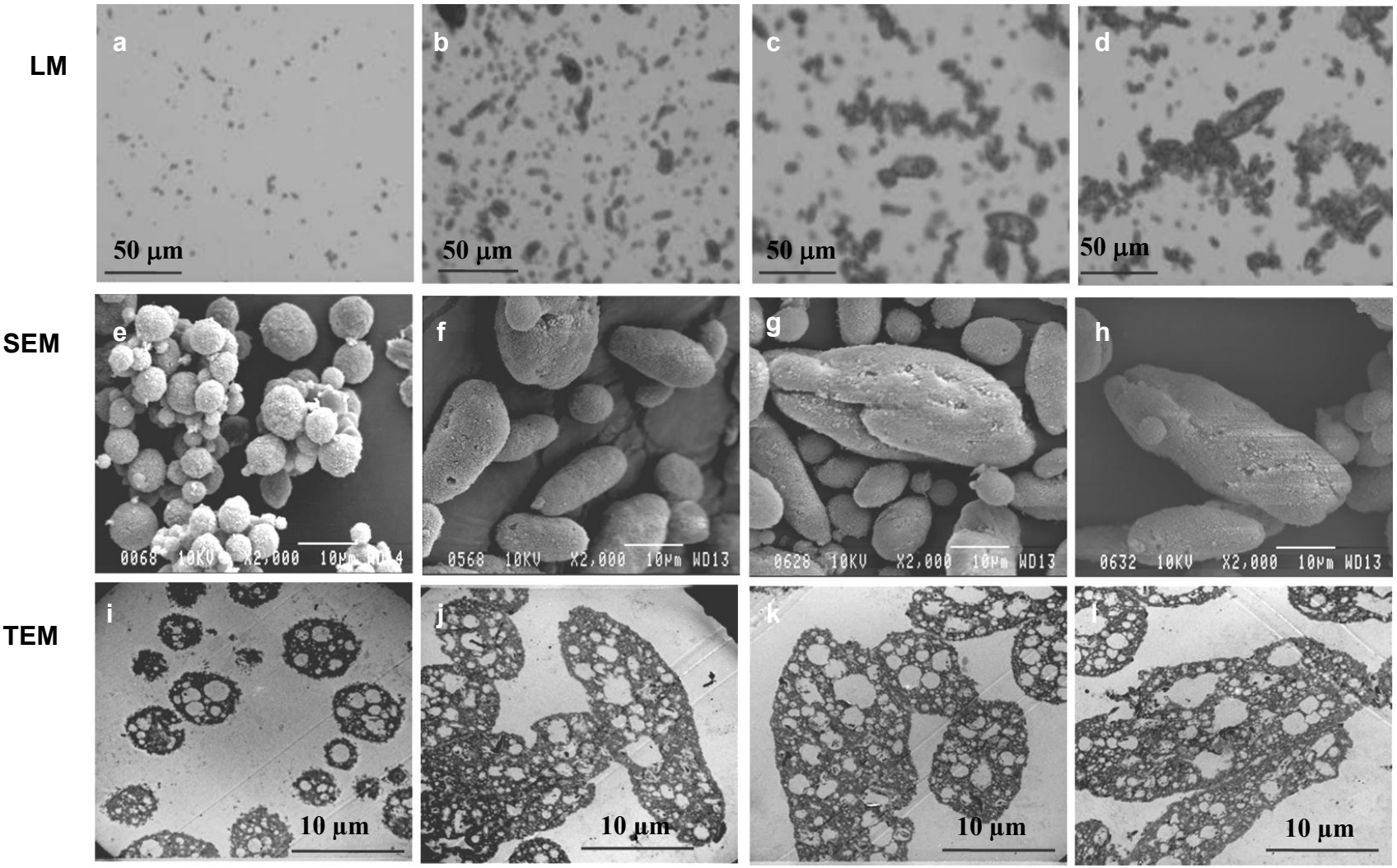

Figure 4.8 Microscopy of glutaraldehyde (GTA)-treated kafirin microparticles. . **a, e, i** - Control; **b, f, j** - 10% GTA; **c, g, k** - 20% GTA; **d, h, i** -30% GTA. LM – Light microscopy; SEM – Scanning electron microscopy; TEM – Transmission electron microscopy.

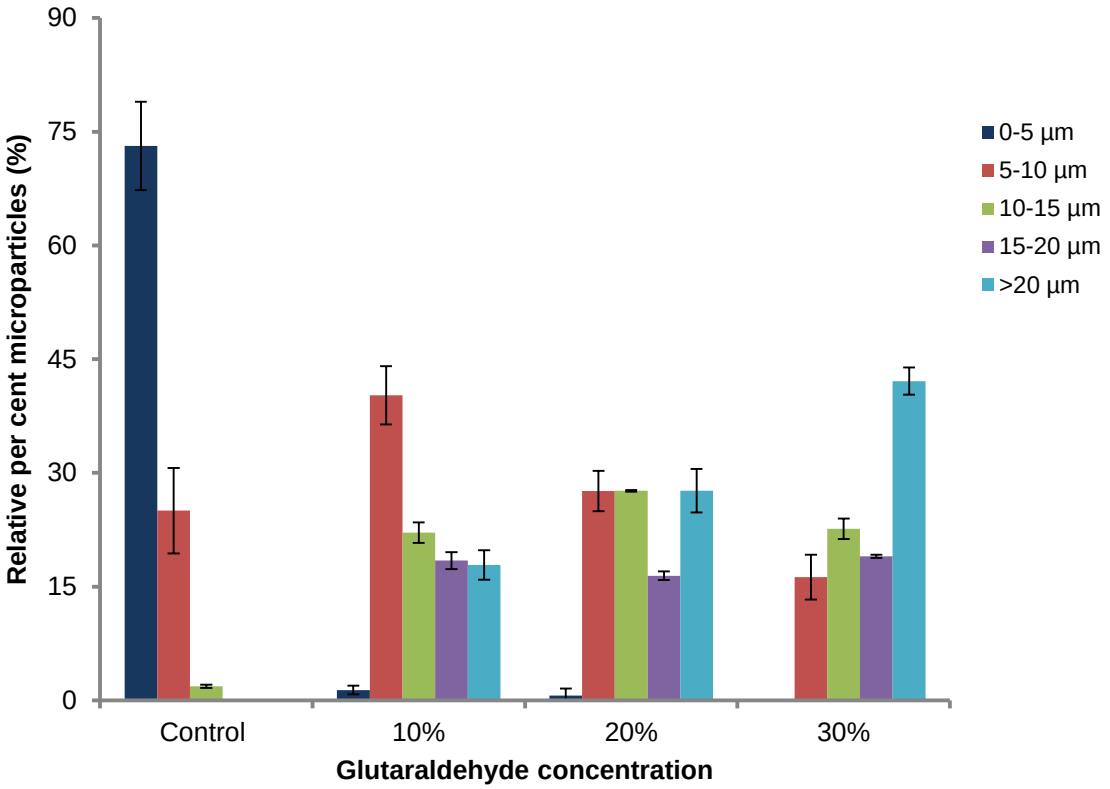

Figure 4.9 Particle size distribution of glutaraldehyde-treated kafirin microparticles. Error bars are standard deviations for two replicate measurements each of at least 100 particles.

As with increasing severity of wet heat treatment, the average microparticle size increased with severity of the glutaraldehyde treatment, from 1-5 µm of the control to >20 µm with 30% glutaraldehyde. Ezpeleta, Rache, Gueguen and Orecchioni (1997) reported a similar increase in particle size of vicilin microparticles with glutaraldehyde treatment. The relative proportion of microparticles of size >20 µm was also increased, up to about 45% with 30% glutaraldehyde (Figure 4.9). Glutaraldehyde treatment also resulted in particles that were of more elongated oval shape than heat-treated microparticles. Unlike heat treatment, the size of the vacuoles in the microparticles did not change with glutaraldehyde treatment. This is presumably, because there was no heating involved with the glutaraldehyde treatments therefore the expansion of entrapped air was not possible.

AFM indicated that the kafirin microparticles had a surface characterized by a rough morphology (marked X) (Figure 4.10A-E). Figure 4.10A illustrates the surface of a single control microparticle. More detailed study showed that the microparticle surface was composed of nanosized protuberances. Figure 4.10B shows the surface of a single heat-treated microparticle. In this case, more detailed study showed that nano-sized protuberances

of irregular shape and size (≈50–300 nm) were responsible for the final surface topography. As viewed by SEM (Figures 4.3, 4.5 and 4.8) the morphology is most likely due to non-linear (random) aggregation of the structural units (polypeptides). Similar nanostructure images have been reported with zein nanoparticles precipitated from aqueous ethanol (Xu et al., 2011) and with zein film droplets deposited onto silica (Panchapakesan, Sozer, Dogan, Huang and Kokini, 2012). Non-linear protein aggregation with heat treatment is a generic property of polypeptides (Krebs et al., 2007). As explained by these authors, non-linear protein aggregation is fast and non-specific, which decreases the likelihood of substantial structural rearrangements during the aggregation process. Furthermore, as the non-linear protein aggregation is not specific, there is no directionality to the aggregates, probably resulting in the round shapes. AFM of transglutaminase treated microparticles showed similar morphology as with heat treatment **(**Figure 4.10D).

On the contrary, with glutaraldehyde treatment, the presumed kafirin nanostructures were spindle-shaped with a unidirectional orientation, probably due to linear glutaraldehyde-protein linkage, as discussed (Figure 4.10E**)**. These nanostructures were ≈100–350 nm long and ≈20–100 nm wide (Figure 4.10Ei). The image in Figure 4.10Eii is probably a cross-sectional view of the spindles (represented by circular shapes). No reference to similar shaped protein particle structures visualized by AFM could be found in the literature. The spindle-shape formed with glutaraldehyde treatment suggests a linear polymerization of the kafirin polypeptides during their reaction with glutaraldehyde. This is in agreement with Migneault et al. (2004) who suggested that glutaraldehyde-protein reaction results in a cross-linked structure consisting of a linear aldol-condensed oligomer of glutaraldehyde linked to Schiff base (imine) from the protein. The variation in size of nanostructures viewed by AFM is probably dependent on how homogenous the nanoparticles were in the sites viewed. The nanostructures viewed from rough areas (R, Figure 4.10A-E) had larger diameter compared to those from flat areas (F, Figure 4.10A-E). This was probably because of the broadening phenomenon, where the side of the AFM probe is involved in imaging (reviewed by Shakesheff, Davies, Jackson, Roberts, Tendler, Brown, Watson, Barrett, and Shaw, 1994). The broadening effect is due to tip-sample convolution, which results when the radius of curvature of the tip is similar to, or greater than, the size of the feature that is imaged (reviewed by Shakesheff et al., 1994).

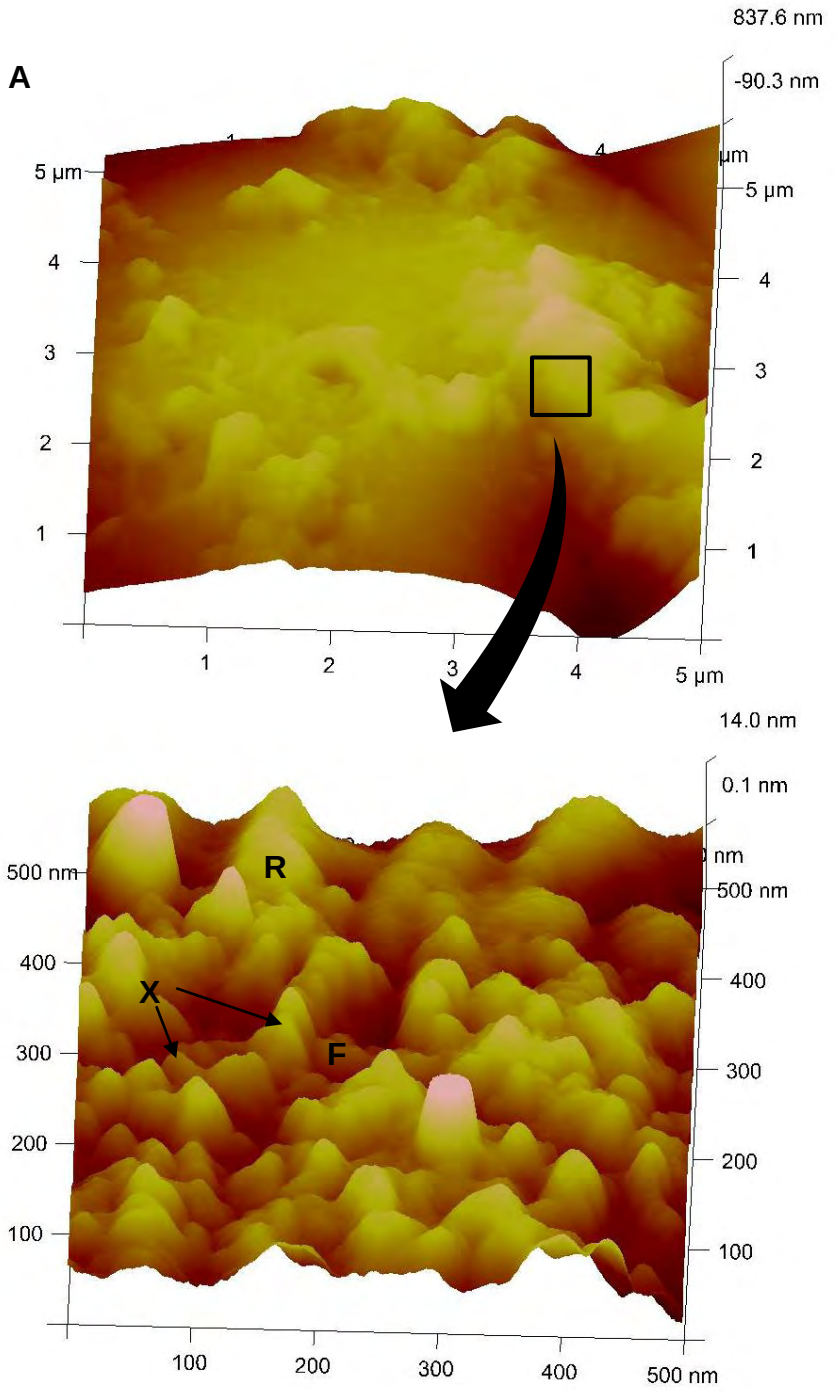

Figure 4.10 AFM topographs of treated kafirin microparticles at two different levels of magnification.

A. Control (22ºC). **B**. Heat treatment (96ºC).

C. Maltodextrin.

D. Transglutaminase treatment (0.6% transglutaminase + maltodextrin).

E. Glutaraldehdye treatment (30%). (**i**) Side view. (**ii**) View from end of nanostructures.

F-flat area, R- rough area. X –nanostructures (nanosized protuberances).

B

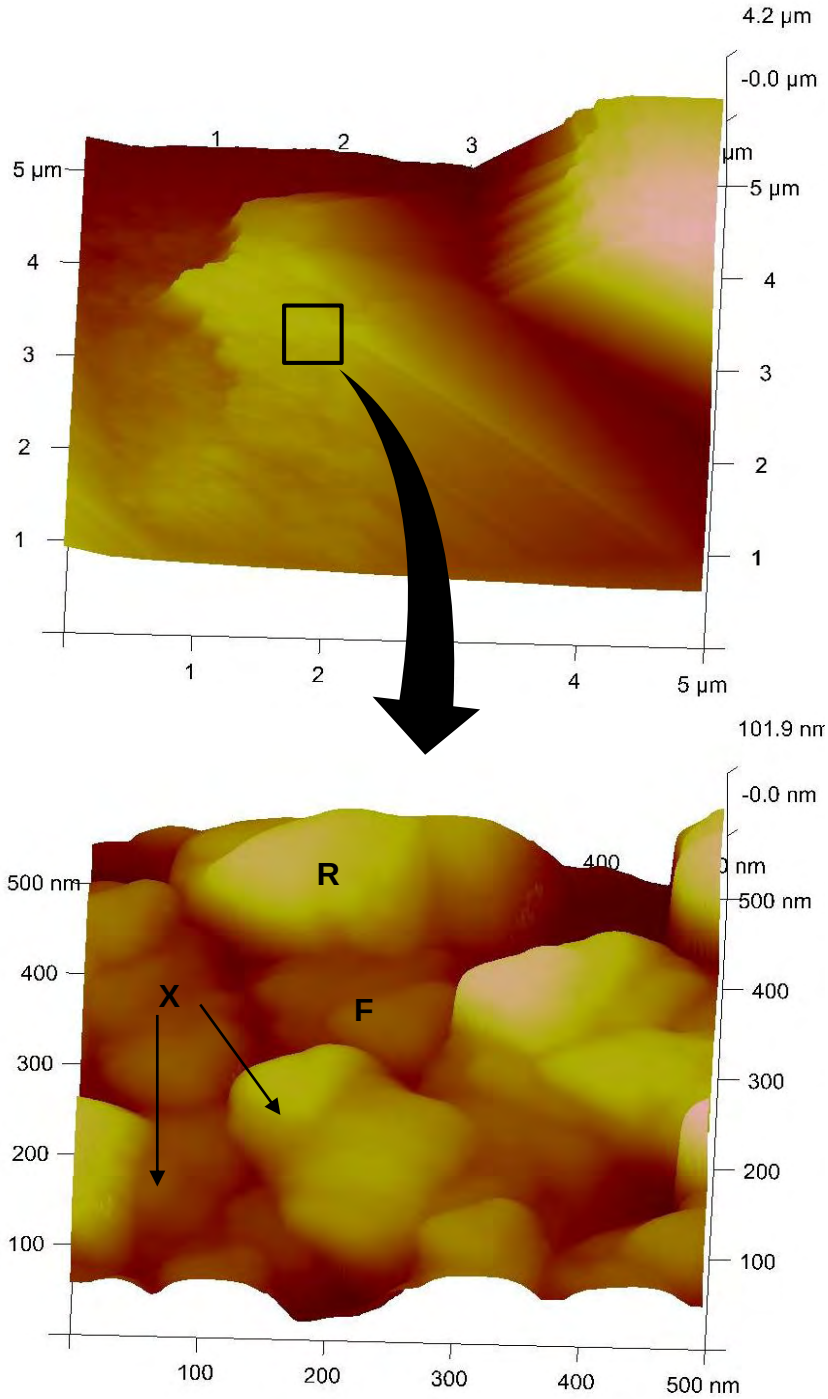
4.2 µm
-0.0 µm
µm
5 µm
4
3
2
1
1
2
3
5 µm
4
3
2
1
1
2
4
5 µm
101.9 nm
-0.0 nm
nm
500 nm
400
300
200
100
R
F
X
400
500 nm
400
300
200
100
100
200
300
400
500 nm

C

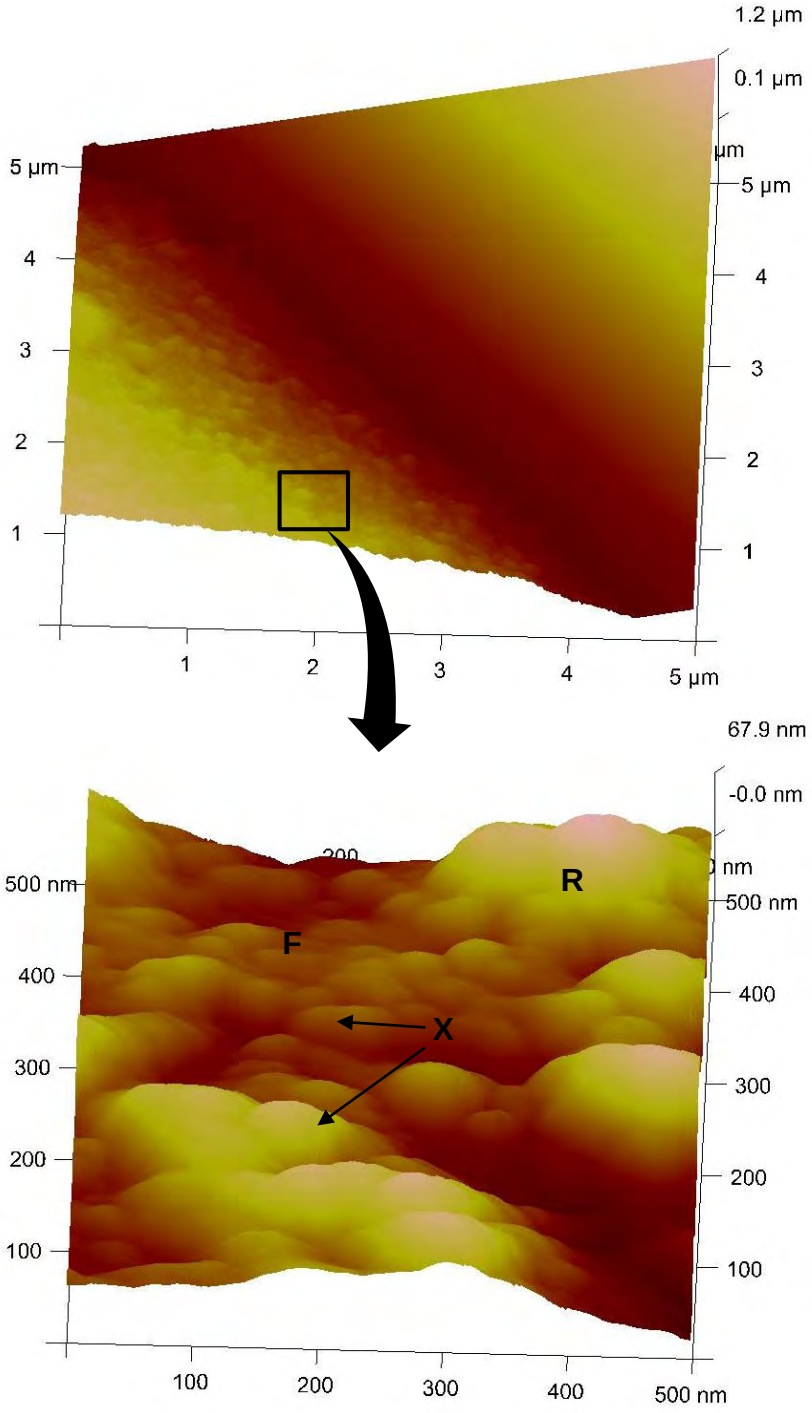
1.2 µm
0.1 µm
µm
5 µm
4
3
2
1
5 µm
4
3
2
1
67.9 nm
-0.0 nm
500 nm
400
300
200
100
R
F
X
500 nm
400
300
200
100

D

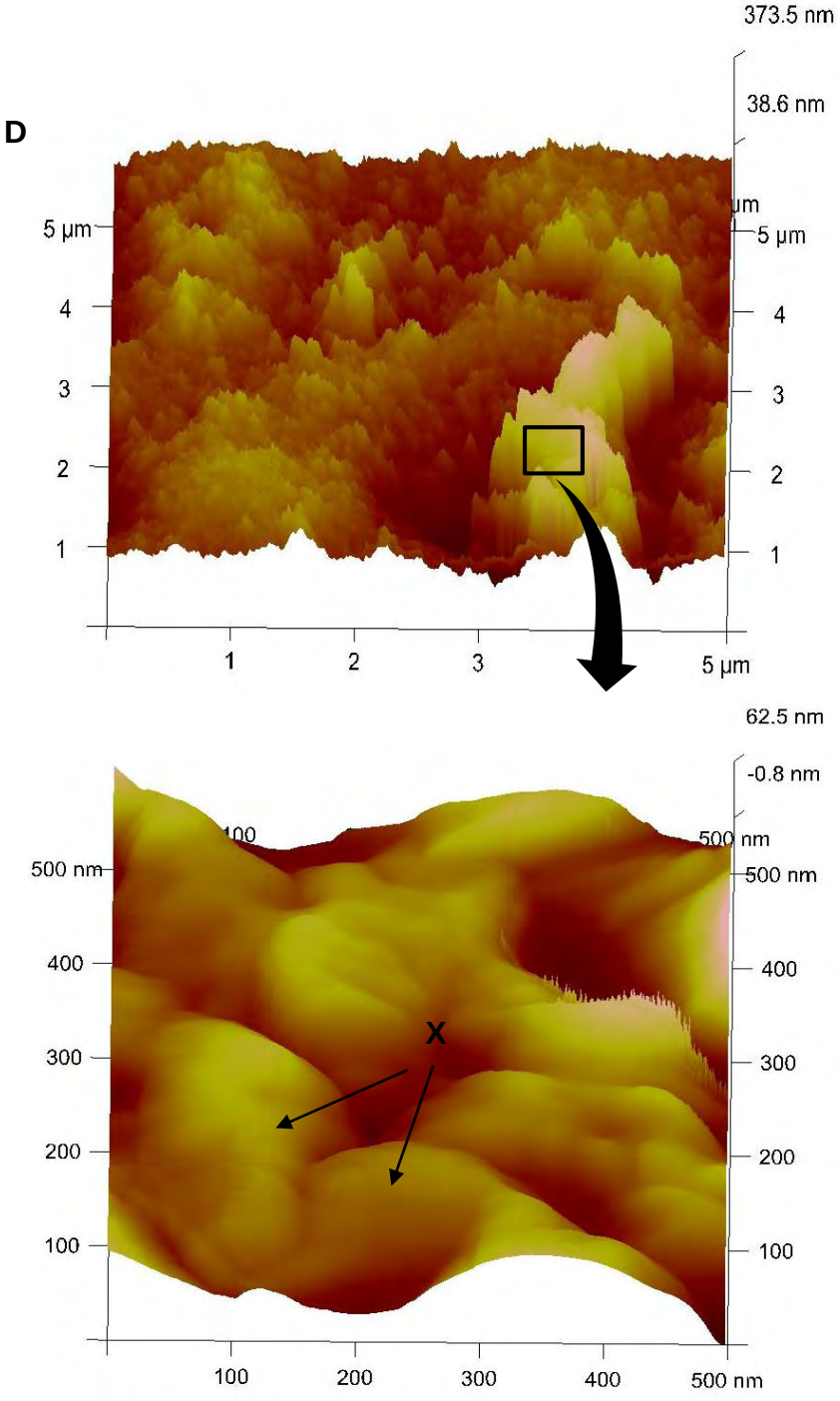
373.5 nm
38.6 nm
5 µm
4
3
2
1
1
2
3
5 µm
62.5 nm
-0.8 nm
500 nm
400
300
200
100
X
100
200
300
400
500 nm

E (i)

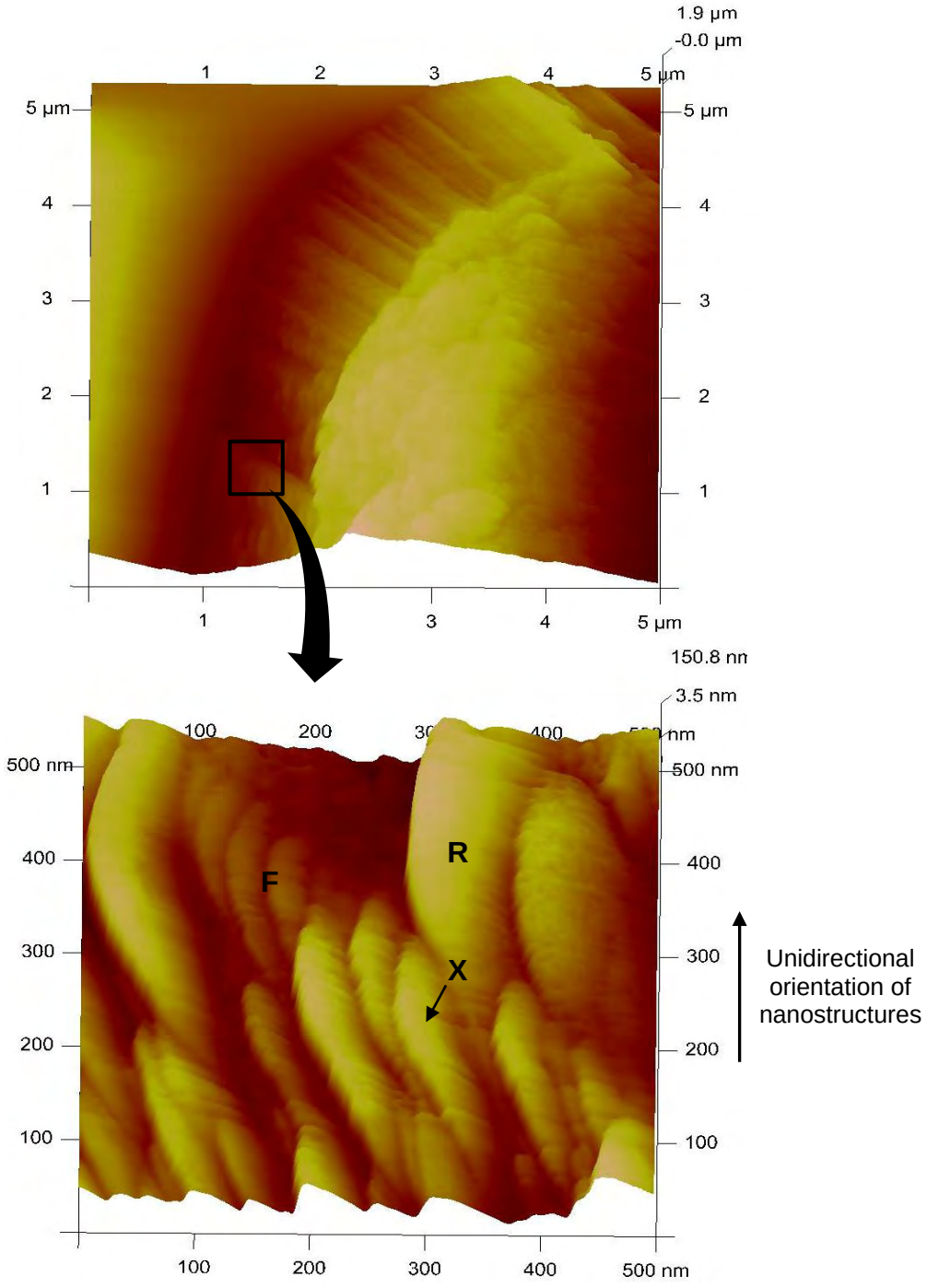
1.9 µm
-0.0 µm
5 µm
150.8 nm
3.5 nm
500 nm
R
F
X
Unidirectional orientation of nanostructures

E (ii)

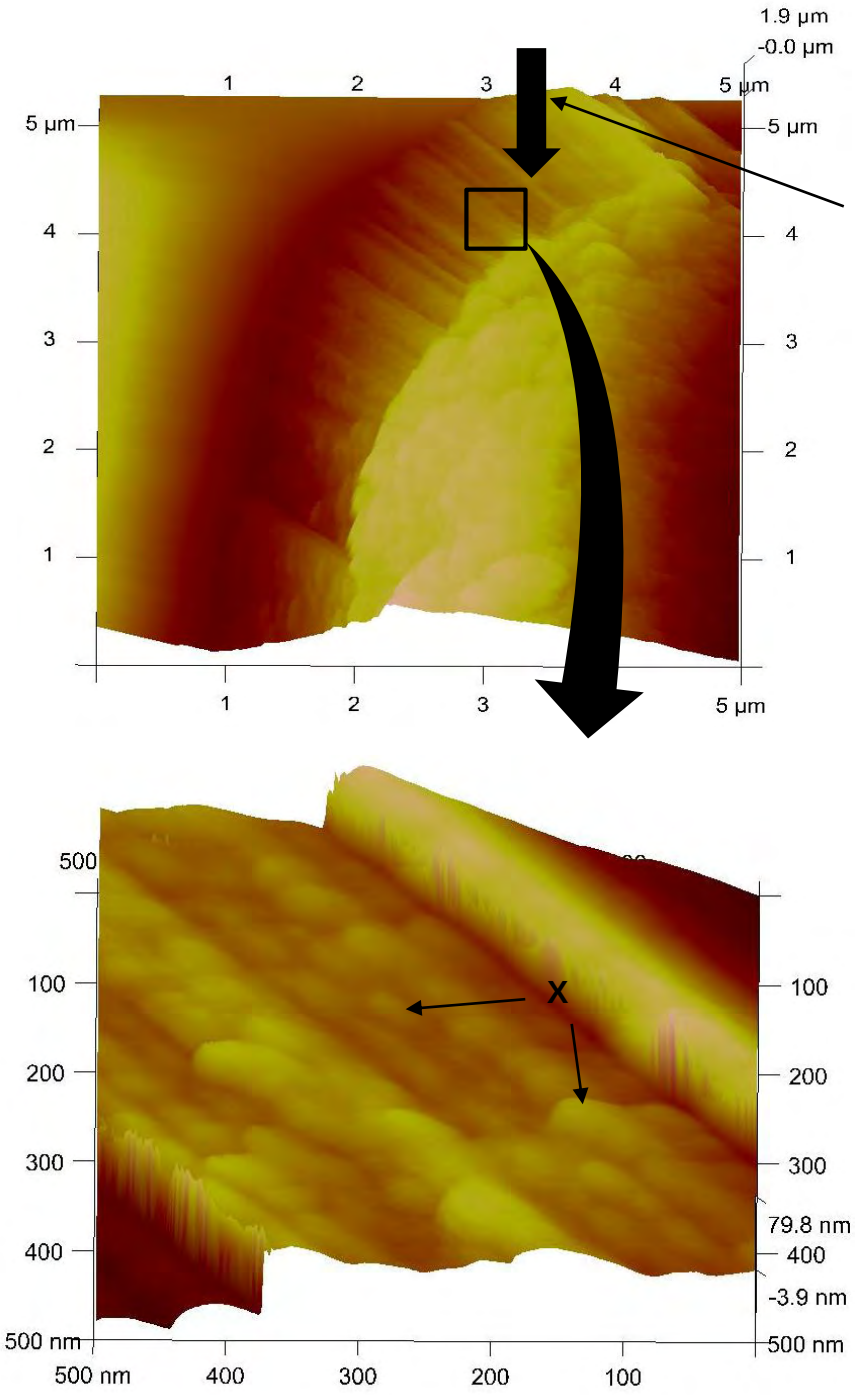

4.1.4.2 *Protein structure of treated kafirin microparticles*

SDS-PAGE of treated kafirin microparticles

SDS-PAGE under non-reducing conditions, of the wet heat-treated kafirin microparticles showed no change in band pattern compared with the control until the severity of the treatment was at 96^{o}C (Figure 4.11A). The highest band intensity was at 16–27 kDa with SDS-PAGE under both non-reducing and reducing conditions, which are the monomeric α-, β- and γ-kafirins (Shull et al., 1991). Bands 44–53 kDa and 78–93 kDa, probably dimers and trimers, respectively, based on classification by El Nour et al. (1998), were seen showing the occurrence of polymerized kafirin. The 96^{o}C heat treatment, under non-reducing conditions, however, showed a fainter trimer band and disappearance of an oligomer band (Figure 4.11A, arrows in Lane 4). This is considered indicative of polymerization of the different kafirin species, which then become too large to enter the separating gel (Ezeogu, Duodu and Taylor, 2005). The absence of visible change in band pattern at lower treatment temperatures may be due to the electrophoresis technique not being sufficiently sensitive to show a lower degree of polymerization. Under reducing conditions, all the treatments showed similar band patterns with very low levels of kafirin trimers and oligomers. This indicated that the kafirin polymers formed by heat treatment were the result of disulphide cross-linking, and that the linkages were broken on reduction, as demonstrated by the high level of kafirin monomers, as described by (Emmambux and Taylor, 2009).

Despite the changes in the physical appearance of the kafirin microparticles with transglutaminase treatment, there was no evidence of polymerization with SDS-PAGE (Figure 4.11B). However, with very high enzyme concentration (9.4% transglutaminase), which was over 15 fold the levels transglutaminase treatment used by other workers (Autio, Kruus, Knaapila, Gerber, Flander and Buchert, 2005; Bruno et al., 2008), a band approximately 39 kDa, probably a monomeric transglutaminase (Motoki and Seguro, 1998), was detected (Figure 4.11B, Lane 6). In addition, with the 9.4% transglutaminase treatment, faint 63 kDa and 118 kDa bands were detected using SDS-PAGE under reducing conditions, indicative of presence of kafirin trimers and oligomers, possibly formed by transglutaminase catalysed cross-linking of kafirin proteins. This suggested a low reactivity of kafirin with transglutaminase enzyme.

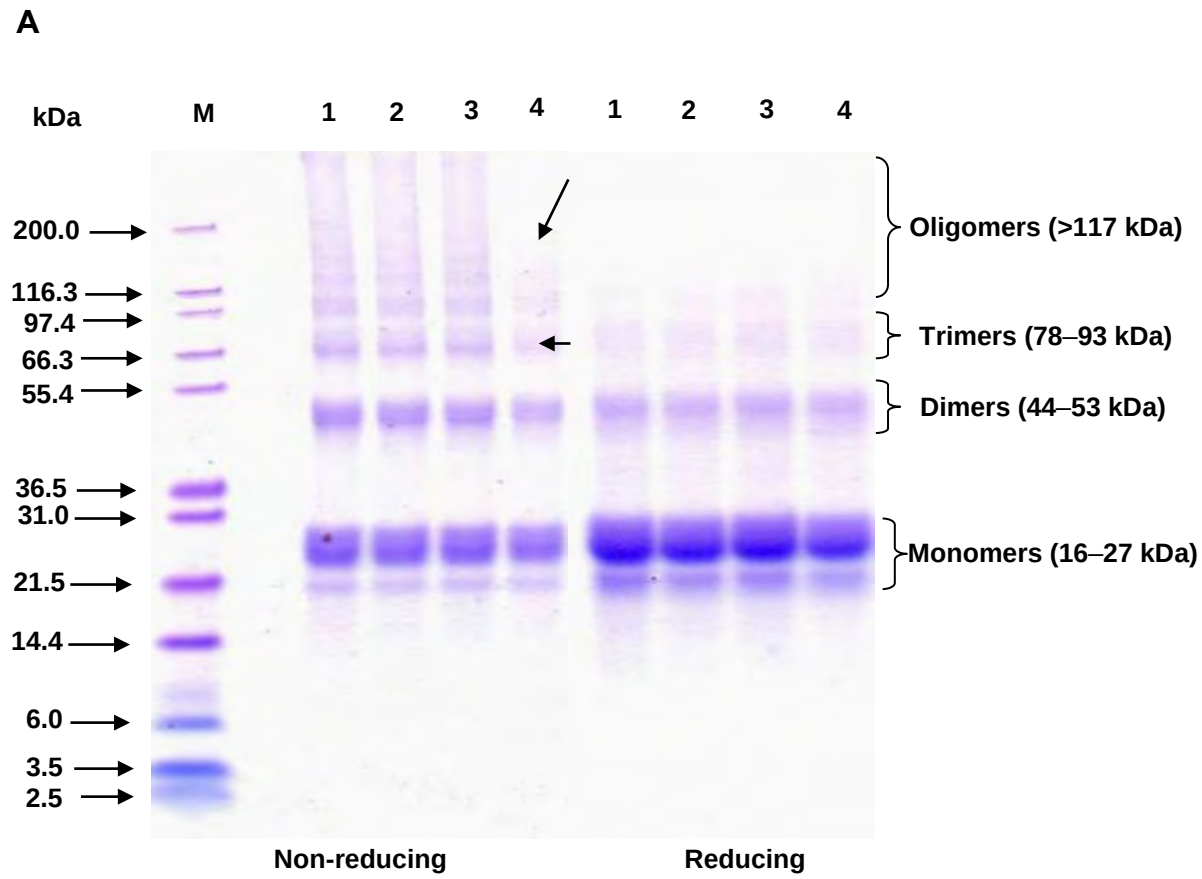

Figure 4.11 SDS-PAGE of treated kafirin microparticles. Protein loading, 10 µg.

A. Heat treatment. Lanes M: Molecular markers; 1: Control (22ºC); 2: 50ºC; 3: 75ºC; 4: 96ºC. Arrows in Lane 4 under non-reducing conditions show fading and disappearance of bands.

B. Transglutaminase (TG) treatment. Lanes M: Molecular markers; 1: TG; 2: Maltodextrin 3: 0.1% TG + maltodextrin; 4: 0.3% TG + maltodextrin; 5: 0.6% TG + maltodextrin; 6: 9.4% TG + maltodextrin*.

C. Glutaraldehyde treatment. Lanes M: Molecular markers; 1: Control; 2: 10%; 3: 20%; 4: 30%.

*The very high enzyme concentration (9.4% transglutaminase), which was over 15-fold the level of transglutaminase treatment in literature was tested only for SDS-PAGE to check whether it could have a cross-linking effect on the kafirin microparticles.

B

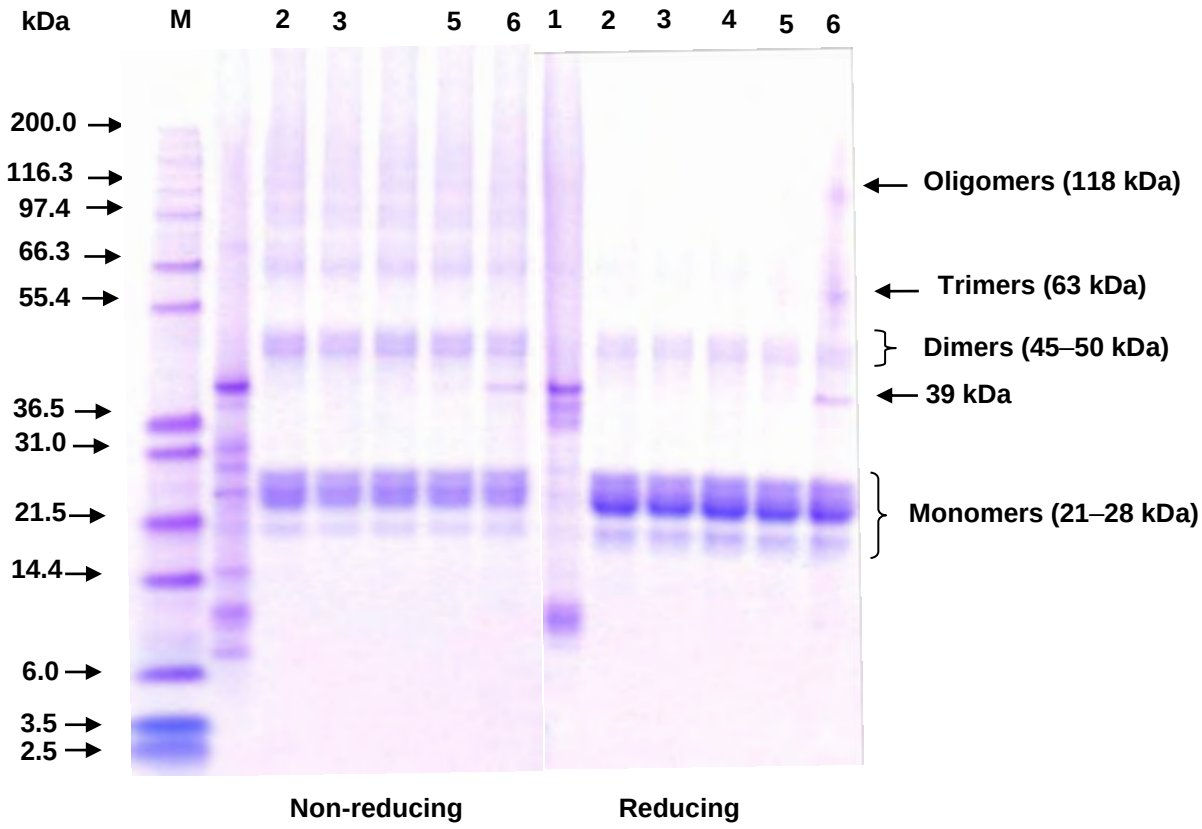
kDa
M
2
3
5
6
1
2
3
4
5
6
200.0
116.3
97.4
66.3
55.4
36.5
31.0
21.5
14.4
6.0
3.5
2.5
Oligomers (118 kDa)
Trimers (63 kDa)
Dimers (45–50 kDa)
39 kDa
Monomers (21–28 kDa)
Non-reducing
Reducing

C

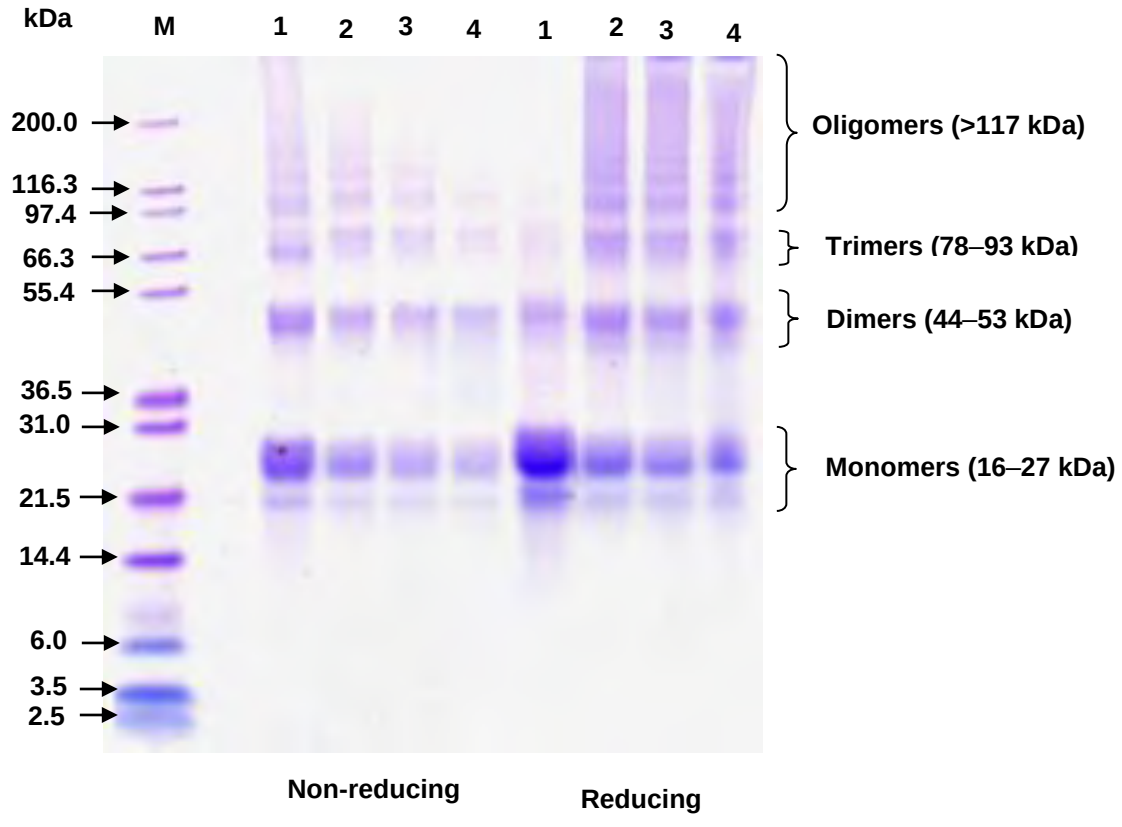
kDa
M
1
2
3
4
1
2
3
4
200.0
116.3
97.4
66.3
55.4
36.5
31.0
21.5
14.4
6.0
3.5
2.5
Oligomers (>117 kDa)
Trimers (78–93 kDa)
Dimers (44–53 kDa)
Monomers (16–27 kDa)
Non-reducing
Reducing

As stated, this is probably because of kafirin's very low lysine content (Belton et al., 2006). A similar poor cross-linking reaction was reported when wheat gliadin and the low molecular weight (LMW) glutenin subunits, which are also low in lysine, were cross-linked with transglutaminase (Autio et al., 2005).

In contrast, glutaraldehyde treatment of kafirin microparticles resulted in a progressive reduction of monomer (16–27 kDa), dimer (44–53 kDa), trimer (78–93 kDa) and oligomer (>117 kDa) bands under non-reducing conditions (Figure 4.11C). This is indicative of an increase in kafirin polymerization with increase in glutaraldehyde concentration, hence a reduction in the proportion of kafirin that could migrate into the separating gel. With SDS-PAGE under reducing conditions, the intensity of the kafirin monomer bands was much higher in the control than with the glutaraldehyde treatments. This indicated that the glutaraldehyde cross-linked the kafirin in such a way that breaking of the intermolecular disulphide bonds did not depolymerize it. Thus, the major cause of kafirin cross-linking with glutaraldehyde was not by disulphide bonding. It has been shown that cross-linking proteins with glutaraldehyde involves free amino groups of peptide chains and the carbonyl groups of the aldehyde (Rayment, 1997; Gerrard, Brown and Fayle, 2003) to form non-disulphide covalent bonds.

FTIR of heat, transglutaminase and glutaraldehyde treated kafirin microparticles

The kafirin microparticle secondary structure as analysed by FTIR showed a α-helical component of 48.7% for the control (Table 4.1) as determined at the Amide I band (≈1650–1620 cm^{-1}) based on the work by Duodu et al. (2001). Native kafirin is about 60% α-helical (reviewed by Belton et al., 2006), whereas Taylor et al. (2009a) found the secondary structure of kafirin microparticles between 50–56% α-helical conformation. These authors attributed the reduction in the proportion of α-helical conformation to protein aggregation during the formation of kafirin microparticles by self-assembly. The difference in the proportion of α-helical conformation in the control kafirin microparticles found in the present study compared to that reported by Taylor et al. (2009a) may be attributed to a number of factors, including differences in kafirin batches, method of kafirin extraction and drying effect on secondary structure measurements, as was suggested by Gao et al. (2005). Heat treatment of kafirin microparticles reduced further the relative proportion of α-helical conformation by up to about 17% compared to the control. The other amine bands (II and III) were not elaborated,

in this study, as they are less sensitive with FTIR spectroscopy in determining of protein secondary structure (reviewed by Jackson and Mantsch, 1995).

Table 4.1 Effects of heat, transglutaminase and glutaraldehyde treatments on the protein secondary structure of kafirin microparticles determined by FTIR

Treatment		Relative proportion of α-helical conformation at Amide I band (%)
Control	22°C	48.7 e (0.6)
Heat		
	50°C	45.5 d (0.3)
	75°C	40.9 ab (0.2)
	96°C	40.6 a (0.5)
Transglutaminase		
	Maltodextrin	41.9 b (0.8)
	0.1% TG + Maltodextrin	41.2 ab (0.8)
	0.3% TG + Maltodextrin	41.9 b (1.1)
	0.6% TG + Maltodextrin	43.3 c (0.8)
Glutaraldehyde		
	10%	44.5 d (0.6)
	20%	45.1 d (0.2)
	30%	45.1 d (0.8)

Values followed by different letters are significantly different ($p<0.05$). Values in the brackets are standard deviations (n=3). Control (22°C) is the same for heat and glutaraldehyde treatments. Amide I band ≈ 1650–1620 cm^{-1}.

The change in protein secondary structure with heat treatment has been related to the kafirin polymerization (Duodu et al., 2001; Byaruhanga et al., 2006). It has been suggested that thermal treatment disrupts the hydrogen bonds that stabilize the protein conformation, causing loss of the α-helix and β-sheet structures and creating new β-sheet arrangements (Emmambux and Taylor, 2009). Thus, it appears that the increase in size of the kafirin microparticles with increasing heat treatment was as a result of a further process of assisted-assembly caused by wet heat-induced kafirin disulphide-bonded polymerization, as described by Emmambux and Taylor (2009).

Treatment of the kafirin microparticles with transglutaminase appeared to result in slight changes to the protein secondary structure in comparison with microparticles to which only maltodextrin had been added. Similar observations were made by Eissa, Puhl, Kadla and

Khan (2006) studying the conformational changes of β-lactoglobulin treated with transglutaminase. These authors noted changes in microstructural properties, which were not reflected to the same extent in the molecular structure (protein secondary structure). In the present study, the essential absence of lysine in kafirin may have been a reason for the very small change in secondary structure. In addition, it has been proposed by Eissa et al. (2006) that there may be little effect of transglutaminase treatment on C=O stretching mode, probably due to the low number of the bonds created by the activity of the enzyme in comparison to the backbone bonds in the protein. When kafirin microparticles treated with transglutaminase and/or maltodextrin are compared to control without any treatment (control at 22^{o}C), it appears that there is a substantial difference in protein structure with about an 11–15% reduction in the relative proportion of α-helical conformation. This was probably because of the effect of maltodextrin, which constitutes the largest proportion of the transglutaminase enzyme mixture. A similar change in protein secondary structure as a result of reaction between dextrin and gliadin has been reported (Secundo and Guerrieri, 2005), which presumably was Maillard reaction. Maillard reaction has been shown to reduce the α-helical conformation of protein (Sun, Hayakawa and Izumori, 2004).

Despite the SDS-PAGE evidence of kafirin polymerization with glutaraldehyde treatment, FTIR indicated that it caused only a small reduction in the relative proportion of α-helical conformation (7–9%) (Table 4.1). There was no change in the protein secondary structure with increase in glutaraldehyde concentration. As stated, cross-linking protein with glutaraldehyde involves the free amino groups of the proteins and carbonyl groups of the aldehyde (Rayment, 1997). However, N–H bending contributes only less than 20% to Amide I band (Pelton and McLean, 2000; Surewicz et al., 1993). This is probably the reason for the small change in protein secondary structure with glutaraldehyde treatment. The present findings are consistent with a report by Caillard, Remondetto and Subirade (2009) on soy protein hydrogels, which showed little alteration in protein secondary structure with glutaraldehyde treatment despite a large effect on gel physical appearance and functional properties.

4.1.4.3 *Protein digestibility of heat, transglutaminase and glutaraldehyde treated kafirin microparticles*

Heat treatment resulted in up to 39% reduction in the IVPD of kafirin microparticles (Table 4.2). The reduction in IVPD with wet heat treatment is a characteristic of kafirin proteins and is due to disulphide cross-linking of these proteins (Hamaker et al., 1987; Duodu et al., 2003). Reduction in the IVPD of kafirin has been associated with reduction in proportion α-helical conformation at the amide I band (Emmambux and Taylor, 2009). The reduction in IVPD of kafirin microparticles with heat treatment agrees with the data on the protein secondary structure (Table 4.1).

Table 4.2 Effects of kafirin microparticle treatment with heat, transglutaminase and glutaraldehyde on their *in vitro* protein digestibility (IVPD)

Treatment		IVPD (%)
Control	22°C	92.2 e (0.4)
Heat		
	50°C	90.2 de (1.8)
	75°C	73.5 b (0.7)
	96°C	57.3 a (1.5)
Transglutaminase		
	Maltodextrin	90.0 de (0.1)
	0.1% TG + Maltodextrin	85.2 c (0.4)
	0.3% TG + Maltodextrin	86.3 cd (4.3)
	0.6% TG + Maltodextrin	88.7 cde (0.0)
Glutaraldehyde		
	10%	91.3 e (1.8)
	20%	91.9 e (2.8)
	30%	92.5 e (0.3)

Values followed by different letters are significantly different ($p<0.05$). Values in the brackets are standard deviations (n=3). Control (22°C) is the same for heat and glutaraldehyde treatments.

Transglutaminase treatment had little effect on IVPD of the kafirin microparticles, with a reduction of only about 1–5%, compared to their control kafirin microparticles to which only

maltodextrin was added. Similar findings were reported by Seguro, Kumazawa, Kuraishi, Sakamoto and Motoki (1996) and Roos, Lorenzen, Sick, Schrezenmeir and Schlimme (2003) working on transglutaminase-treated casein. This small effect of transglutaminase on IVPD of kafirin microparticles was probably due to the very low kafirin lysine content as discussed. Additionally, it has been suggested by Lundin, Golding and Wooster (2008) that the little effect of transglutaminase on protein digestibility may be because the cross-linked regions of the protein molecules are probably are not involved in the proteolytic reaction. However, the reduction in IVPD of transglutaminase-treated microparticles was slightly higher (4–8%) when compared with the control microparticles held at 22^{o}C. This was probably because the transglutaminase enzyme is prepared in maltodextrin (sugar) carrier base constituting 99%, which may participate in Maillard reaction with the proteins. Maillard reaction has been shown to inhibit protein digestibility (Friedman, 1996).

Despite the glutaraldehyde treatment causing kafirin polymerization, it did not significantly affect kafirin microparticle IVPD. This is consistent with the lack of change in protein secondary structure and is probably a result of an increase in protein void volume caused by the glutaraldehyde cross-linking. It has been suggested that polymeric forms of glutaraldehyde are involved in the cross-linking with protein (Migneault et al., 2004; Wine, Cohen-Hadar, Freeman and Frolow, 2007). These glutaraldehyde polymers may create long methylene bridges between peptides (Farris et al., 2010). Hence, the protein polymer chains may be kept far apart in a glutaraldehyde-protein complex, thereby allowing easier accessibility of pepsin enzyme to hydrolyse internal peptide bonds.

4.1.4.4 *Mechanical properties of heat, transglutaminase and glutaraldehyde treated kafirin microparticles*

These treatments reduced the slope of force-deformation curves obtained with AFM of kafirin microparticles (Figure 4.12, Table 4.3). Heat and glutaraldehyde treatments resulted in the greatest decrease in slope. The slope of a force-deformation curve is a measure of the elastic stiffness of the material (Lee, Wei, Kysar and Hone, 2008) and has been shown to directly correspond to the surface elastic modulus of nanoparticles (Krake and Damasche, 2000; Safanama, Marashi, Hesari, Firoozi, Aboutalebi and Jalilzadeh, 2012).

Various reasons may account for the differences in the elastic moduli of the kafirin microparticles with different treatments. In the case of glutaraldehyde treatment, it has been

suggested that molecular structure of the long methylene bridges formed between the glutaraldehyde cross-linked proteins may lead to a decrease in the intermolecular forces between polymer chains causing a plasticizer effect (Marquié, Tessier, Aymard and Guilbert, 1997).

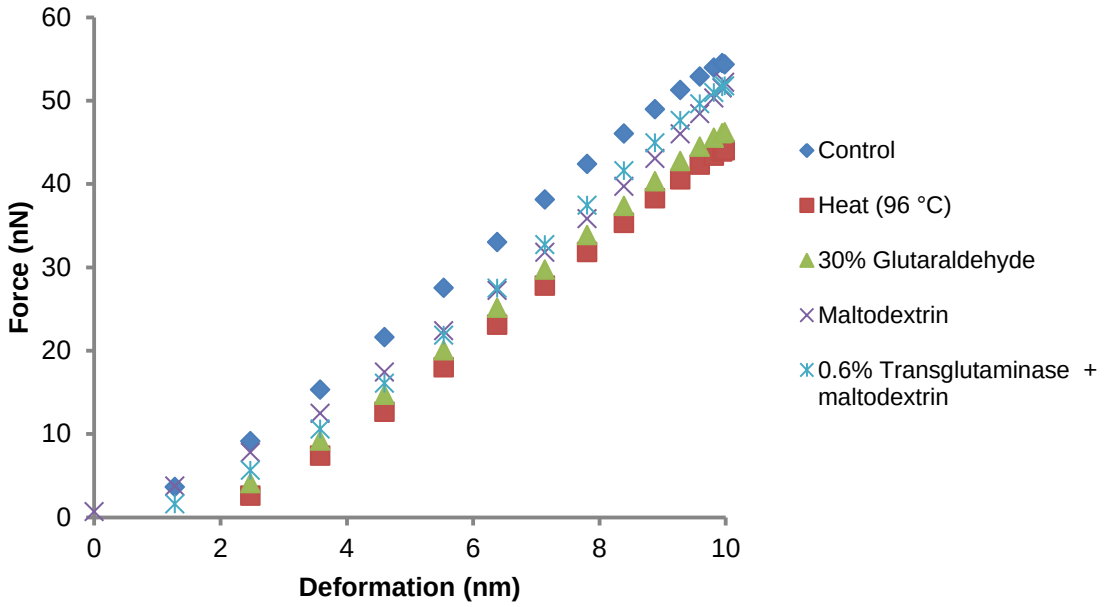

Figure 4.12 Representative linear portion of the force-deformation curves for heat, transglutaminase and glutaraldehyde treated kafirin microparticles, determined by AFM.

Table 4.3 Slope of linear portion of force-deformation curves of heat, transglutaminase and glutaraldehyde treated kafirin microparticles determined by AFM

Treatment		Slope (nN/nm)
Control	22 °C	6.18 c (0.27)
Heat	96°C	4.81 a (0.11)
Transglutaminase		
	Maltodextrin	5.42 b (0.23)
	0.6% TG + Maltodextrin	5.12 ab (0.30)
Glutaraldehyde	30%	4.83 a (0.32)

Values are mean slopes of curves for each treatment. Values followed by different letters are significantly different ($p<0.05$). Figures in the brackets are standard deviations (n=3)

In addition, non-linear protein aggregation is characterized by less elastic behaviour (Chen et al., 2006), which probably accounted for the higher elastic modulus of the control and the transglutaminase-treated kafirin microparticles compared to glutaraldehyde. With heat

treatment, the reduction in the elastic stiffness was probably due to the increase in the microparticle vacuole size. It is known that the elastic modulus of particles decreases with increase in their porosity (Phani and Niyogi, 1987). However, it is important to note that this AFM technique measures only a very small portion of the microparticles (reviewed by Kim, Cheng, Liu, Wu and Sun, 2010), hence the results have to be treated with caution.

4.1.4.5 *Kafirin microparticle further self-assembly*

This study shows that modification of kafirin microparticles with wet heat or glutaraldehyde treatment result in two structures that while similar in size and external morphology, are formed by significantly different mechanisms. It is also apparent that in both cases the larger kafirin microparticle structures had undergone some form of further assisted-assembly during the treatments and were not just formed as a result of 'gluing' the original microparticles together. The 'gluing together' of microparticles was observed when sorghum condensed tannins were encapsulated using kafirin microparticles (Taylor et al., 2009b). Furthermore, with both the heat and glutaraldehyde treatments, there was kafirin polymerization and although the treatments only resulted in a small changes in secondary structure from α-helical to β-sheet as shown by FTIR, there was a considerable proportion of β-sheet present, 59.4% and 54.9% for the most rigorous heat treatment and glutaraldehyde treatment, respectively (Table 4.1). A large proportion of β-sheet presence is considered indicative of protein aggregation (Mizutani et al., 2003) and the universal energetic minimum for aggregated protein (reviewed by Gorbenko and Kinnunen, 2006). Zein can self-assemble into aggregates as globules (Guo et al., 2005), fibrils (Erickson, Campanella and Hamaker, 2012), and spherical micro- and nano-particles (Wang and Padua, 2010) depending on the conditions of formation, all of which have a large proportion of β-sheet structure.

Wang and Padua (2010) working with zein dissolved in 70% ethanol showed that at low mass fraction zein formed spheres. With increasing zein concentration, they noted various different geometries formed by connecting, melting or deformation of spheres. They concluded that spheres were the basis of all other microphases. In this study, the heat-treated microparticles appeared to be formed by coalescence of spherical nanoparticles, in agreement with Wang and Padua (2010). Further work by Wang and Padua (2012) showed that at nanoscale, zein formed stripes, rings and discs with a periodicity characteristic of β-sheet. They indicated that these β-sheets self-assembled into stripes, which curled into rings and then the rings stacked into spheres. However, in this study AFM indicated the glutaraldehyde-treated microparticles

were formed from spindle-shaped nanostructures with little change in secondary structure but with a large proportion of β-sheet structure present. It appears unlikely that these structures formed from spheres. Further work is needed in order to understand the kafirin self-assembly process at a molecular level, under the different conditions used in this study so that the self-assembly process can be further manipulated to enable the formation of different structures.

4.1.5 Conclusions

Heat treatment increases the size of kafirin microparticles and enlarges the pores within these microstructures. While glutaraldehyde treatment, as with heat increases the size of the microparticles, it also results in the formation of presumed kafirin nanostructures with generally spindle shapes, probably due to formation of a linear kafirin-glutaraldehyde linkage. On the contrary, transglutaminase treatment has little effect on the size of individual microparticles but results in agglomeration of kafirin microparticles into large lumps. Cross-linking the formed kafirin microparticles using wet heat or glutaraldehyde treatment apparently causes further assisted-assembly by two significantly different mechanisms. Heat treatment, involves kafirin polymerization by disulphide bonding with the microparticles being formed from round, coalesced nanostructures. Kafirin polymerization in glutaraldehyde treated microparticles is not by disulphide bonding and the nanostructures are spindle-shaped.

4.1.6 References

American Association of Cereal Chemists (AACC International), 2000. Crude protein-combustion, Standard Method 46-30. Approved Methods of the AACC (10th ed.). The Association: St Paul, MN.

Autio, K., Kruus, K., Knaapila, A., Gerber, N., Flander, L., Buchert, J., 2005. Kinetics of transglutaminase-induced cross-linking of wheat proteins in dough. Journal of Agricultural and Food Chemistry 53, 1039–1045.

Belton, P.S., Delgadillo, I., Halford, N.G., Shewry, P.R., 2006. Kafirin structure and functionality. Journal of Cereal Science 44, 272–286.

Bruno, M., Giancone, T., Torrieri, E., Masi, P., Moresi, M., 2008. Engineering properties of edible transglutaminase cross-linked caseinate-based films. Food Bioprocess Technology 1, 393–404.

Byaruhanga, Y.B., Emmambux, M.N., Belton, P.S., Wellner, N., Ng, K.G., Taylor, J.R.N., 2006. Alteration of kafirin film structure by heating with microwave energy and tannin complexation. Journal of Agricultural and Food Chemistry 54, 4198–4207.

Caillard, R., Remondetto, G.E., Subirade, M., 2009. Physicochemical properties and microstructure of soy protein hydrogels co-induced by Maillard type cross-linking and salts. Food Research International 42, 98–106.

Duodu, K.G., Taylor, J.R.N., Belton, P.S., Hamaker, B.R., 2003. Factors affecting sorghum protein digestibility. Journal of Cereal Science 38, 117–131.

Eissa, A.S., Puhl, C., Kadla, J.F., Khan, S.A., 2006. Enzymatic cross-linking of β-lactoglobulin: conformational properties using FTIR spectroscopy. Biomacromolecules 7, 1707−1713.

El Nour, N.A., Peruffo, A.D.B., Curioni, A., 1998. Characterisation of sorghum kafirins in relations to their cross-linking behaviour. Journal of Cereal Science 28, 197–207.

Emmambux, N. M., Taylor, J.R.N., 2003. Sorghum kafirin interaction with various phenolic compounds. Journal of the Science of Food and Agriculture 83, 402–407.

Emmambux, N.M., Taylor, J.R.N., 2009. Properties of heat-treated sorghum and maize meal and their prolamin proteins. Journal of Agricultural and Food Chemistry 57, 1045–1050.

Erickson, D.P., Campanella, O.H., Hamaker, B.R., 2012. Functionalizing maize zein in viscoelastic dough systems through fibrous, β-sheet-rich protein networks: An alternative, physiochemical approach to gluten-free breadmaking. Trends in Food Science and Technology 24, 74–81.

Ezeogu, L.I., Duodu, K.G., Taylor, J.R.N., 2005. Effects of endosperm texture and cooking on the in vitro starch digestibility of sorghum and maize flours. Journal of Cereal Science 42, 33–44.

Ezpeleta, I., Rache, J.M., Gueguen, J., Orecchioni, A.M., 1997. Properties of glutaraldehyde cross-linked vicilin nano- and microparticles. Journal of Microencapsulation 14, 557–565.

Farris, S., Song, J., Huang, Q., 2010. Alternative reaction mechanism for the cross-linking of gelatin with glutaraldehyde. Journal of Agricultural and Food Chemistry 58, 998–1003.

Friedman, M., 1996. Food browning and its prevention: an overview. Journal of Agricultural and Food Chemistry 44, 631−653.

Gan, C.-Y., Cheng, L.-H., Easa, A.M., 2008. Evaluation of microbial transglutaminase and ribose cross-linked soy protein isolate-based microcapsules containing fish oil. Innovative Food Science and Emerging Technologies 9, 563–569.

Gao, C., Taylor, J., Wellner, N., Byaruhanga, Y.B., Parker, M.L., Mills, E.N.C., Belton, P.S., 2005. Effect of preparation conditions on protein secondary structure and biofilm formation of kafirin. Journal of Agricultural and Food Chemistry 53, 306–312.

Gerrard, J.A., Brown, P.K., Fayle, S.E., 2003. Maillard crosslinking of food proteins II: the reactions of glutaraldehyde, formaldehyde and glyceraldehyde with wheat proteins in vitro and in situ. Food Chemistry 80, 35–43.

Gong, S., Wang, H., Sun, Q., Xue, S.-T., Wang, J.-Y., 2006. Mechanical properties and in vitro biocompatibility of porous zein scaffolds. Biomaterials 27, 3793–3799.

Gorbenko, G.P., Kinnunen, P.K.J., 2006. The role of lipid-protein interactions in amyloid-type protein fibril formation. Chemistry and Physics of Lipids 141, 72–82.

Guo, Y., Liu, Z., An, H., Li, M., Hu, J., 2005. Nano-structure and properties of maize zein studied by atomic force microscopy. Journal of Cereal Science 41, 277–281.

Hamaker, B.R., Kirleis, A.W., Mertz, E.T., Axtell, J.D., 1986. Effect of cooking on the protein profiles and in vitro digestibility of sorghum and maize. Journal of Agricultural and Food Chemistry 34, 647−649.

Hamaker, B.R., Kirleis, A.W., Butler, L.G., Axtell, J.D., Mertz, E.T., 1987. Improving the in vitro protein digestibility of sorghum with reducing agents. Proceedings of the National Academy of Sciences of the United States of America 84, 626–628.

Hou, Q., De Bank, P.A., Shakesheff, K.M., 2004. Injectable scaffolds for tissue regeneration. Journal of Materials Chemistry 14, 1915–1935.

Jackson, M., Mantsch, H.H., 1995. The use and misuse of FTIR spectroscopy in the determination of protein structure. Critical Reviews in Biochemistry and Molecular Biology 30, 95–120.

Kim, K., Cheng, J., Liu, Q., Wu, X.Y., Sun, Y., 2010. Investigation of mechanical properties of soft hydrogel microcapsules in relation to protein delivery using a MEMS force sensor. Journal of Biomedical Materials Research Part A 92, 103–113.

Kim, S., Kang, Y., Krueger, C.H., Sen, M., Holcomb, J.B., Chen, D., Wenke, J.C., Yang, Y., 2012. Sequential delivery of BMP-2 and IFG-1 using a chitosan gel with gelatin microspheres enhances early osteoblastic differentiation. Acta Biomaterialia 8, 1768–1777.

Krake, B., Damasche, B., 2000. Measurement of nanohardness and nanoelasticity of thin gold films with scanning force microscope. Applied Physics Letters 77, 361–363.

Krebs, M.R.H., Devlin, G.L., Donald, A.M., 2007. Protein particulates: another generic form of protein aggregation? Biophysical Journal 92, 1336–1342.

Lee, C., Wei, X., Kysar, J.W., Hone, J., 2008. Measurement of the elastic properties and intrinsic strength of monolayer graphene. Science 321, 385–388.

Lehtinen, K.E.J., Zachariah, M.R., 2001. Effect of coalescence energy release on the temporal shape evolution of nanoparticles. Physical Review B 63 205402-1–205402-7.

Lundin, L., Golding, M., Wooster, T.J., 2008. Understanding food structure and function in developing food for appetite control. Nutrition and Dietetics 65 (Suppl. 3), S79–S85.

Marquié, C., Tessier, A.-M., Aymard, C., Guilbert, S., 1997. HPLC determination of the reactive lysine content of cottonseed protein films to monitor the extent of cross-linking by formaldehyde, glutaraldehyde, and glyoxal. Journal of Agricultural and Food Chemistry 45, 922–926.

Migneault, I., Dartiguenave, C., Bertrand, M.J., Waldron, K.C., 2004. Glutaraldehyde: behavior in aqueous solution, reaction with proteins, and application to enzyme crosslinking. BioTechniques 37, 790−802.

Mizutani, Y., Matsumura, Y., Imamura, K., Nakanishi, K., Mori, T., 2003. Effects of water activity and lipid addition on secondary structure of zein in powder systems. Journal of Agricultural and Food Chemistry 51, 229–235.

Motoki, M., Seguro, K., 1998. Transglutaminase and its use for food processing. Trends in Food Science and Technology 9, 204–210.

Muthuselvi, L., Dhathathreyan, A., 2006. Simple coacervates of zein to encapsulate gitoxin. Colloids and Surfaces B: Biointerfaces 51, 39–43.

Panchapakesan, C., Sozer, N., Dogan, H., Huang, Q., Kokini, J.L., 2012. Effect of different fractions of xeon on the mechanical and phase properties of zein films at nano-scale. Journal of Cereal Science 55, 174–182.

Parris, N., Cooke, P.H., Hicks, K.B., 2005. Encapsulation of essential oils in zein nanospherical particles. Journal of Agricultural and Food Chemistry 53, 4788–4792.

Patel, A., Hu, Y., Tiwari, J.K., Velikov, K.P., 2010. Synthesis and characterisation of zein–curcumin colloidal particles. Soft Matter 6, 6192–6199.

Pelton, J.T., McLean, L.R., 2000. Spectroscopic methods for analysis of protein secondary structure. Analytical Biochemistry 277, 167–176.

Phani, K.K., Niyogi, S.K., 1987. Young's modulus of porous brittle solids. Journal of Materials Science 22, 257–263.

Rayment, I., 1997. Reductive alkylation of lysine residues to alter crystallization properties of properties. Methods in Enzymology 276, 171–179.

Reddy, N., Yang, Y., 2011. Potential of plant proteins for medical applications. Trends in Biotechnology 29, 490–498.

Roos, N., Lorenzen, P.C., Sick, H., Schrezenmeir, J., Schlimme, E., 2003. Cross-linking by transglutaminase changes neither the in vitro proteolysis nor the in vivo digestibility of caseinate. Kieler Milchwirtschaftliche Forschungsberichte 55, 261–276.

Safanama, D.S., Marashi, P., Hesari, A.Z., Firoozi, S., Aboutalebi, S.H., Jalilzadeh, S., 2012. Elastic modulus measurement of nanocomposite materials by atomic force microscopy. International Journal of Modern Physics: Conference Series 5, 502–509.

Secundo, F., Guerrieri, N., 2005. ATR-FT/IR study on the interactions between gliadins and dextrin and their effects on protein secondary structure. Journal of Agricultural and Food Chemistry 53, 1757−1764.

Seguro, K., Kumazawa, Y., Kuraishi, C., Sakamoto, H., Motoki, M., 1996. The ε-(γ-glutamyl)lysine moiety in crosslinked casein is an available source of lysine for rats. Journal of Nutrition 126, 2557–2562.

Shakesheff, K.M., Davies, M.C., Jackson, D.E., Roberts, C.J., Tendler, S.J.B., Brown, V.A., Watson, R.C., Barrett, D.A., Shaw, P.N., 1994. Imaging the surface of silica microparticles with the atomic force microscope: a novel sample preparation method. Surface Science Letters 304, L393–L399.

Shull, J.M., Watterson, J.J., Kirleis, A.W., 1991. Proposed nomenclature for the alcohol-soluble proteins (kafirins) of *Sorghum bicolor* (L. Moench) based on molecular weight, solubility and structure. Journal of Agricultural and Food Chemistry 39, 83–87.

Sun, Y., Hayakawa, S., Izumori, K., 2004. Modification of ovalbumin with a rare ketohexose through the Maillard reaction: effect on protein structure and gel properties. Journal of Agricultural and Food Chemistry 52, 1293–1299.

Surewicz, W.K., Mantsch, H.H., Chapman, D., 1993. Determination of protein secondary structure by Fourier transform infrared spectroscopy: a critical assessment. Biochemistry 32, 389−394.

Taylor, J., Taylor, J.R.N., 2002. Alleviation of the adverse effects of cooking on sorghum protein digestibility through fermentation in traditional African porridges. International Journal of Food Science and Technology 37, 129–137.

Taylor, J., Taylor, J.R.N., Belton, P.S., Minnaar, A., 2009a. Formation of kafirin microparticles by phase separation from an organic acid and their characterization. Journal of Cereal Science 50, 90–105.

Taylor, J., Taylor, J.R.N., Belton, P.S., Minnaar, A., 2009b. Kafirin Microparticle encapsulation of catechin and sorghum condensed tannins. Journal of Agricultural and Food Chemistry 57, 7523–7528.

Wang, H.-J., Lin, Z.-X., Liu, X.-M., Sheng, S.-Y., Wang, J.-Y., 2005. Heparin-loaded zein microsphere film and hemocompatibility. Journal of Controlled Release 105, 120–131.

Wang, Y., Padua, G.W., 2010. Formation of zein microphases in ethanol-water. Langmuir 26, 12897–12901.

Wang, Y., Padua, G.W., 2012. Nanoscale characterization of zein self-assembly. Langmuir 28, 2429−2435.

Weiss, P., Layrolle, P., Clergeau, L.P., Enckel, B., Pilet, P., Amouriq, Y., Daculsi, G., Giumelli, B., 2007. The safety and efficacy of an injectable bone substitute in dental sockets demonstrated in a human clinical trial. Biomaterials 28, 3295−3305.

Wine, Y., Cohen-Hadar, N., Freeman, A., Frolow, F., 2007. Elucidation of the mechanism and end products of glutaraldehyde crosslinking reaction by x-ray structure analysis. Biotechnology and Bioengineering 98, 711–718.

Xiao, D., Davidson, P.M., Zhong, Q., 2011. Spray dried zein capsules with coencapsulated nisin and thymol as antimicrobial delivery system for enhanced antilisterial properties. Journal of Agricultural and Food Chemistry 59, 7393–7404.

Xu, H., Jiang, Q., Reddy, N., Yang, Y., 2011. Hollow nanoparticles from zein for potential medical applications. Journal of Materials Chemistry 21, 18227–18235.

Zhang, W., Zhong, Q., 2009. Microemulsions as nanoreactors to produce whey protein nanoparticles with enhanced heat stability by sequential enzymic cross-linking and thermal pretreatments. Journal of Agricultural and Food Chemistry 57, 9181–9189.

CHAPTER 2

4.2 IMPROVEMENT IN WATER STABILITY AND OTHER RELATED FUNCTIONAL PROPERTIES OF THIN CAST KAFIRIN PROTEIN FILMS

4.2.1 Abstract

Improvement in the water stability and other related functional properties of thin (<50 µm) kafirin protein films was investigated. Thin conventional kafirin films and kafirin microparticle films were prepared by casting in acetic acid solution. Thin kafirin films cast from microparticles were more stable in water than conventional cast kafirin films. Treatment of kafirin microparticles with heat and transglutaminase resulted in slightly thicker films with reduced tensile strength. In contrast, glutaraldehyde treatment resulted in up to 43% increase in film tensile strength. The films prepared from microparticles treated with glutaraldehyde were quite stable in ambient temperature water, despite the loss of plasticizer. This was probably due to the formation of covalent cross-linking between free amino groups of the kafirin polypeptides and carbonyl groups of the aldehyde. Thus, such thin glutaraldehyde-treated kafirin microparticle films appear to have good potential for use as biomaterials in aqueous applications.

4.2.2 Introduction

Films and other biomaterials made from proteins draw much interest as a consumer- and environment-friendly option to synthetic polymer products (Poole, Church and Huson, 2008; Bourtoom, 2009). Some of the applications or potential uses of protein biomaterials include packaging materials and food coatings (Krochta, 2002), carriers of antimicrobial agents (Pérez-Pérez, Regalado-González, Rodríguez-Rodríguez, Barbosa-Rodríguez, and Villaseñor-Ortega, 2006) and drug-eluting coating film for cardiovascular devices (Wang et al., 2005). However, with respect to films made from cereal proteins such as zein, their poor mechanical properties and water stability compared to similar materials made from synthetic polymers are major limitations (Lawton, 2002; Reddy et al., 2008).

Protein film functional properties can be modified by physical treatments such as heat (Byaruhanga et al., 2005), γ-irradiation (Soliman, Eldin and Furuta, 2009), chemicals such as aldehydes (Sessa et al., 2007) or enzymes such as transglutaminase (Chambi and Grosso, 2006). Most of these modifications have been done on films with >50 μm thickness. For example, Sessa et al. (2007) worked on 700 to 900 μm thick zein films, Chambi and Grosso (2006) worked on 750 μm thick gelatin and casein films, while Hernández-Muñoz, Kanavouras, Lagaron and Gavara (2005) study was on 55 μm thick gliadin films.

Kafirin, the storage prolamin protein in sorghum, is relatively hydrophobic compared to other cereal proteins such as zein (Duodu et al., 2003; Belton et al., 2006). Thus, kafirin has a potential for use in biomaterials that are stable in water. Research has shown that thin cast kafirin films (<50 μm) produced from kafirin microparticles have some superior functional properties such as better film surface characteristics and lower water vapour permeability, than the conventional cast films from kafirin protein (Taylor et al., 2009c). The objective of this study was to investigate various treatments to improve the water stability and other related functional properties of thin kafirin films. Specifically, the use of heat, transglutaminase and glutaraldehyde treated kafirin microparticles to produce films was explored.

4.2.3 Materials and methods

4.2.3.1 *Materials*

Kafirin was extracted from mixture of two very similar white, tan-plant non-tannin sorghum cultivars PANNAR PEX 202/606, as described (Emmambux and Taylor, 2003). Briefly, whole milled sorghum grain was mixed with 70% (w/w) aqueous ethanol containing 3.5% (w/w) sodium metabisulphite and 5% (w/w) sodium hydroxide and then heated at 70^{o}C for 1 h with vigorous stirring. The clear supernatant was recovered by centrifugation and the ethanol evaporated. Kafirin was precipitated by adjusting the pH of the protein suspension to 5.0. The precipitated kafirin was recovered by vacuum filtration, freeze-drying, defatting with hexane at ambient temperature and air-drying.

4.2.3.2 *Preparation of conventional cast kafirin films*

Conventional kafirin films were prepared by the casting method described by Taylor et al. (2005b) from a 2% (w/w protein basis) kafirin solution in glacial acetic acid, containing 40% (w/w with respect to protein) plasticizer (a 1:1:1 w/w mixture of glycerol: polyethylene glycol 400: lactic acid). It has been shown that this plasticizer combination is effective in kafirin films (Taylor et al., 2009c). Films were dried overnight at 50°C in an oven (not forced draft) on a level surface.

4.2.3.3 *Preparation of kafirin microparticle films*

To prepare kafirin microparticle films, firstly, kafirin microparticles were prepared using acetic acid solvent according to Taylor et al. (2009c) with some modification. Plasticizer (0.66 g) was mixed with glacial acetic acid (4.34 g) and added to kafirin (1.9 g, 84% protein) with gentle stirring until fully dissolved. The kafirin solution was held at ambient temperature (22°C) for 16 h to equilibrate. Then, kafirin microparticles were prepared by adding 73.1 g distilled water to 6.9 g kafirin solution at a rate of 1.4 mL/min using a Watson-Marlow Bredel peristaltic pump (Falmouth, U.K.), while mixing using a magnetic stirrer at 600 rpm at ambient temperature. This suspension contained 2% (w/w) kafirin protein and 5.4% (w/w) (0.9 M) acetic acid.

To cast the films, 4.0 g suspensions of kafirin microparticles were centrifuged at 3150 *g* for 10 min. The clear supernatants were carefully removed and replaced by 25% (w/w) (4.2 M)

acetic acid and then left to equilibrate at ambient temperature for 12 h. Then, 32 mg plasticizer (40% w/w on kafirin protein basis) was added and films cast in the bottom dishes (90 mm diameter) of 100 mm × 15 mm borosilicate glass Petri dishes (Schott Glas, Mainz, Germany) by drying overnight at 50°C in an oven (not forced draught). All the films were assessed visually and photographed using a flatbed scanner.

Preparation of films from heat-treated kafirin microparticles

Kafirin microparticle film preparation suspension (4.0 g), described above, was washed with distilled water three times to remove the acetic acid. Treatment of kafirin microparticles with heat was done by heating the microparticles suspended in water, at 50°C, 75°C and 96°C for 1 h. A control film preparation mixture was maintained at ambient temperature for the same period. Then, supernatants were replaced with 25% acetic acid, plasticizer added and films were cast as described.

Preparation of films from transglutaminase-treated kafirin microparticles

The supernatants in the 4.0 g kafirin microparticle suspensions were removed by centrifugation and washed with distilled water as described above. The supernatants were replaced with 0.1%, 0.3% and 0.6% (w/w) microbial transglutaminase (Activa WM), activity 100 U/g (Ajinomoto Foods Europe, S.A.S., France) (on protein basis) in 0.02 M Tris–HCl buffer (pH 7.0). The buffer had been pre-heated to 50°C prior to dissolving the enzyme. For control films, 25% pure maltodextrin in 0.02 M Tris–HCl buffer, pH 7.0 was used as the transglutaminase enzyme is supplied in a 99% maltodextrin carrier base. Transglutaminase reaction was carried out at 30°C for 12 h. Optimal transglutaminase reaction temperature is 50°C (Ando, Adashi, Umeda, Matsuura, Nonaka, Uchio, Tanaka and Motoki, 1989) but complete films could not be formed when this temperature was used, probably because of heat induced cross-linking of the kafirin proteins. The films were cast as described.

Preparation of films from glutaraldehyde-treated kafirin microparticles

These were prepared by adding 10%, 20% and 30% (w/w) glutaraldehyde (Saarchem, Krugersdorp, South Africa) (as a proportion of protein) to 4.0 g film preparation mixtures in 25% acetic acid (pH 2.0). Reaction with glutaraldehyde was carried out at ambient temperature for 12 h and the films cast as described.

4.2.3.4 *SEM*

The film surfaces were examined using SEM as described (Taylor et al., 2009c). Strips of the films were mounted on an aluminium stub using a double-sided transparent tape, sputter-coated with gold and viewed using a Jeol JSM-840 Scanning Electron Microscope (Tokyo, Japan).

4.2.3.5 *SDS-PAGE*

Films were characterized by SDS-PAGE under reducing and non-reducing conditions. An X Cell SureLock™ Mini-Cell electrophoresis unit (Invitrogen Life Technologies, Carlsbad, CA, USA) was used with 15-well 1 mm thick pre-prepared Invitrogen NuPAGE® 4–12% Bis-Tris gradient gels. The loading was ≈10 µg protein. Invitrogen Mark12™ Unstained Standard was used. Proteins were stained with Coomassie® Brilliant Blue R250 overnight, destained and photographed.

4.2.3.6 *FTIR spectroscopy*

FTIR spectroscopy was performed as described (Taylor et al., 2009c). Briefly, the films were dried for a week in a desiccator. Then small pieces of the films were scanned in a Vertex 70v FT-IR spectrophotometer (Bruker Optik, Ettlingen, Germany), using 64 scans, 8 cm^{-1} band and an interval of 1 cm^{-1} in the Attenuated Total Reflectance (ATR) mode at wavenumber 600–4000 cm^{-1}. At least four replicates were performed for each treatment. The FTIR spectra were Fourier-deconvoluted with a resolution enhancement factor of 2 and a bandwidth of 12 cm^{-1}. The proportions of the α-helical conformations (≈1650 cm^{-1}) and the β-sheet structures (≈1620 cm^{-1}) were calculated by measuring the heights of the peaks assigned to the secondary structures on the FTIR spectra. The relative proportions of the α-helical conformations were calculated as described (section 4.1.3.9).

4.2.3.7 *Water vapour transmission (WVT) and water vapour permeability (WVP)*

These were measured using a modified method based on ASTM E96-97 method (American Society for Testing & Materials, 1997b) as described by Taylor et al. (2005b). Briefly, the thicknesses of the films were measured in five different places using the micrometer gauge (Braive Instruments) and the average calculated after conditioning the films for 72 h in a 50% relative humidity (RH) chamber. Cast films (31 mm diameter) were mounted on top of

modified Schott bottles containing distilled water to a level where the bottle neck had a constant diameter. The bottles with films secured at the top were placed in a forced draught incubator at 29^{o}C with an average RH of 16% over the period of the test. Weight loss was recorded daily for 12 days. Three replicate measurements were performed for each treatment. Graphs of water loss against time were plotted for each treatment and gradients of the best-lines-of-fit recorded. WVT was calculated by dividing the gradient of the line with the area of the film. The WVP was calculated thus:

$$\text{WVP} = \frac{(\text{gradient (g/h)} \times \text{thickness of film (mm)})}{\text{Area (m}^2) \times P_o \text{ (kPa)} \times (RH_1\text{-}RH_2)/100}$$

Where:

P_o = saturated vapour pressure at 25^{o}C = 3.17 kPa

RH_1 = Relative humidity inside the bottle (i.e. 100%)

RH_2 = Relative humidity outside the bottle

4.2.3.8 *Water stability*

Complete conventional cast kafirin films and kafirin microparticle films were immersed in water (22^{o}C) containing 0.02% (w/v) sodium azide in separate transparent plastic containers then mounted on an orbital shaker set at a gentle speed of 70 rpm and monitored over a period of 48 h. To determine the extent to which the films would maintain their physical integrity in water under vigorous shaking, complete films were immersed in distilled water containing sodium azide at 22°C, and then mounted on an orbital shaker set at speed of 300 rpm for 72 h. At the end of the shaking period, the films were visually assessed and photographed using a flatbed scanner in the plastic containers.

4.2.3.9 *Water uptake and weight loss of films in water*

These were measured according to Soliman et al. (2009) with some modification. Films (90 mm diameter) were dried in a desiccator for 72 h and then weighed. The dried films were immersed in distilled water for 24 h at 22^{o}C with gentle agitation on a rocking platform set at 30 rpm. The water on the film surfaces was removed by placing the films between paper towels and then weighed. The films were then dried in a desiccator as before and weighed again. The film water uptake and weight loss in water were calculated thus:

$$\% \text{ Water uptake} = \frac{(\text{Mass after immersion} - \text{Initial dry mass})}{\text{Initial dry mass}} \times 100$$

$$\% \text{ Weight loss in water} = \frac{(\text{Initial dry mass} - \text{Mass after immersion and drying})}{\text{Mass after immersion and drying}} \times 100$$

4.2.3.10 *Surface density*

Film surface density was measured based on the procedure of Soliman et al. (2009). Films (90 mm diameter) were weighed. The weight of each film was divided by its area to calculate the surface density (mg/cm^2).

4.2.3.11 *Tensile properties*

The films were conditioned at 50% relative humidity and 25°C for 72 h in a desiccator maintained using 4.99 M calcium chloride (Stokes and Robinson, 1949). Then the film strips 60 mm x 10 mm were cut. The thicknesses of the films were measured in five different places using a micrometer gauge (Braive Instruments, Hermalle-sous-Argenteau, Belgium) and the average calculated. Tensile properties of the films were studied as described (Taylor et al., 2005b), based on ASTM D882–97 method (American Society for Testing and Materials (ASTM), 1997a), using a TA-XT2 Texture Analyser (Stable Micro Systems, Goldalming, U.K.). For soaked films, the films were air-dried at ambient temperature for 30 min before measuring tensile properties.

4.2.3.12 *IVPD*

This was performed by a pepsin digestion procedure based on that of Hamaker et al. (1986). Prior to IVPD assay, the films were freeze-fractured in liquid nitrogen and ground into powder using a mortar and pestle. Accurately weighed film powder (10 mg) was digested with a P7000-100G pepsin (Sigma, Johannesburg, South Africa), activity 863 units/mg protein for 2 h at 37^{o}C and the products of the digestion were pippeted off. The residue was washed with distilled water and dried at 100^{o}C overnight. The residual protein was determined by Dumas nitrogen combustion method (AACC International, 2000) method 46-30. IVPD was calculated by the difference between the total protein and the residual protein after pepsin digestion divided by the total protein and expressed as a percentage.

4.2.3.13 *Statistical analyses*

All the experiments were repeated at least twice. The film FTIR, thickness, water vapour WVT, WVP, tensile properties, water uptake, weight loss in water, IVPD data were analysed by one-way analysis of variance (ANOVA). These measured parameters were the dependent variables while and heat, transglutaminase and glutaraldehyde treatments were the independent variables. Significant differences among the means were determined by Fischer's least significant difference (LSD) test. The calculations were performed using Statistica software version 10 (StatSoft, Tulsa, OK).

4.2.4 Results and discussion

4.2.4.1 *Water stability of conventional cast kafirin films and cast kafirin microparticle films*

Conventional cast kafirin films disintegrated into many small fragments in water, while the cast kafirin microparticle films remained largely intact (Figure 4.13). The better stability of kafirin microparticle films in water was probably due to changes in kafirin protein secondary structure during microparticle preparation. During the formation of kafirin microparticles, there is a reduction in the proportion of protein α-helical conformation, probably with corresponding increase in β-sheet conformation (Taylor et al., 2009a). Subirade, Kelly, Guéguen and Pézolet (1998) suggested that β-sheet conformation may be essential for protein-protein interactions and network formation in protein films from plant origins, whereby intermolecular H-bonding between β-sheets probably act as junction zones that stabilize the film network. Additionally, the characteristic presence of large voids within the kafirin microparticles, when prepared by coacervation (Taylor et al., 2009a) enhances protein solubility in the casting solution, probably thereby improving the film matrix cohesion. Because of the better water stability of cast kafirin films prepared from microparticles they were investigated further using various treatments: heat, transglutaminase and glutaraldehyde, to enhance this and other related film functional properties

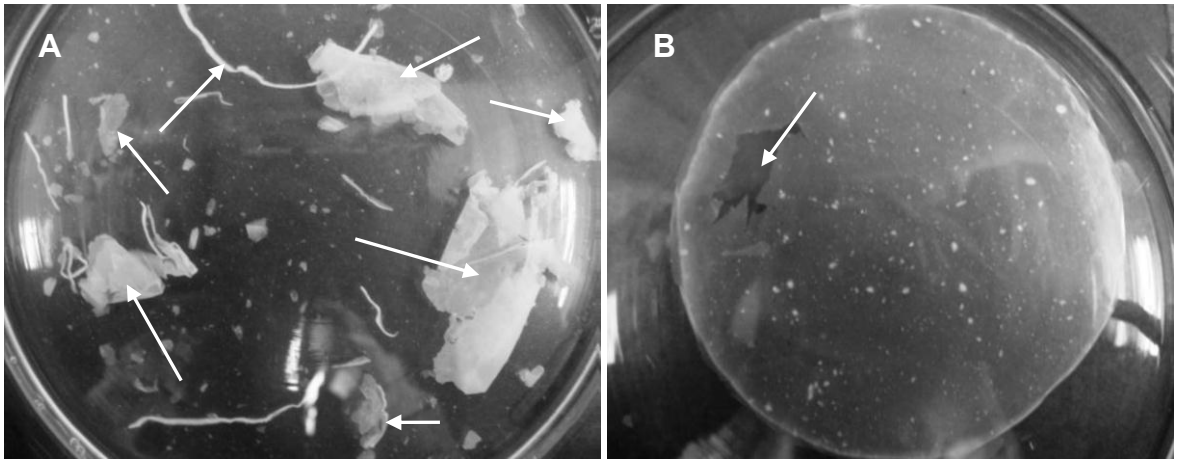

Figure 4.13 Appearance of kafirin films cast in acetic acid, after immersion in water for 48 h at room temperature with gentle shaking (70 rpm). Films photographed in transparent plastic tubs while immersed in water. **A**. Conventional kafirin film. Arrows point to film fragments. **B.** Kafirin microparticle film. Arrow points to torn section of film. (Pictures taken by Miss Amy J. Taylor on behalf of the candidate).

4.2.4.2 *Film physical appearance*

Treating kafirin microparticles with heat at moderate temperature (50^{o}C) did not change the clarity of the films made from them (Figure 4.14A- b). However, when viewed by SEM the film surfaces were rough (Figure 4.14A- f). Higher temperature treatment (75^{o}C and 96^{o}C) resulted in the formation of opaque and incomplete films (arrows, Figure 4.14A- c, d). These films had a rough surface and the microparticles were poorly fused. The outline of individual microparticle shapes was clearly visible with gaps in between them (arrows, Figure 4.14A-g, h), which was similar to the appearance of biomaterials made from zein microparticles such as films (Dong et al., 2004) and sponges (Wang et al., 2008). Byaruhanga et al. (2005) working on cast films prepared from microwave-heated kafirin reported formation of films with rough surface and, attributed this to undissolved lumps of kafirin. Likewise, in the present study the poor fusion of the heated kafirin microparticles was probably due to reduction in their solubility in the aqueous acetic acid casting solution. Hamaker et al. (1986) suggested that the reduction in solubility of kafirin proteins as a result of thermal treatment is probably due to disulphide cross-linking of kafirin proteins.

In contrast, transglutaminase-treated kafirin microparticle films were as clear as their control (Figure 4.14B, i–l). However, these films had a rough surface when viewed by SEM (Figure 4.14B, m–p), indicating poor fusion of the microparticles.

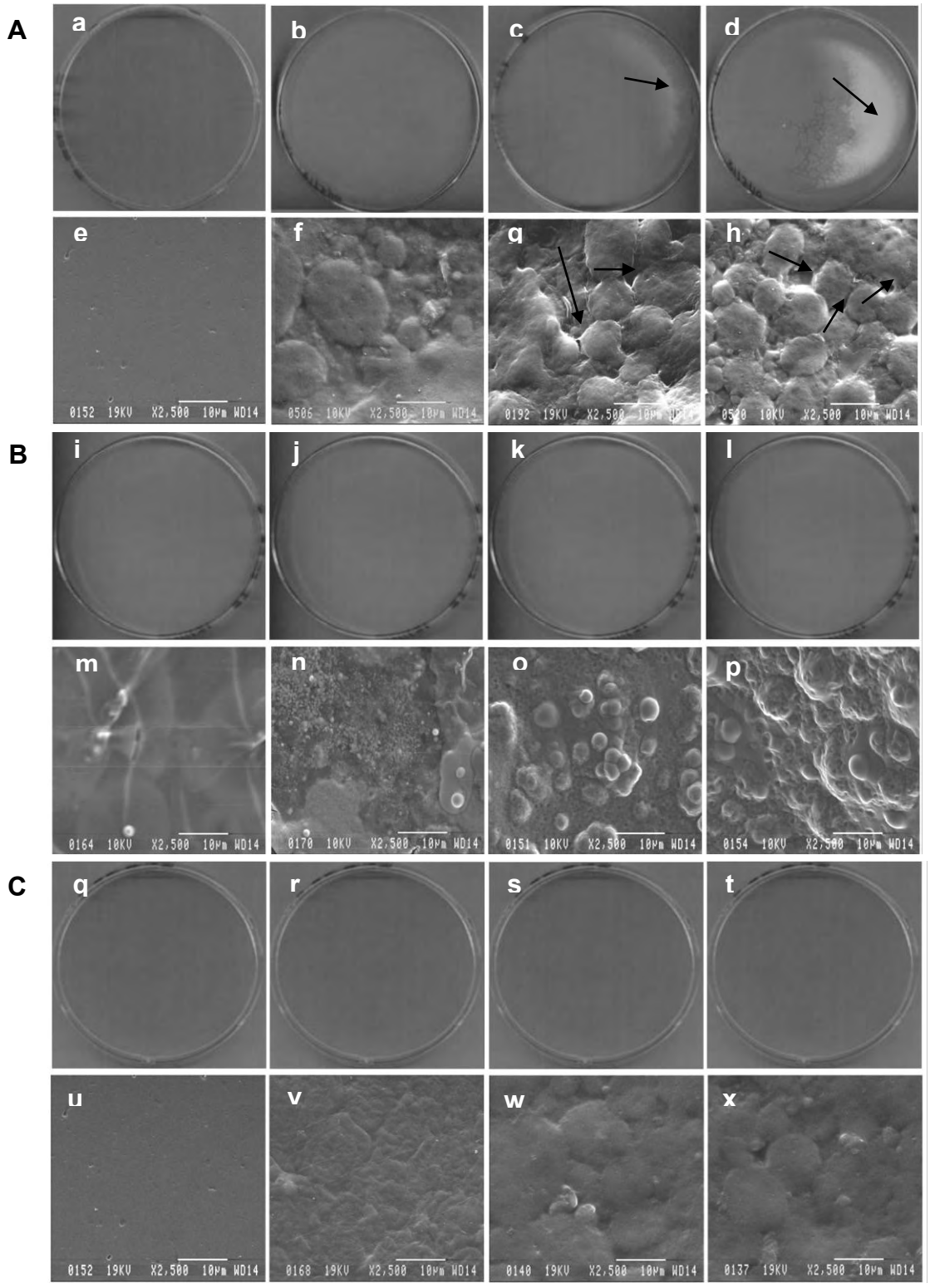

Figure 4.14 Physical appearance of films prepared from treated kafirin microparticles. **A.** Heat treatment. a-d: photographs, e-h: SEM. **a, e** - control; **b, f** - 50°C; **c, g** - 75°C; **d, h** - 96°C. Arrows: **c, d**- opaque incomplete sections; **g, h** –gaps. **B.** Transglutaminase (TG) treatment. i-l: photographs; m-p: SEM. **i, m** - Maltodextrin; **j, n** - 0.1% TG + Maltodextrin; **k, o** - 0.3% + Maltodextrin; **l, p** - 0.6% TG + Maltodextrin. **C.** Glutaraldehyde treatment. q-t: photographs, u-x: SEM. **q, u** - control; **r, v** - 10%; **s, w** - 20%; **t, x** - 30%.

Tang, Jiang, Wen, Yang (2005) also reported a rough and uneven surface of films prepared from transglutaminase-treated SPI. In the present study, Maillard reaction due to the presence of maltodextrin may have caused poor solubility of the microparticles, thereby resulting in the uneven film surface.

Treating kafirin microparticles with glutaraldehyde did not change the clarity of the films, irrespective of the concentration of glutaraldehyde (Figure 4.14C, q–t). However, these glutaraldehyde-treated kafirin microparticle films were slightly rough (Figure 4.14C, v–x), probably due to reduction in solubility of the kafirin microparticles as a result of glutaraldehyde cross-linking of the kafirin proteins. Notwithstanding this, the glutaraldehyde-treated kafirin microparticles were clearly better fused than the heat-treated and transglutaminase-treated microparticles.

4.2.4.3 *Film chemical structure*

SDS-PAGE under non-reducing and reducing conditions of films prepared from heat-treated kafirin microparticles and untreated control had highest band intensity at 16–28 kDa (Figure 4.15A), which are the monomeric α-, β- and γ- kafirins (Shull et al., 1991). In addition, bands of approximately 42–58 kDa and 61–88 kDa, identified as dimers and trimers, respectively (El Nour et al., 1998), were present in all the films, indicative of kafirin polymerization. Treating kafirin microparticles with heat did not result in any change in band pattern with SDS-PAGE under non-reducing conditions. This was probably because despite the differences in heat treatment temperatures, all the film-forming mixtures were subjected to 50^{o}C for a long time (12 h) during evaporation to prepare the films. With heat treatment at 96^{o}C some oligomers (≈94–183 kDa) (arrow in Figure 4.15A, lane 4 under reducing conditions) resistant to reduction by mercaptoethanol remained. These may be attributed to concealed covalent cross-links induced by heat that are inaccessible to the reducing agent, as suggested by Duodu et al. (2003).

Despite changes in the physical appearance of films, there was no evidence of transglutaminase-induced kafirin polymerization (Figure 4.15B). This was probably because kafirin has very low lysine content (Belton et al., 2006), which renders it a poor substrate for the transglutaminase reaction that produces ε-(γ-glutamyl)-lysine bridges. For a lysine-poor protein, the transglutaminase-catalysed protein reaction may progress through deamidation, an alternative reaction pathway (Larré, Chiarello, Blanloeil, Chenu and Gueguen, 1993).

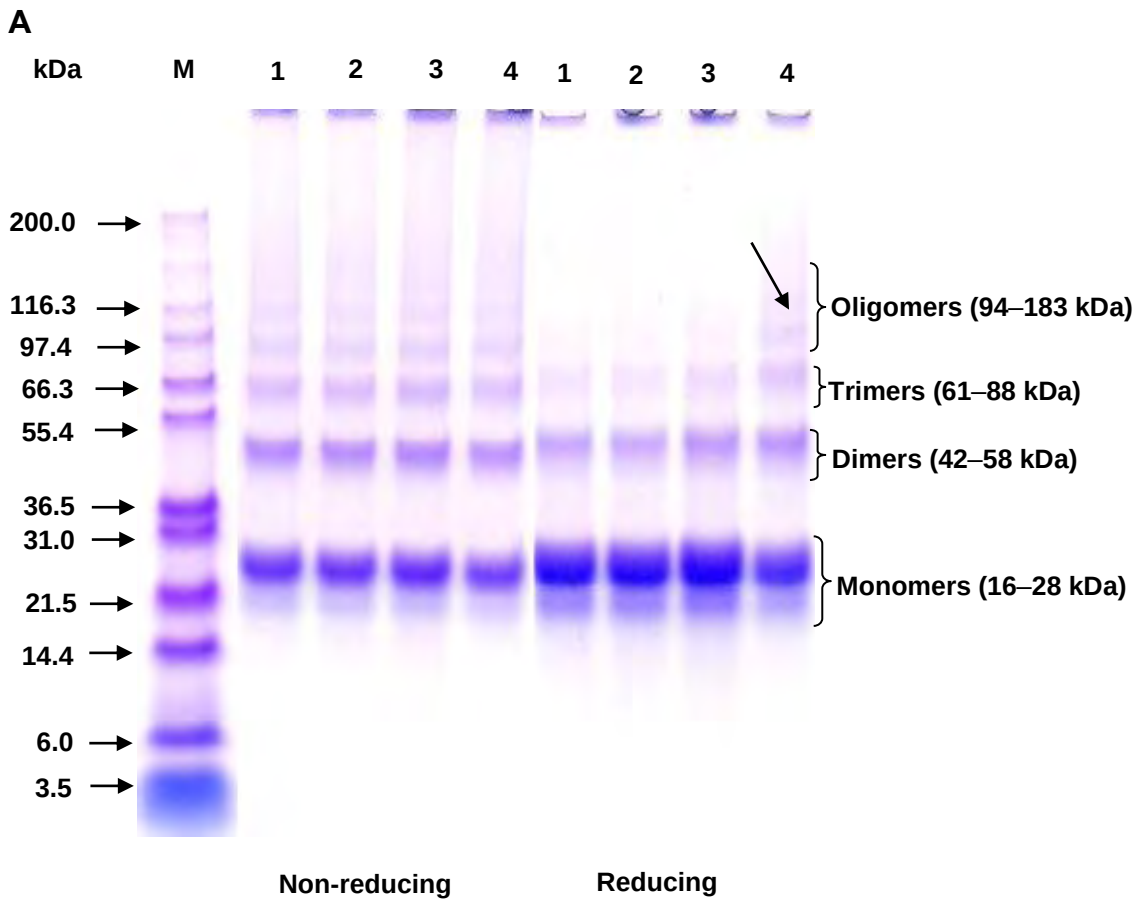

Figure 4.15 SDS-PAGE of films prepared from treated kafirin microparticles. Protein loading, 10 µg.

A. Heat treatment. Lanes M: Molecular markers; 1: Control (22ºC); 2: 50ºC; 3: 75ºC; 4: 96ºC. Arrow: reduction-resistant oligomers.

B. Transglutaminase (TG) treatment. Lanes M: Molecular markers; 1: Maltodextrin; 2: 0.1% TG + Maltodextrin; 3: 0.3% TG + Maltodextrin; 4: 0.6% TG + Maltodextrin.

C. Glutaraldehyde treatment. Lanes M: Molecular markers; 1: Control; 2: 10%; 3: 20%; 4: 30%.

B

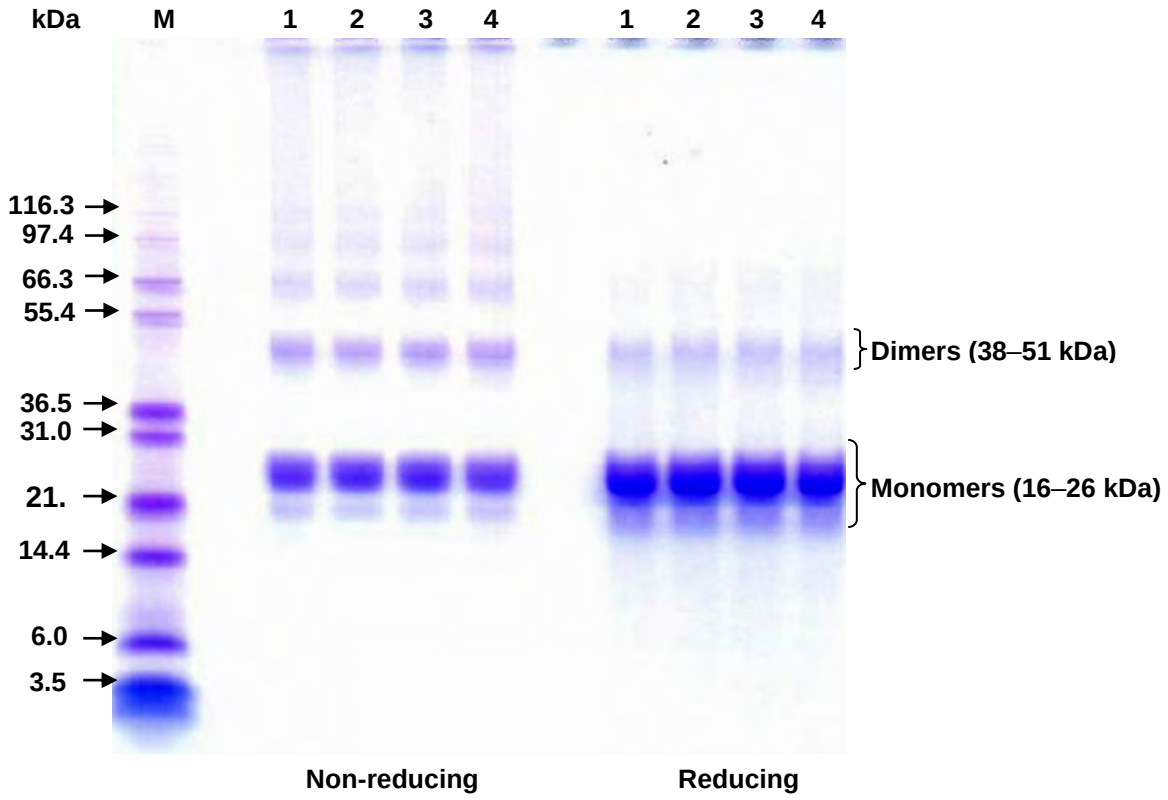
kDa
M
1
2
3
4
1
2
3
4
116.3
97.4
66.3
55.4
36.5
31.0
21.
14.4
6.0
3.5
Dimers (38–51 kDa)
Monomers (16–26 kDa)
Non-reducing
Reducing

C

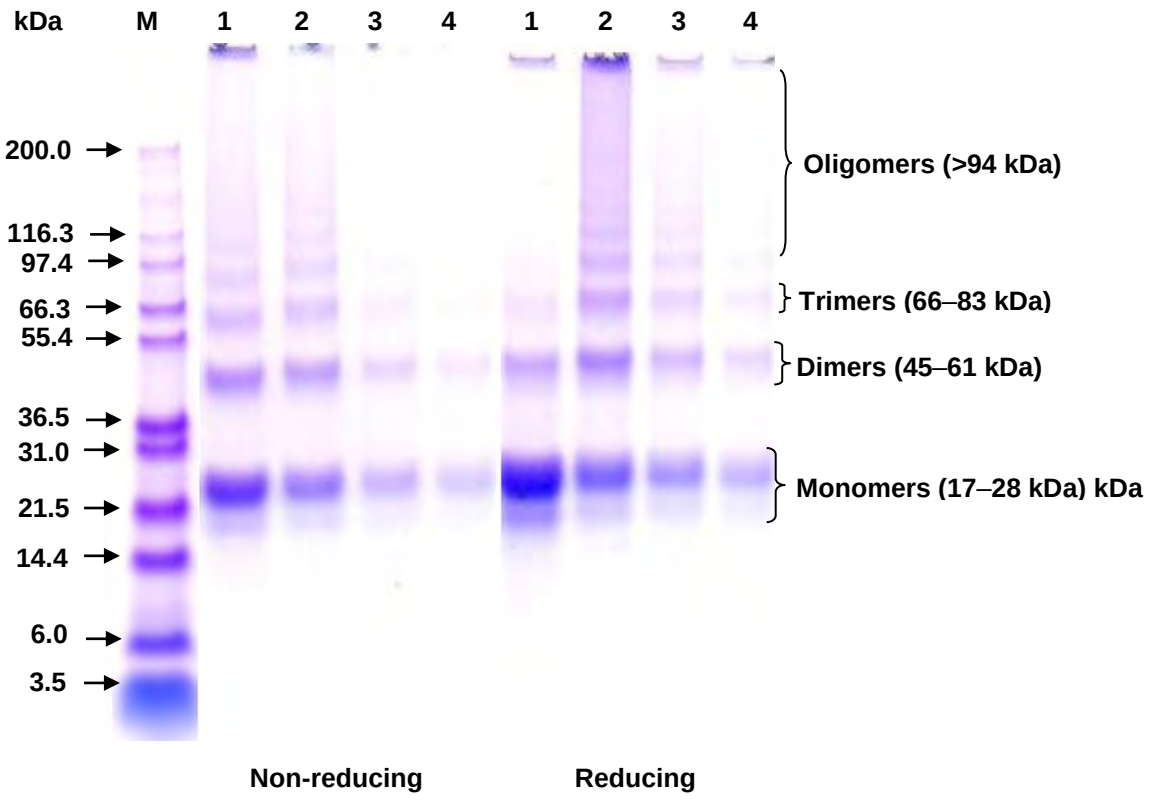
kDa
M
1
2
3
4
1
2
3
4
200.0
116.3
97.4
66.3
55.4
36.5
31.0
21.5
14.4
6.0
3.5
Oligomers (>94 kDa)
Trimers (66–83 kDa)
Dimers (45–61 kDa)
Monomers (17–28 kDa) kDa
Non-reducing
Reducing

The results in the present study are consistent with those of Motoki, Seguro, Nio and Takinami (1986) working on glutamine-specific deamidation of α_{s1}-casein by transglutaminase, who found no changes in molecular weights. Similarly, Flores, Cabra, Quirasco, Farres and Galvez (2010) working on maize protein isolate emulsions found a similar electrophoretic band pattern for deamidated and non-deamidated emulsions, despite their difference in emulsion stability. The fact that films prepared from transglutaminase-treated kafirin microparticles were rough (Figure 4.14B, n–p) may be attributed to an increase in negative charges in the kafirin due to deamidation, probably making the microparticles less soluble in the acetic acid casting solution.

Glutaraldehyde treatment of the kafirin microparticles resulted in the reduction in monomer (17–28 kDa), dimer (45–61 kDa), trimer (66–83 kDa) and oligomer (>94 kDa) band intensities with the SDS-PAGE under non-reducing conditions (Figure 4.15C). With SDS-PAGE under reducing conditions, there was an increase in intensities of dimer, trimer and oligomer bands for 10% glutaraldehyde treatment (Figure 4.15C, lane 2), indicating the presence of polymerized kafirin proteins. The presence of polymerized kafirin under reducing conditions was expected as cross-links with glutaraldehyde are formed between free amino groups of peptide chains and the carbonyl groups of the aldehyde (Migneault et al., 2004) and not disulphide linkages. Similar protein polymerization through non-disulphide bonding was reported by Sessa, Mohamed and Byars (2008) working on zein films treated with glutaraldehyde. Treatments with higher glutaraldehyde concentrations (20% and 30%) resulted in the monomer, dimer and trimer bands being much fainter and an almost complete absence of oligomer bands. These observations indicate the formation of highly polymerized kafirin polymers of MW > 200 kDa at higher glutaraldehyde concentrations, which were too large to migrate into the separating gel. A similar result was reported by Reddy et al. (2008) who found disappearance of molecular weight bands, when they cross-linked pre-formed wheat gluten fibres with high concentration of glutaraldehyde.

With regard to protein secondary structure, treating the kafirin microparticles with heat decreased the relative proportion of α-helical conformation in the films by up to 11%, at the Amide I band (wavenumber ≈1650–1620 cm^{-1}) (Table 4.4), as determined by FTIR. There was a decrease in the relative proportion of α-helical conformation with increase in heating temperature. Byaruhanga et al. (2006) reported a similar decrease in proportion of α-helical conformation with concomitant increase in β-sheet conformation when they heated kafirin

and kafirin film with microwave energy. Similarly, Emmambux and Taylor (2009) reported a reduction in α-helical conformation when they studied the protein secondary structure of cooked kafirin. It has been suggested that during thermal treatment the hydrogen bonds stabilizing protein structure are disrupted, causing loss of the α-helical and β-sheet conformation and creating new β-sheet arrangements (Duodu et al., 2001). Loss of α-helical conformation can be indicative of protein aggregation (Mizutani et al., 2003). In the present study, the relative proportion of α-helical conformation in the Amide I band for control films was 53.9%. Taylor et al. (2009c) reported a lower percentage (50.5%) for similar kafirin microparticle films. These differences can be attributed to the kafirin batch variations. Such differences have been reported previously by Taylor et al. (2009a), when they compared the proportion of α-helical conformation in their study with the data by Gao et al. (2005) on kafirin extracted and dried under similar conditions.

Table 4.4 Effects of treating kafirin microparticles with heat, transglutaminase and glutaraldehyde on the protein secondary structure of films prepared from them, as determined by FTIR

Treatment		Relative proportion of α-helical conformation at Amide I band (%)
Control	22ºC	53.9 e (0.1)
Heat		
	50ºC	52.2 d (0.9)
	75ºC	50.7 c (0.1)
	96ºC	48.0 a (0.6)
Transglutaminase		
	Maltodextrin	50.8 c (0.7)
	0.1% TG + Maltodextrin	50.4 c (0.4)
	0.3% TG + Maltodextrin	49.3 b (0.3)
	0.6% TG + Maltodextrin	48.5 a (0.5)
Glutaraldehyde		
	10%	50.6 c (0.5)
	20%	51.0 c (0.9)
	30%	52.2 d (0.3)

Values followed by different superscript letters are significantly different ($p<0.05$). Numbers in the parentheses are standard deviations (n=4). Control for heat and glutaraldehyde treatments is the same. Amide I band (≈1650–1620 cm^{-1}). TG- Transglutaminase

Transglutaminase treatment of kafirin microparticles resulted in up to 5% reduction in the relative proportion of α-helical conformation with respect to control films with maltodextrin treatment. As with heat treatment, there was a progressive decrease in the relative proportion of α-helical conformation with increase in concentration of transglutaminase. This was probably due to transglutaminase-induced deamidation of kafirin proteins, as discussed. In a similar study using proteins from soymilk residue, Chan and Ma (1999) also found a reduction in the α-helical conformation with acid-induced deamidation. Similarly, working on gluten, Matsudomi, Kato and Kobayashi (1982) reported a decrease in α-helical conformation with increase in deamidation. Wagner and Gueguen (1995) proposed that a reduction in proportion of α-helical conformation as a result of deamidation may be caused mainly by the increased electrostatic repulsion and the decreased hydrogen bonding.

In contrast to the trend with heat and transglutaminase treatments, there was a progressive increase in the relative proportion of α-helical conformation with increase in glutaraldehyde concentration. Selling, Woods, Sessa and Biswas (2008) reported a similar increase in α-helical conformation of zein fibres treated with glutaraldehyde. As with transglutaminase treatment, the changes in the protein secondary structure due to treatment with glutaraldehyde were generally small compared to heat treatment. This is consistent with findings by Caillard et al. (2009) on soy protein hydrogels cross-linked using glutaraldehyde, which showed changes in gel physical appearance and functional properties that were not reflected to the same extent by alterations in the protein secondary structure.

4.2.4.4 *Film functional properties*

Film WVT and WVP

Heat treatment resulted in films 20–29% thicker than their control (Table 4.5). However, these films were still thinner than those reported in similar studies. For example, the films reported by Sessa et al. (2007) were about 30 times in thickness compared to the kafirin microparticle films in the present study. The WVT of the films prepared from all the treated kafirin microparticles was generally similar to that of the control. The WVT values were within the range reported for unmodified kafirin microparticle films (Taylor et al., 2009c) and whey proteins films (Kaya and Kaya, 2000). Treating kafirin microparticles with heat resulted in films that were 20–29% thicker than their control.

Table 4.5 Effects of treating kafirin microparticles with heat, transglutaminase glutaraldehyde on the thickness, water vapour transmission (WVT) and water vapour permeability (WVP) of films

Treatment		Thickness (μm)	WVT ($g\ h^{-1}\ m^{-2}$)	WVP ($g\ mm\ m^{-2}\ h^{-1}\ kPa^{-1}$)
Control	22°C	16.3 ab (1.0)	33.0 a (3.2)	0.17 a (0.01)
Heat				
	50°C	20.3 c (0.9)	34.9 ab (1.3)	0.22 b (0.01)
	75°C	19.6 bc (0.3)	38.4 b (0.8)	0.24 b (0.00)
	96°C	21.0 c (0.4)	34.5 ab (2.9)	0.23 b (0.02)
Transglutaminase				
	Maltodextrin	22.7 cd (3.3)	34.0 ab (3.9)	0.24 b (0.01)
	0.1% TG + Maltodextrin	25.3 de (0.3)	37.9 b (1.6)	0.30 c (0.01)
	0.3% TG + Maltodextrin	28.0 e (1.1)	34.5 ab (0.0)	0.30 c (0.01)
	0.6% TG + Maltodextrin	26.5 e (0.6)	34.5 ab (0.1)	0.29 c (0.01)
Glutaraldehyde				
	10%	16.3 ab (2.4)	31.5 a (1.3)	0.16 a (0.03)
	20%	15.8 a (1.7)	33.0 a (3.2)	0.16 a (0.01)
	30%	16.1 ab (3.6)	33.0 a (1.3)	0.17 a (0.03)

Values in the same column but with different letters are significantly different ($p<0.05$). Numbers in parentheses are standard deviations (n=3). Control for heat and glutaraldehyde treatments is the same. TG- Transglutaminase

These differences in thickness were reflected by the roughness of the film surfaces noted using SEM (Figure 4.14). The WVP of the heat-treated kafirin microparticle films was higher by 29–41% compared to the control, probably because these films were thicker, therefore they probably had more pinholes. A linear increase in WVP with film thickness has been reported by Park and Chinnan (1995), which may be attributed to changes in film structure due to thickness as well as swelling of hydrophobic films, which may alter their structure too. Similar results were reported by Taylor et al. (2009c) who found that thicker kafirin films had higher WVP than thinner kafirin microparticle films. In addition, the fact that the heat treatment resulted in gaps especially at higher temperature (Figure 4.14A- g, h) may have led to increase in WVP.

As with heat treatment, treating the kafirin microparticles with transglutaminase increased the thickness of the films, probably because the films were rough as result of the poor fusion of the microparticles with transglutaminase. The WVP of the films increased by 11–23% as a result of transglutaminase treatment. As with the heat treatment, the poor fusion of the

transglutaminase-treated kafirin microparticles may have resulted in the increase in film WVP. When compared to the other treatments, the WVP for films prepared from transglutaminase-treated kafirin microparticles were 25–88% higher. This is probably because the suggested excess negative charges resulting from transglutaminase-induced deamidation of kafirin may have caused electrostatic repulsion within the film matrix leading to greater interstitial spacing than with the other treatments, thereby resulting in higher WVP.

Glutaraldehyde treatment did not change the thickness or the WVP of the films, despite the fact that the films were rougher than the control as observed by SEM (Figure 4.14). Micard, Belamri, Morel and Guilbert (2000) also found no change in the WVP of gluten films treated with formaldehyde. In the present study, formation of additional non-disulphide covalent cross-links as result of the treatment with the glutaraldehyde may be a reason for the similarity in WVP. Chambi and Grosso (2006) proposed that bonding at molecular level, which stabilizes the protein network, could compensate for morphological differences in influencing the film functional properties.

Film water stability, water uptake and weight loss in water

Treating the kafirin microparticles with transglutaminase resulted in poor water stability of the kafirin microparticle films (Figure 4.16A), probably due to the poor fusion of the kafirin microparticles (Figure 4.14B). In addition, the poor water stability of the films prepared from transglutaminase-treated kafirin microparticles was also probably due to transglutaminase-induced deamidation. In contrast, treating kafirin microparticles with glutaraldehyde resulted in films that were resistant to disintegration in water (Figure 4.16B). SEM of the films after soaking in water for 72 h with vigorous agitation (Figure 4.17) showed the presence of fewer holes (arrows in Figure 4.17) in the films prepared from glutaraldehyde-treated kafirin microparticles, indicating that less physical damage occurred. There was an increase in film stability in water with increasing glutaraldehyde concentration. Increase in water stability has been reported when glutaraldehyde is used to modify a number of similar protein biomaterials such as zein films (Sessa et al., 2007), gliadin films (Hernández-Muñoz et al., 2005), zein fibres (Selling et al., 2008) and gluten fibres (Reddy et al., 2008).

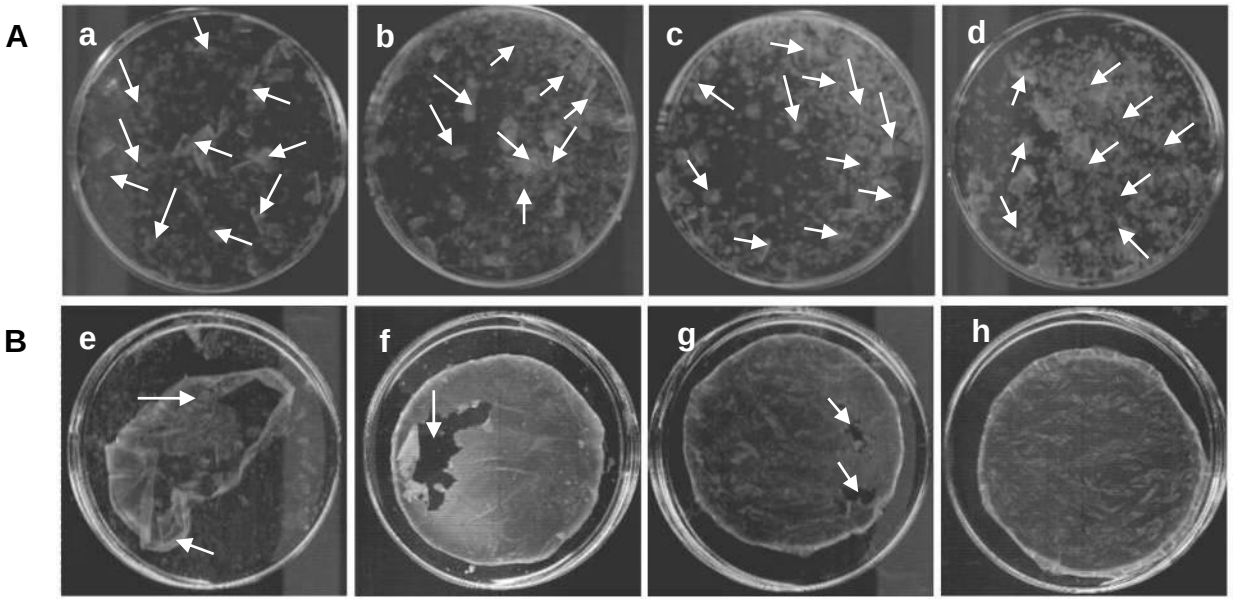

Figure 4.16 Water stability of films prepared from treated kafirin microparticles. The films were photographed in Petri dishes in water: **A.** Transglutaminase (TG) treatment (a–d). **a**: Maltodextrin; **b**: 0.1% TG + Maltodextrin; **c**: 0.3% TG + Maltodextrin; **d**: 0.6% TG + Maltodextrin. Arrows: film fragments. **B.** Glutaraldehyde treatment (e–h). **e**: Control; f: 10%; **g**: 20%; **h**: 30%; Arrows- **e**: fragmented film; **f, g**: disintegrated section of film. Heat treatment resulted in incomplete films hence no data was obtained as complete films were required for a meaningful comparison.

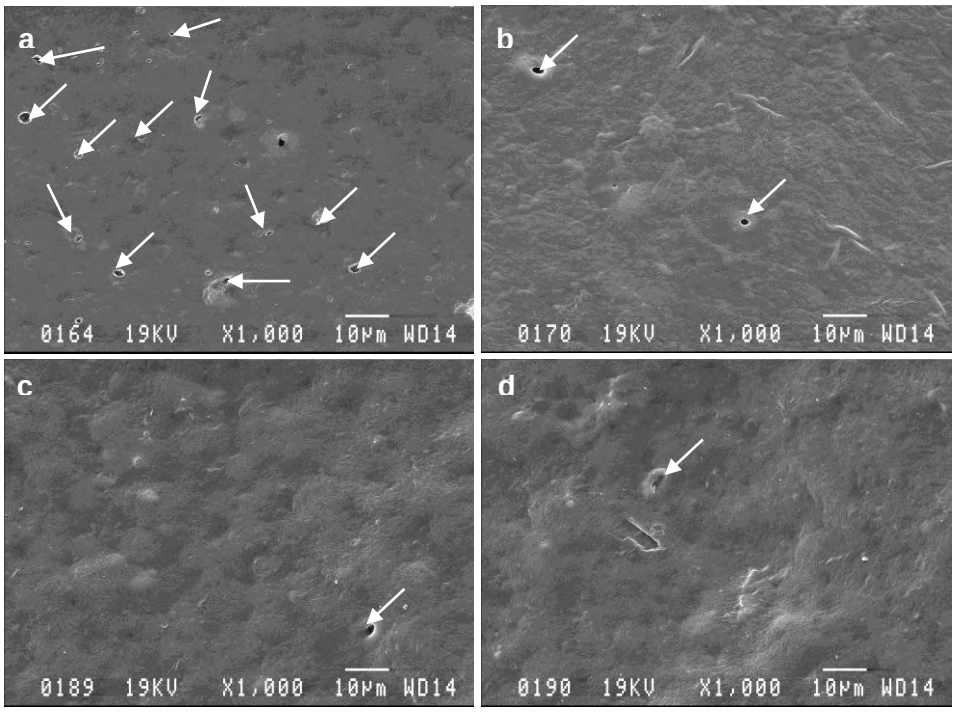

Figure 4.17 SEM of kafirin microparticle films after vigorous agitation in water for 72 h at 22^{o}C: **a**: Control; **b**: 10% GTA; **c**: 20% GTA; **d**: 30% GTA. Arrows point to the holes probably caused by physical damage by water agitation. GTA- Glutaraldehyde.

An interesting finding in the present study was that the glutaraldehyde-treated microparticle films maintained their integrity in water. This was despite the fact that they were several magnitudes thinner than the biomaterials reported in these previous studies. Glutaraldehyde treatment resulted in reduction of both film water uptake and film weight loss in water (Table 4.6). Similar reductions in film water uptake and weight loss in water as result of glutaraldehyde treatment has been reported by Orliac, Rouilly, Silvestre and Rigal (2002) working on sunflower protein isolate films. Likewise, glutaraldehyde treatment has been shown to cause reductions in weight loss in water with gliadin films (Hernández-Muñoz et al., 2005). As kafirin is a relatively hydrophobic protein (Duodu et al., 2003), the weight loss in water of the kafirin microparticle films was mainly due to loss of plasticizer through diffusion into the water. This is consistent with the fact that the film weight loss in water was equivalent to 88–95% of the plasticizer content. It has been shown that protein film weight loss in water corresponds to hydrophilic plasticizer content (Hernández-Muñoz et al., 2005). The reduction in film water uptake or weight loss in water as a result of glutaraldehyde treatment is probably due to the covalent bonding leading to the formation of a more stable cross-linked network resistant to water. Reddy et al. (2008) proposed two reasons for improvement in film water stability after treatment with glutaraldehyde. First, treatment with glutaraldehyde may result in fewer hydrophilic groups. This is because there is preferential reaction of the aldehydes with the free amino groups of the basic amino acids, which are the primary water-bonding sites on proteins. Second, the formation of higher molecular weight proteins by glutaraldehyde treatment may result in better water resistance. This latter explanation concurs with SDS-PAGE findings (Figure 4.15C), which showed presence of polymerized proteins in glutaraldehyde-treated kafirin microparticle films.

Table 4.6 Effects of glutaraldehyde treatment on the water uptake and weight loss in water of kafirin microparticle films

Glutaraldehyde treatment	Water Uptake of film (g/100 g dry film)	Film Weight Loss in water (g/100 g dry film)
Control	29.2 c (0.4)	31.8 b (0.6)
10%	27.0 b (1.2)	29.9 a (0.9)
20%	26.0 b (0.9)	29.3 a (0.4)
30%	23.4 a (1.4)	29.1 a (0.3)

Values in the same column but with different letters are significantly different ($p<0.05$). Numbers in parentheses are standard deviations (n=3).

As shown (Figure 4.14A), treating kafirin microparticles with heat resulted in formation of incomplete films, especially when subjected to higher temperature treatments. Therefore, no data was obtained from water resistance tests for heat cross-linked films, as complete films were required for a meaningful comparison. In addition, as transglutaminase treatment resulted in poor water stability of the films (Figure 4.16A), the determination of water uptake and weight loss in water was not feasible for these films.

Film tensile properties before and after soaking

There was a progressive reduction in maximum stress with increase in treatment temperature (Figure 4.18A; Table 4.7). The reduction in film maximum stress was probably because, as noted by SEM (Figure 4.14A), these films had poorly fused microparticles, indicating poor structural cohesion of film matrix. Similarly, transglutaminase treatment resulted in a 24-53% reduction in film maximum stress, with respect to control films with maltodextrin treatment (Figure 4.18B, Table 4.7). As with heat treatment, the poor fusion of the microparticles due to treatment with transglutaminase (Figure 4.14B) could probably be a reason for weakness of these films. In addition, transglutaminase induced deamidation may have been a contributing factor.

Surface density was determined for glutaraldehyde-treated kafirin microparticle films, as they showed evidence of stability in water. Glutaraldehyde treatment slightly increased the film surface density, while it resulted in varied effects on film tensile strength, depending on concentration of glutaraldehyde (Table 4.7; Figure 4.18C). With 10% glutaraldehyde treatment, there was a 43% increase in film maximum tensile stress, and 58% increase in maximum strain. However, at higher glutaraldehyde concentration (20% and 30%), there was a 42–43% reduction in film breaking stress. This was accompanied by about four-fold increase in maximum strain. Increase in the film maximum stress as a result of glutaraldehyde treatment is presumably due to formation of additional cross-links, as discussed. Similar increases in protein film tensile strength have been reported when glutaraldehyde is used to cross-link many proteins, such as gliadin (Hernández-Muñoz et al., 2005), zein (Parris and Coffin, 1997; Sessa et al., 2007) and sunflower protein isolate (Orliac et al., 2002). On the other hand, the fact that there was a reduction in maximum stress accompanied by increase in maximum strain at higher glutaraldehyde concentration was probably due to a plasticizing effect of excess glutaraldehyde molecules in the protein network.

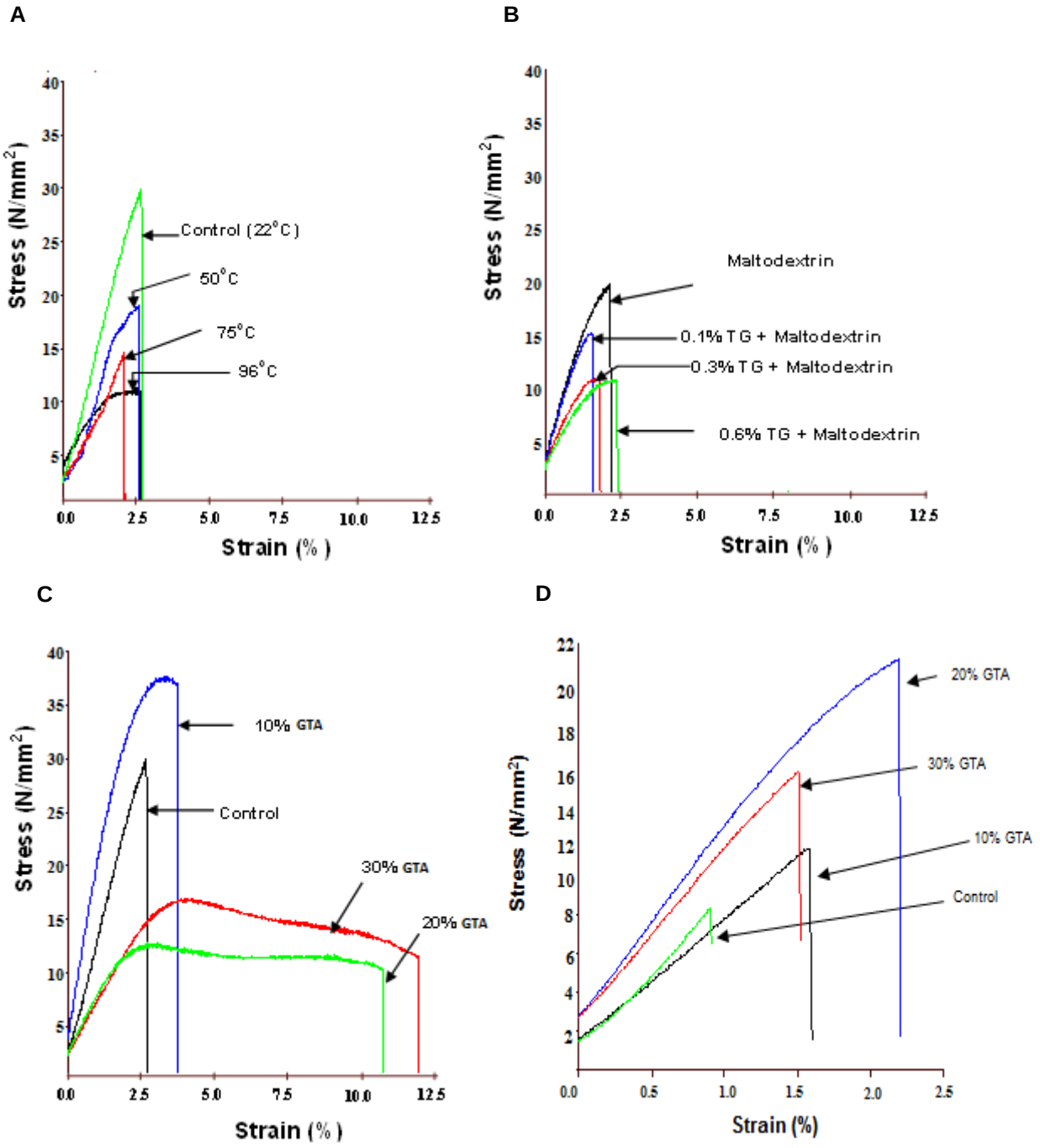

Figure 4.18 Typical stress-strain curves of films prepared from treated kafirin microparticles determined by a TA-XT2 Texture Analyser. **A**. Heat treatment. **B**. Transglutaminase (TG) treatment. **C.** Glutaraldehyde (GTA) treatment. **D**. Effect of glutaraldehyde treatment on tensile properties of kafirin microparticle films after soaking in water.

Table 4.7 Effects of treating kafirin microparticles with heat, transglutaminase and glutaraldehyde on the surface density, tensile properties and *in vitro* protein digestibility (IVPD) of films made from them

Treatment		Surface Density (mg/cm^2)	Maximum Stress (N/mm^2)	Maximum Strain (%)	IVPD (%)	IVPD* (Percentage of control)
	Before soaking in water					
Control	22°C	3.42 a (0.01)	24.3 e (5.2)	2.6 a (0.2)	37.7 e (0.8)	
Heat						
	50°C		18.6 cd (0.7)	3.5 ab (1.1)	37.1 e (0.3)	98.4
	75°C		13.5 ab (0.5)	2.6 ab (0.6)	36.6 de (0.2)	97.1
	96°C		10.7 a (1.4)	3.0 ab (0.4)	35.0 cd (0.8)	92.8
Transglutaminase						
	Maltodextrin		19.7 d (1.1)	2.5 a (0.5)	34.0 bc (0.6)	90.2
	0.1% TG + Maltodextrin		15.0 bc (0.5)	2.1 a (0.6)	32.8 b (1.2)	87.0
	0.3% TG + Maltodextrin		10.2 a (1.2)	2.1 a (0.4)	31.0 a (1.0)	82.2
	0.6% TG + Maltodextrin		9.3 a (0.2)	2.0 a (0.6)	30.3 a (0.4)	80.4
Glutaraldehyde						
	10%	3.45 ab (0.02)	34.8 f (3.7)	4.1 b (0.4)	39.7 f (0.9)	105.3
	20%	3.49 b (0.02)	13.9 b (2.1)	12.2 c (0.4)	40.7 fg (1.2)	108.0
	30%	3.56 c (0.04)	14.2 b (2.6)	13.9 d (2.1)	42.2 h (0.2)	111.9
	After soaking films in water for 24 h and drying in air at room temperature for 30 min					
Glutaraldehyde						
	Control		6.6 a (2.2)	0.8 a (0.2)		
	10%		11.8 b (1.1)	1.6 b (0.2)		
	20%		16.2 b (4.4)	1.7 b (0.5)		
	30%		12.7 b (4.2)	1.7 b (0.4)		

Values in a column followed by different letters are significantly different ($p<0.05$). Numbers in the parentheses are standard deviations (n=3). Control for heat and glutaraldehyde treatments is the same. TG- Transglutaminase. * Values calculated from the mean IVPD values expressed as per cent of IVPD of control 22°C.

Similar results were reported by Marquié et al. (1997) working on cottonseed protein films who noted a decrease in film maximum puncture force. Likewise, increase in elongation at break has been reported for other protein films cross-linked using glutaraldehyde such as zein films (Parris and Coffin, 1997). Marquié et al. (1997) proposed that molecular structure of the long methylene bridges formed between the glutaraldehyde cross-linked proteins may lead to a decrease in the intermolecular forces between polypeptide chains.

Concerning the tensile properties of films that had been soaked for 24 h in water, glutaraldehyde treatment resulted in retention of far higher tensile strength than the control (Table 4.7; Figure 4.18D). This agrees with the data on film water stability (Figures 4.16B and 4.17), water uptake and weight loss in water (Table 4.6), which showed that glutaraldehyde treatment resulted in kafirin microparticle films with better integrity even after soaking in water. These data on tensile strength retention compare favourably with published data for similar glutaraldehyde treatments, despite the differences in type of protein from which the film is prepared and film thickness. For example, in the study by Sessa et al. (2007) tensile strength of soaked zein films was ≈31% of the pre-soaked film tensile strength with 8% glutaraldehyde treatment, which compares closely with 34% obtained with 10% glutaraldehyde treatment in the present study. Better retention of tensile strength after soaking in water has also been reported for other glutaraldehyde-treated biomaterials such as gluten fibres (Reddy et al., 2008). The tensile strain of kafirin microparticle films was reduced after soaking in water, probably due to the washing out of the plasticizer. No data were obtained for heat and transglutaminase treatments as they produced films that were not useful for tensile test after soaking.

Film IVPD

Heat treatment of kafirin microparticles slightly reduced the IVPD of the films made from them (Table 4.7). Byaruhanga et al. (2005) reported a reduction in IVPD of cast kafirin films as a result of heat treatment. Reduction in IVPD of wet heated-kafirin is a known phenomenon, which is attributed to disulphide cross-linking (Duodu et al., 2003). However, in the present study, the small IVPD reduction may be attributed the prolonged heat treatment for all the films as discussed. As with heat treatment, treating kafirin microparticles with transglutaminase reduced film IVPD. A reduction in protein digestibility has been reported for soy protein isolate treated with transglutaminase (Tang, Li, Yang, 2006). The film IVPD

was lower with transglutaminase treatment than with heat treatment. This is probably due to the fact maltodextrin (a carbohydrate), which is the transglutaminase enzyme carrier base constituting 99% of the enzyme material, may interact with kafirin (a protein) through Maillard reaction, thereby reducing further the IVPD.

On the contrary, treatment with glutaraldehyde increased the IVPD of the kafirin microparticle films by up to some 12%. The increase in protein digestibility as a result of glutaraldehyde treatment may probably be due to an increase in void volume. Migneault et al. (2004) suggested that it is polymeric forms of glutaraldehyde (polyglutaraldehydes) that are involved in the cross-linking of proteins. These glutaraldehyde polymers may form long distance methylene bridges between protein chains, probably creating easier access of the pepsin enzyme to the peptide bonds in the kafirin. Overall, the changes in IVPD of the kafirin microparticle films as a result of all the three treatments were not large compared to the control (maximum of 20% change). This was probably because irrespective of the treatments, all the film-forming mixtures were subjected to the same relatively high temperature (50^{o}C) for a long time (12 h) during solvent evaporation.

4.2.5 Conclusions

Thin kafirin films cast from microparticles are more stable in water than conventional cast kafirin films. Glutaraldehyde treatment of the thin kafirin microparticle films renders them quite stable in ambient temperature water, despite the loss of plasticizer. Thus, glutaraldehyde-treated kafirin microparticle films appear to have good potential for use as thin biomaterials in aqueous applications.

4.2.6 References

American Association of Cereal Chemists (AACC International), 2000. Crude protein-combustion, Standard Method 46-30. Approved Methods of the AACC (10th ed.). The Association: St Paul, MN.

American Society for Testing and Materials (ASTM), 1997a. Annual Book of the ASTM Standards. ASTM D882-97: Standard method for tensile properties of thin plastic sheeting. The Society: West Conshohocken, PA.

American Society for Testing and Materials (ASTM), 1997b. Annual Book of the ASTM Standards. ASTM E96-97: Standard test methods for water vapor transmission of materials. The Society: West Conshohocken, PA.

Ando, H., Adashi, M., Umeda, K., Matsuura, A., Nonaka, M., Uchio, R., Tanaka, H., Motoki, M., 1989. Purification and characteristics of a novel transglutaminase derived from microorganisms. Agricultural and Biological Chemistry 53, 2613−2617.

Belton, P.S., Delgadillo, I., Halford, N.G., Shewry, P.R., 2006. Kafirin structure and functionality. Journal of Cereal Science 44, 272–286.

Bourtoom, T., 2009. Edible protein films: properties enhancement. International Food Research Journal 16, 1−9.

Byaruhanga, Y.B., Erasmus, C., Taylor, J.R.N., 2005. Effect of microwave heating of kafirin on the functional properties of kafirin films. Cereal Chemistry 82, 565−573.

Byaruhanga, Y.B., Emmambux, M.N., Belton, P.S., Wellner, N., Ng, K.G., Taylor, J.R.N., 2006. Alteration of kafirin film structure by heating with microwave energy and tannin complexation. Journal of Agricultural and Food Chemistry 54, 4198−4207.

Caillard, R., Remondetto, G.E., Subirade, M., 2009. Physicochemical properties and microstructure of soy protein hydrogels co-induced by Maillard type cross-linking and salts. Food Research International 42, 98–106.

Chambi, H., Grosso, C., 2006. Edible films produced with gelatin and casein cross-linked with transglutaminase. Food Research International 39, 458–466.

Chan, W.-M., Ma, C.-Y., 1999. Acid modification of proteins from soymilk residue (okara). Food Research International 32, 119−127.

Dong, J., Sun, Q., Wang, J.Y., 2004. Basic study of corn protein, zein, as a biomaterial in tissue engineering, surface morphology and biocompatibility. Biomaterials 25, 4691–4697.

Duodu, K.G., Taylor, J.R.N., Belton, P.S., Hamaker, B.R., 2003. Factors affecting sorghum protein digestibility. Journal of Cereal Science 38, 117−131.

Duodu, K.G., Tang, H., Wellner, N., Belton, P.S., Taylor, J.R.N., 2001. FTIR and solid state ^{13}C NMR spectroscopy of proteins of wet cooked and popped sorghum and maize. Journal of Cereal Science 33, 261−269.

El Nour, N.A., Peruffo, A.D.B., Curioni, A., 1998. Characterisation of sorghum kafirins in relations to their cross-linking behaviour. Journal of Cereal Science 28, 197−207.

Emmambux, N.M., Taylor, J.R.N., 2003. Sorghum kafirin interaction with various phenolic compounds. Journal of the Science of Food and Agriculture 83, 402–407.

Emmambux, N.M., Taylor, J.R.N., 2009. Properties of heat-treated sorghum and maize meal and their prolamin proteins. Journal of Agricultural and Food Chemistry 57, 1045–1050.

Flores, I., Cabra, V., Quirasco, M.C., Farres, A., Galvez, A., 2010. Emulsifying properties of chemically deamidated corn (*Zea mays*) gluten meal. Food Science and Technology International 16, 241–250.

Gao, C., Taylor, J., Wellner, N., Byaruhanga, Y.B., Parker, M.L., Mills, E.N.C., Belton, P.S., 2005. Effect of preparation conditions on protein secondary structure and biofilm formation of kafirin. Journal of Agricultural and Food Chemistry 53, 306–312.

Hamaker, B.R., Kirleis, A.W., Mertz, E.T., Axtell, J.D., 1986. Effect of cooking on the protein profiles and in vitro digestibility of sorghum and maize. Journal of Agricultural and Food Chemistry 34, 647−649.

Hernández-Muñoz, P., Kanavouras, A., Lagaron, J.M., Gavara, R., 2005. Development and characterization of films based on chemically cross-linked gliadins. Journal of Agricultural and Food Chemistry 53, 8216−8223.

Kaya, S., Kaya, A., 2000. Microwave drying effects on properties of whey protein isolate edible films. Journal of Food Engineering 43, 91–96.

Krochta, J.M., 2002. Proteins as raw materials for films and coatings: definitions, current status, and opportunities. In: Gennadios, A. (Ed.), Protein-Based Films and Coatings. CRC Press: Boca Raton, FL, pp. 1−41.

Larré, C., Chiarello, M., Blanloeil, Y., Chenu, M., Gueguen, J., 1993. Gliadin modifications catalyzed by guinea pig liver transglutaminase. Journal of Food Biochemistry 17, 267–282.

Lawton, J.W., 2002. Zein: a history of processing and use. Cereal Chemistry 79, 1–18.

Marquié, C., Tessier, A.-M., Aymard, C., Guilbert, S., 1997. HPLC determination of the reactive lysine content of cottonseed protein films to monitor the extent of cross-linking by formaldehyde, glutaraldehyde, and glyoxal. Journal of Agricultural and Food Chemistry 45, 922–926.

Matsudomi, N., Kato, A., Kobayashi, K., 1982. Conformation and surface properties of deamidated gluten. Agricultural and Biological Chemistry 46, 1583−1586.

Micard, V., Belamri, R., Morel, M.-H., Guilbert, S., 2000. Properties of chemically and physically treated wheat gluten films. Journal of Agricultural and Food Chemistry 48, 2948–2953.

Migneault, I., Dartiguenave, C., Bertrand, M.J., Waldron, K.C., 2004. Glutaraldehyde: behavior in aqueous solution, reaction with proteins, and application to enzyme crosslinking. BioTechniques 37, 790−802.

Mizutani, Y., Matsumura, Y., Imamura, K., Nakanishi, K., Mori, T., 2003. Effects of water activity and lipid addition on secondary structure of zein in powder systems. Journal of Agricultural and Food Chemistry 51, 229–235.

Motoki, M., Seguro, K., Nio, N., Takinami, K., 1986. Glutamine-specific deamidation of α_{sl}-casein by transglutaminase. Agricultural and Biological Chemistry 50, 3025−3030.

Orliac, O., Rouilly, A., Silvestre, F., Rigal, L., 2002. Effects of additives on the mechanical properties, hydrophobicity and water uptake of thermomoulded films produced from sunflower protein isolate. Polymer 43, 5417–5425.

Park, H.J., Chinnan, M.S., 1995. Gas and water vapor barrier properties of edible films from protein and cellulosic materials. Journal of Food Engineering 25, 497–507.

Parris, N., Coffin, D.R., 1997. Composition factors affecting the water vapor permeability and tensile properties of hydrophilic zein films. Journal of Agricultural and Food Chemistry 45, 1596−1599.

Pérez-Pérez, C., Regalado-González, C., Rodríguez-Rodríguez, C.A., Barbosa-Rodríguez, J.R., Villaseñor-Ortega, F., 2006. Incorporation of antimicrobial agents in food packaging films and coatings. In: Guevara-González, R.G., and Torres-Pacheco, I. (Eds.), Advances in Agricultural and Food Biotechnology. Research Signpost: Trivandrum, India, pp. 193−216.

Poole, A.J., Church, J.S., Huson, M.G., 2008. Environmentally sustainable fibers from regenerated protein. Biomacromolecules 10, 1−8.

Reddy, N., Tan, Y., Li, Y., Yang, Y., 2008. Effect of glutaraldehyde crosslinking conditions on the strength and water stability of wheat gluten fibers. Macromolecular Materials and Engineering 293, 614–620.

Selling, G.W., Woods, K.K., Sessa, D., Biswas, A., 2008. Electrospun zein fibers using glutaraldehyde as the crosslinking reagent: effect of time and temperature. Macromolecular Chemistry and Physics 209, 1003–1011.

Sessa, D.J., Mohamed, A., Byars, J.A., 2008. Chemistry and physical properties of melt-processed and solution-cross-linked corn zein. Journal of Agricultural and Food Chemistry 56, 7067–7075.

Sessa, D.J., Mohamed, A., Byars, J.A., Hamaker, S.A., Selling, G.W., 2007. Properties of films from corn zein reacted with glutaraldehyde. Journal of Applied Polymer Science 105, 2877–2883.

Shull, J.M., Watterson, J.J., Kirleis, A.W., 1991. Proposed nomenclature for the alcohol-soluble proteins (kafirins) of *Sorghum bicolor* (L. Moench) based on molecular weight, solubility and structure. Journal of Agricultural and Food Chemistry 39, 83–87.

Soliman, E.A., Eldin, M.S.M., Furuta, M., 2009. Biodegradable zein-based films: influence of γ-irradiation on structural and functional properties. Journal of Agricultural and Food Chemistry 57, 2529–2535.

Stokes, R.H., Robinson, R.A., 1949. Standard solutions for humidity control at 25°C. Industrial and Engineering Chemistry 41, 2013.

Subirade, M., Kelly, I., Guéguen, J., Pézolet, M., 1998. Molecular basis of film formation from a soybean protein: comparison between the conformation of glycinin in aqueous solution and in films. International Journal of Biological Macromolecules 23, 241–249.

Tang, C.-H., Jiang, Y., Wen, Q.-B., Yang, X.-Q., 2005. Effect of transglutaminase treatment on the properties of cast films of soy protein isolates. Journal of Biotechnology 120, 296–307.

Tang, C.-H., Li, L., Yang, X.-Q., 2006. Influence of transglutaminase-induced cross-linking on *in vitro* digestibility of soy protein isolate. Journal of Food Biochemistry 30, 718–731.

Taylor, J., Taylor, J.R.N., Belton, P.S., Minnaar, A., 2009c. Preparation of free-standing films from kafirin protein microparticles: mechanism of formation and functional properties. Journal of Agricultural and Food Chemistry 57, 6729–6735.

Taylor, J., Taylor, J.R.N., Dutton, M.F., De Kock, S., 2005b. Identification of kafirin film casting solvents. Food Chemistry 32, 149−154.

Wagner, J.R., Gueguen, J., 1995. Effects of dissociation, deamidation, and reducing treatment on structural and surface active properties of soy glycinin. Journal of Food Biochemistry 43, 1993−2000.

Wang, H.-J., Lin, Z.-X., Liu, X.-M., Sheng, S.-Y., Wang, J.-Y., 2005. Heparin-loaded zein microsphere film and hemocompatibility. Journal of Controlled Release 105, 120–131.

Wang, Q., Yin, L., Padua, G.W., 2008. Effect of hydrophilic and lipophilic compounds on zein microstructures. Food Biophysics 3, 174–181.

CHAPTER 3

4.3 *IN VITRO* BMP-2 BINDING TO KAFIRIN MICROSTRUCTURES, RAT MODEL ASSESSMENT OF KAFIRIN MICROPARTICLE FILM-BMP-2 SYSTEM SAFETY, EVALUATION OF BIODEGRADABILITY OF KAFIRIN MICROPARTICLE FILM IMPLANT AND ASSESSMENT OF KAFIRIN MICROPARTICLE FILM-BMP-2 INDUCED ECTOPIC BONE FORMATION

4.3.1 Abstract

Mammalian collagen, a standard carrier used to enhance the osteoinductive effect of BMP-2, may induce immune response and has a risk of transmitting diseases. The potential of kafirin microstructures as biomaterials for replacement of collagen was investigated. The ability of kafirin microstructures to bind BMP-2 *in vitro* was evaluated. A rat model assessment of glutaraldehyde- and polyphenol-treated kafirin microparticle films, and kafirin microparticle film-BMP-2 system safety was performed. In addition, the biodegradability of these kafirin microparticle film implants and the ability of kafirin microparticle film-BMP-2 system to induce ectopic bone formation were investigated. Compared to collagen standard, the BMP-2 binding capacities of control, heat-treated, transglutaminase-treated and glutaraldehyde-treated kafirin microparticles were 7%, 18%, 34% and 22% higher, respectively, after 24 h binding, probably due mainly to the vacuoles creating a greater surface area in the microparticles. The glutaraldehyde- and polyphenol-treated films, and kafirin microparticle film-BMP-2 system were non-irritant to the animals, probably because kafirin is non-allergenic. Kafirin microparticle film implants degraded slowly, probably because of the low susceptibility of kafirin to mammalian proteolytic enzymes. Kafirin microparticle film-BMP-2 system did not induce ectopic bone morphogenesis, probably mainly due to low BMP-2 dosage and short study duration. These kafirin microstructures could have application as natural, non-animal protein biomaterials such as bioactive scaffolds for hard or soft tissue repair. However, at low BMP-2 levels (107–2140 ng/g) and a short implantation period (28 days), the kafirin microparticle film-BMP-2 system does not induce bone morphogenesis in the rat. Therefore more work needs to be done to optimize BMP-2 loading and release profile with kafirin microstructures.

4.3.2 Introduction

In the previous research chapters, it was established that treatment of kafirin microparticles with heat, transglutaminase and glutaraldehyde modified the functional properties of the kafirin microstructures. It was found that heat and glutaraldehyde cross-linking treatments both increased the microparticle size (Chapter 1). Additionally heat treatment increased the microparticle vacuole size, thereby increasing their internal surface area enabling their potential application for binding to delay or control the release of the encapsulated bioactives. In Chapter 2, it was shown that the thin kafirin microparticle films were relatively stable in ambient temperature water, which was enhanced by treatment with glutaraldehyde, indicating their potential stability in aqueous physiological environment.

Several workers have shown the potential of cereal protein microstructures to bind or carry bioactives or as scaffolds. For example, Taylor et al. (2009b) found that the vacuolated kafirin microparticles could encapsulate antioxidants, probably because of the presence of the holes, which increased the internal surface area for binding these bioactives. Similarly, in a study by Wang et al. (2005), they reported a heparin-loaded zein microsphere films with potential for application as drug-eluting coating film for cardiovascular devices. Likewise, Tu, Wang, Li, Dai, Wang and Zhang (2009) showed that the complexes of zein scaffolds and rabbit mesenchymal stem cells could undergo ectopic bone formation in the thigh muscle pouches of nude mice. To determine whether the kafirin microstructures could be used as biomaterial scaffolds or *in vivo* carriers for other bioactives, such as bone morphogenetic proteins (BMPs), stem cells, heparin among others, it is necessary first to establish their safety. It is also important to determine the binding of the kafirin microstructures with these bioactives.

Safe, slowly biodegradable and effective implantable medical devices are needed in order to promote regeneration of bone tissue. Many conditions occur where bone regeneration is necessary, such as periodontitis, bone tooth cavities, degenerative spinal conditions and severe fractures (reviewed by Bessa et al., 2008). One of the major concerns with medical devices is immune reaction and implant rejection by the body (reviewed by Nag and Banerjee, 2012). There is also a requirement that medical devices have to last for sufficient time in order for complete tissue regeneration to take place (reviewed by Bessa et al., 2008). The thin, water stable kafirin microparticle films (Chapter 2) may have good functional properties for this type of application.

BMPs are multi-functional growth factors that belong to the transforming growth factor β (TGF-β) superfamily (Chen, Zhao and Mundy, 2004), which induce cartilage and bone formation in addition to non-osteogenic developmental processes such as in neural induction (reviewed by Shah, Keppler, and Rutkowski, 2011). According to Shah et al. (2011), there are 23 different members of TGF-β family of which 17 are BMPs. BMP-2 plays a critical role in bone formation and regeneration. While BMP-2 by itself is sufficient to induce bone formation, its rapid distribution from implant site reduces its inductive effect (reviewed by Kim, Kim, Kim, Choi, Chai, Kim and Cho, 2005). Other factors that affect the therapeutic outcome of BMP-2 are its quantity, concentration and time of application (reviewed by King and Cochran, 2002; La, Kang, Yang, Bhang, Lee, Park and Kim, 2010). The ability to immobilize this molecule in certain matrices can be crucial in bone tissue engineering. While mammalian collagen is the current standard carrier for BMP-2 (reviewed by Gautschi, Frey and Zellweger, 2007), it has the potential to induce an immune response due to its xenobiotic origin as well as having a high risk of transmitting Creutzfeldt–Jakob disease (CJD) (reviewed by Bessa et al., 2008, 2010; Silva, Ducheyne and Reis, 2007; Haidar et al., 2009). Therefore, delivery systems that do not elicit an immune response need to be sought.

Kafirin microstructures may be highly suitable for a number of reasons. Firstly, kafirin is a relatively hydrophobic protein (Duodu et al., 2003). This may enhance its ability to bind BMP-2, which has been shown to have a strong affinity for hydrophobic surfaces (Utesch, Daminelli and Mroginski, 2011). Secondly, the fact that kafirin microparticles are vacuolated (Taylor et al., 2009a) may provide a large surface area for BMP-2 binding. Additionally, kafirin is slowly biodegraded by mammalian proteolytic enzymes (Emmambux and Taylor, 2009) attributed to kafirin hydrophobicity as enzymes function in an aqueous environment (Duodu et al., 2003), which might prolong the degradation period of the kafirin microstructures in the body. Most importantly, kafirin is non-allergenic (Ciacci et al., 2007).

The present study investigated the potential of modified kafirin microstructures to bind BMP-2. A rat model assessment of the safety of kafirin microparticle film implants and kafirin microparticle film-BMP-2 system was performed. In addition, the biodegradability of kafirin microparticle film implants in the rat model was evaluated. Also, the ability of kafirin microparticle film-BMP-2 to induce ectopic bone formation in the rodent model was investigated.

4.3.3 Materials and methods

4.3.3.1 *Materials*

Kafirin was extracted from a mixture of two similar white, tan-plant non-tannin sorghum cultivars PANNAR PEX 202 and 606 and used to prepare kafirin microparticles as described in Chapter 1. All the other materials used in the study are specified in the relevant sections of the text.

4.3.3.2 *Binding BMP-2 with kafirin microparticles*

The BMP-2 binding study was performed by the candidate under the guidance of Dr Nicolaas Duneas of Altis Biologics.

Medium exchange for kafirin microparticles

As kafirin microparticles were stored in 0.9 M acetic acid, the carrier medium was exchanged to 20 mM acetic acid. The kafirin microparticle suspensions were centrifuged at 3150 *g* for 20 min. Then the supernatants were carefully decanted off, replaced with 20 mM acetic acid (pH 3.3), re-suspended for 15 min on a rocking platform, and centrifuged as before. The supernatant were replaced with fresh 20 mM acetic acid. This process was repeated three times. Then, the volume of 20 mM acetic acid was adjusted to give a solids content of at least 6% (w/w).

Binding BMP-2 with kafirin microparticles

Kafirin microparticle suspensions containing 100 mg protein were weighed into 5 mL cryovials. Then, 0.5 mL 1000 ppm Tween® 20 (polyoxyethylene sorbitan monolaurate) (Merck-Schuchardt, Munich, Germany) was added and vortex-mixed. Similarly, 100 mg porcine collagen standard (Altis Biologics, Pretoria, South Africa) was weighed and treated the same way as the kafirin microparticles. Porcine BMP complex (0.778 mg/mL) (pH 3.3) with BMP-2 abundance of 0.00085% (w/w) as a proportion of BMP complex (Altis Biologics) (1.5 mL) was added to kafirin microparticles or collagen standard and vortex-mixed to give a BMP complex to carrier protein ratio of approximately 1:100. The reaction volumes of the mixtures were adjusted to 4.5 mL using 20 mM acetic acid and the contents mixed well. Samples were drawn from clear supernatants after centrifugation at 3150 *g* for 20 min. An initial 50 µL sample was drawn from unbound sample and transferred into

microwells of a microplate (Greiner Bio-One, Frickenhausen, Germany) to account for time 0. Then, the cryovials were placed on a rocking platform set at 50 rpm and 50 µL sample material was subsequently drawn from clear supernatants of each sample treatment after 5, 10, 30, 60, 120 and 1440 min intervals. Controls containing kafirin microparticles, collagen without BMP complex and BMP complex without binding material (kafirin microparticle or collagen) were included. The reaction mixture had pH 3.0. and ionic strength of 20 mM.

4.3.3.3 *SDS-PAGE*

To characterize the proteins BMP binding residues (kafirin microparticles or collagen loaded with BMP complex), SDS-PAGE under reducing and non-reducing conditions was performed as described in Chapter 1. Then silver-stain was used after destaining the gels according to the protocol provided for PlusOne Silver Staining kit, Protein (GE Healthcare Bio-Sciences AB, Uppsala, Sweden).

4.3.3.4 *SEM*

Suspensions of kafirin microparticles and collagen standard loaded with BMP complex were prepared for SEM and analysed as described in Chapter 1.

4.3.3.5 *Lowry protein assay*

The concentration of protein in the clear supernatants was measured by the Lowry protein assay (Lowry, Rosebrough, Farr and Randall, 1951) using a Bio-Rad DC Protein Assay kit (Bio-Rad Laboratories, Hercules, CA) to establish evidence of kafirin microparticle binding to BMP-2. The Lowry protein assay was used to measure free protein in the clear supernatants to give an inverse indication of BMP-2 binding. Controls containing kafirin microparticles or collagen without BMP complex were included. The protein concentrations of the supernatants were obtained by subtracting the protein concentration in supernatant of controls from the treatments with BMP complex.

4.3.3.6 *Enzyme-linked immunosorbant assay (ELISA)*

For confirmation of kafirin microparticle binding to BMP-2, BMP-2 ELISA was used to measure the amount of BMP-2 in the clear supernatants of treatments, which with Lowry protein assay, showed BMP binding profiles that were closely similar to collagen standard. A

Quantikine® BMP-2 Immunoassay kit (R&D Systems, Minneapolis, MN) was used. This is a quantitative sandwich enzyme immunoassay technique, whereby a monoclonal antibody specific for BMP-2 is pre-coated onto a microplate. The standards and samples are pipetted into the wells and the immobilized antibody binds any BMP-2 present. Any unbound substances are washed out from the wells and then an enzyme-linked monoclonal antibody specific for BMP-2 is added to the wells. Then the unbound antibody-enzyme reagent is removed by washing and a colour reagent solution containing a mixture of hydrogen peroxide and tetramethylbenzidine (a chromogen) is added to the wells. Colour develops in proportion to the amount of BMP-2 bound in the initial step. The absorbances were read at 450 nm with correction readings at 570 nm. The BMP-2 concentration in the supernatants was inversely related to binding.

4.3.3.7 *Subcutaneous bioassay using rat model*

The subcutaneous bioassay using rat model was performed to accomplish three objectives. First, was to assess the safety of kafirin microparticle film implants and kafirin microparticle film-BMP-2 system in the rat model. The second objective was to evaluate the biodegradability of kafirin microparticle film implants in the rat tissue. The third was to establish whether the kafirin microparticle film-BMP-2 system was capable of promoting ectopic bone morphogenesis in the rat model. Collagen was used as standard. Because of their good water stability, kafirin microparticle film implants were used in the rat study. In addition, recombinant human BMP-2 (rhBMP-2) was used in the animal study to preclude possible infection from the porcine BMP complex, which contained unpurified BMP-2.

Kafirin microparticle film preparation

Control kafirin microparticle films and a 20% glutaraldehyde-treated kafirin microparticle films were prepared as described in Chapter 2. Kafirin microparticle films treated with polyphenols were prepared as described below. The work on the polyphenol-treated kafirin microparticle films was performed as a previous study by Taylor et al. (2009b) had shown that kafirin microparticles could bind polyphenol but information on the safety and biodegradability of kafirin microstructure-polyphenol system in an animal model was lacking.

Treatment of kafirin microparticle films with polyphenol extract

Polyphenol extract was obtained from Black non-tannin sorghum grain bran. To obtain the bran, the sorghum grains were hand cleaned and sorted to remove foreign objects, damaged and diseased grain. Dehulling was performed using a Tangential Abrasive Dehulling Device (TADD) Model 4E-115 (Venables Machine Works, Saskatoon, SK, Canada). Equal amounts of the sorghum grain (approximately 75 g) were placed into each of the eight compartments of the equipment's chamber holding disc and dehulled for at least 2 min to remove the bran that collected into the holding bag. The collected sorghum brans were then sieved through a 1000 µm aperture test sieve respectively and ground into a powder using a coffee mill (IKA A11, Staufen, Germany). These were further passed through a 500 µm aperture test sieve, packed under vacuum and then stored at 4^{o}C until required for extraction. Then the polyphenols were extracted from the Black sorghum bran according to a protocol by Emmambux and Taylor (2003). Briefly, Black sorghum bran (10 g) was mixed with 150 mL distilled water and stirred for 30 min before adjusting to pH 2.0 using 1.0 M HCl. The mixture was then incubated for 30 min in a shaking water bath at 37^{o}C. Then, the pH was further adjusted to pH 6.0 using 1.0 M NaOH and the incubation continued in the shaking water bath for 30 min. The sample was centrifuged at 7500 *g* for 15 min. Total polyphenol content of the extract was determined using the Folin-Ciocalteu method (Singleton and Rossi, 1965). Polyphenol-treated kafirin microparticle films were prepared by soaking the films in an aqueous extract of polyphenols for 12 h at room temperature.

Washing out plasticizer from kafirin microparticle film

Plasticizer was washed out of the kafirin microparticle films to create a porous matrix for diffusion of BMP-2 molecules to enhance binding and to reduce impurities due to plasticizer content. This is based on the knowledge that a plasticiser acts by disrupting intermolecular chain forces and increasing the free volume of the polymer network (reviewed by Cuq et al., 1998). Hence, when the plasticizer is washed off the film would be expected to become porous due to the voids left at molecular level. The plasticizer in the films was washed out by soaking in distilled water as described in Chapter 2. To decide on whether use of wet or dried kafirin microparticle films would be more suitable for binding rhBMP-2 for the animal study, both wet and dry kafirin microparticle films were prepared. For the wet kafirin microparticle films, the water on the film surfaces after soaking was removed by placing the films in between a paper towel before using the films for binding rhBMP-2 without drying. The dry

kafirin microparticle films were prepared by further drying the films in a desiccator for 72 h before use. The wet kafirin microparticle films were eventually used for rhBMP-2 binding for the rat study based on the rhBMP-2 binding data.

Preparation of rhBMP-2 loaded kafirin microparticle films and collagen

The rhBMP-2 (Invitrogen, Carlsbad, CA) was dissolved in 0.01 M phosphate buffered saline (pH 7.4) (Sigma-Aldrich, St. Louis, MO) to make a 400 ng/mL rhBMP-2 solution. Two doses, a low rhBMP-2 dose (106.7 ng rhBMP-2/g kafirin microparticle film or collagen) and high dose (2140 ng rhBMP-2/g kafirin microparticle film or collagen) were prepared by diffusion loading according to the protocol of Patel et al. (2008), whereby the rhBMP-2 was dripped onto 75 mg kafirin microparticle film or collagen using a micropipette. These loadings were equivalent to 8 ng and 160 ng rhBMP-2 per implant for low dose and high dose, respectively. Then, the implants were incubated at 4^{o}C for 24 h and then dried in air. Kafirin microparticle films and collagen without rhBMP-2 were used as controls.

4.3.3.8 *Sterilization of implant materials*

The dried film dosages were folded into approximately 1 cm × 0.75 cm and placed into individual 2 mL Eppendorf tubes (one per dose). The collagen dosages were also placed in individual 2 mL Eppendorf tubes (one per dose). The Eppendorf tubes containing individual dosages were then packed into a cardboard box. Then, the implant materials were sterilised using γ-irradiation (25 kGry), performed by Synergy Sterilisation (Johannesburg, South Africa). Tables 4.8 and 4.9 provide summaries of the constituents of the treatments for assessment of safety, biodegradability and ectopic bone growth.

Table 4.8 Summary of the constituents of the BMP-2 loaded kafirin microparticle film or collagen and controls for safety and biodegradability assessment

Material	Treatment	Composition
Kafirin microparticle film	Control kafirin microparticle film	75 mg untreated kafirin microparticle film
	20% glutaraldehyde treated kafirin microparticle film	75 mg 20% glutaraldehyde treated kafirin microparticle film
	Polyphenol treated kafirin microparticle film	75 mg polyphenol treated kafirin microparticle film
	BMP-2 loaded control kafirin	75 mg kafirin microparticle film + 8 ng

Material	Treatment	Composition
	microparticle film Low loading	rhBMP-2
	BMP-2 loaded control kafirin microparticle film High loading	75 mg kafirin microparticle film + 160 ng rhBMP-2
Collagen	Control collagen	75 mg collagen without BMP-2
	BMP loaded collagen Low loading	75 mg collagen+ 8 ng rhBMP-2
	BMP loaded collagen High loading	75 mg collagen + 160 ng rhBMP-2

Table 4.9 Summary of the constituents of the BMP-2 loaded kafirin microparticle film or collagen and controls for assessment of biodegradability and ectopic bone growth

Material	Treatment	Composition
Kafirin microparticle film	Control kafirin microparticle film	75 mg kafirin microparticle film without BMP-2
	BMP-2 loaded kafirin microparticle film Low loading	75 mg kafirin microparticle film + 8 ng rhBMP-2
	BMP-2 loaded kafirin microparticle film High loading	75 mg kafirin microparticle film + 160 ng rhBMP-2
Collagen	Control collagen	75 mg collagen without BMP-2
	BMP-2 loaded collagen Low loading	75 mg collagen+ 8 ng rhBMP-2
	BMP-2 loaded collagen High loading	75 mg collagen + 160 ng rhBMP-2

4.3.3.9 *Implantation*

The implant materials were prepared by the candidate while implantation procedures were performed by Prof Vinny Naidoo who is a veterinarian. Sprague–Dawley rats (20) (SA Vaccine Producers, Johannesburg, South Africa) with a weight range of 155–223 g were used in the study. Rats were allowed autoclaved potable water and irradiated food (Rat Chow, Epol, Johannesburg, South Africa) *ad libitum*. This protocol was approved by the University of Pretoria Animal Use and Care Committee (approval number H016-11) (see Annex 1) prior to commencement of the study, according to the South African national standard for the use and care of laboratory animals. The rats were pair-housed in the Biomedical Research Centre

of the University of Pretoria in Eurostandard type III cages (Techniplast, Buguggiate, Italy). Animals were housed on wood shaving and had access to cardboard cartons and tissue paper for enrichment. Four paravertebral skin incisions of 1.5 cm were made with a scalpel blade just caudal to the point of the scapula by a veterinarian. A blind pouch was created subcutaneously by blunt dissection with scissors. After insertion of the implants, the incisions were closed with cyanoacrylate. Treatments were randomised to the available sites by numbering the wound sites 1 to 4 starting on the top left of the dorsum moving in a clockwise direction and subsequently allocating the treatments to a site using a table of random numbers.

4.3.3.10 *Examination of appearance of implants*

The appearances of skin at the sites of the implants were visually assessed by the candidate over the period of the animal experiment.

4.3.3.11 *Histological evaluations*

Independent histological examinations were performed by Idexx Laboratories (Pretoria, South Africa), which is an independent international laboratory. Idexx Laboratories deals in services that include pet-side diagnostic tests, reference laboratory services, digital radiography among other services (http://www.idexxsa.co.za/AboutIDEXX/tabid/103/Default.aspx). The implant treatment identities were coded by the candidate to ensure a blind independent evaluation by Idexx Laboratories.

4.3.3.12 *Safety assessment*

On Day 7, eight animals were euthanized by a veterinarian using isoflurane overdose in a saturated glass chamber and the implants removed for examination by Idexx Laboratories for further evaluation. Animals were also submitted for full necropsy and histopathological evaluation of the major organs (adrenal, brain, gonad, heart, intestines, kidney, liver, lung, pancreas, spleen, stomach, thymus and urinary bladder) by Idexx Laboratories.

4.3.3.13 *Assessment for ectopic bone growth*

On Day 28, the remaining 12 animals were euthanized as above and subjected to radiology to determine whether bone morphogenesis had taken place. Following implant removal by Idexx Laboratories, the implants were sectioned so that half the implants per treatment could be frozen for quantification of alkaline phosphatase enzyme activity. In addition, the gross appearance of the dissected implants was examined using a Zeiss Discovery V20 stereo microscope (Jena, Germany). The alkaline phosphatase enzyme activity test and the gross appearance of the implants were analysed by the candidate. The other half of the implants were placed in 10% buffered formalin for independent histological examination, which was performed by Idexx Laboratories.

Histopathology

This was performed by Idexx Laboratories. After fixation for 2 days, selected blocks of tissue as well as a cross-section of the implantation site were sectioned and processed in an automatic histological tissue processor (Pathcentre Enclosed Tissue Processor, Thermo Scientific, Johannesburg, South Africa). After overnight tissue processing, wax blocks were produced and histological sections of 6 µm were cut on a HM450 Sliding Microtome (Thermo Scientific). The slides were then stained with haematoxylin and eosin staining using a Shandon Varistain Gemini ES automatic slide stainer (Thermo Scientific). Status of the implant materials was examined. Additionally, the implant sites were evaluated for foreign body reaction, granulomatous reaction, osteolysis, osteogenesis (bone morphogenesis) and skin ulceration. Standard histopathology was performed on the animal organs. Photographs of specific morphological findings were taken and histological scoring for tissue response to the implants was recorded according to similar studies (Babensee, 1990; Bensaid, Triffitt, Blanchat, Oudina, Sedel and Petite, 2003). Results were graded as follows: negative/none (-), mild (+), moderate (++), severe (+++).

Alkaline phosphatase activity

Alkaline phosphatase (ALP) activity of cells on the implants was assayed by the candidate using an adenosine 3',5'-cyclic monophosphate (cAMP) direct enzyme immunoassay kit (Catalogue number CA200, Sigma, St. Louis, MO). This assay is based on the competitive binding technique in which cAMP present in a sample competes with a fixed amount of

alkaline phosphatase-labelled cAMP for sites on a rabbit polyclonal antibody. During the incubation, the polyclonal antibody becomes bound to the goat anti-rabbit antibody coated onto the microplate. Following a wash to remove excess conjugate and unbound sample, a substrate solution (a solution of *p*-nitrophenyl phosphate in buffer) is added to the wells to determine the bound enzyme activity. The colour development is stopped and the absorbance is determined. The intensity of the colour is inversely proportional to the concentration of cAMP in the sample, which is used as measure of ALP activity. The ALP assay was performed according to the manufacturer's instructions. Briefly, the implants were frozen in liquid nitrogen and ground using a mortar and pestle. The ground implant were weighed and homogenized in 0.1 M HCl to stop endogenous phosphodiesterase activity. The ALP activity test was performed on the homogenised samples. The absorbance readings were done at 405 nm with a correction at 570 nm using a microplate reader.

4.3.3.14 *Statistical analyses*

One-way analysis of variance (ANOVA) was used to analyse numerical data with Statistica software version 10 (StatSoft, Tulsa, OK). The dependent variables were the BMP-2 binding capacity and the ALP activity while the independent variables were the BMP-2 carrier materials i.e. collagen standard and kafirin microparticles or kafirin microparticle films. With Lowry protein assay, BMP-2 ELISA and ALP activity tests, four microwells were used per treatment for at least two replicate experiments. The mean differences were assessed by Fischer's Least Significant Difference (LSD) test. Histopathology data were obtained by the histological scoring system for tissue response in four replicate implant sites, by the Idexx Laboratories.

4.3.4 Results and discussion

4.3.4.1 *Binding BMP-2 with kafirin microparticles*

With the Lowry protein assay, there was an increase in protein concentration in the clear supernatant with time (Figure 4.19), which seems counter intuitive. It was expected that if the collagen or kafirin microparticles were to bind the BMP, the concentration of free proteins in the clear supernatant after centrifugation would decrease. Otherwise, in case of no BMP binding, the free protein concentration in the supernatant was expected to be unchanged. The inconsistent result was probably because the Lowry protein assay is based on the reaction of

protein with an alkaline copper tartrate solution and Folin reagent (Lowry et al., 1951). Hence, it is not specific for the BMP. However, Lowry protein assay can be used as indication of collagen binding to BMP (Dr Nicolaas Duneas, Altis Biologics, personal communication). The assay has also been used in other studies such as in the investigation of the synergy between recombinant TGF-β1 and BMP-7 in inducing endocrine bone formation in a baboon (Ripamonti, Duneas, Van Den Heever, Bosch and Crooks, 1997) as part of biochemical analyses. Kafirin microparticles heat-treated at 75^{o}C had binding profile closely following the trend obtained with collagen, suggesting that the ability of these kafirin microparticles to bind BMP-2 was probably similar to the collagen standard.

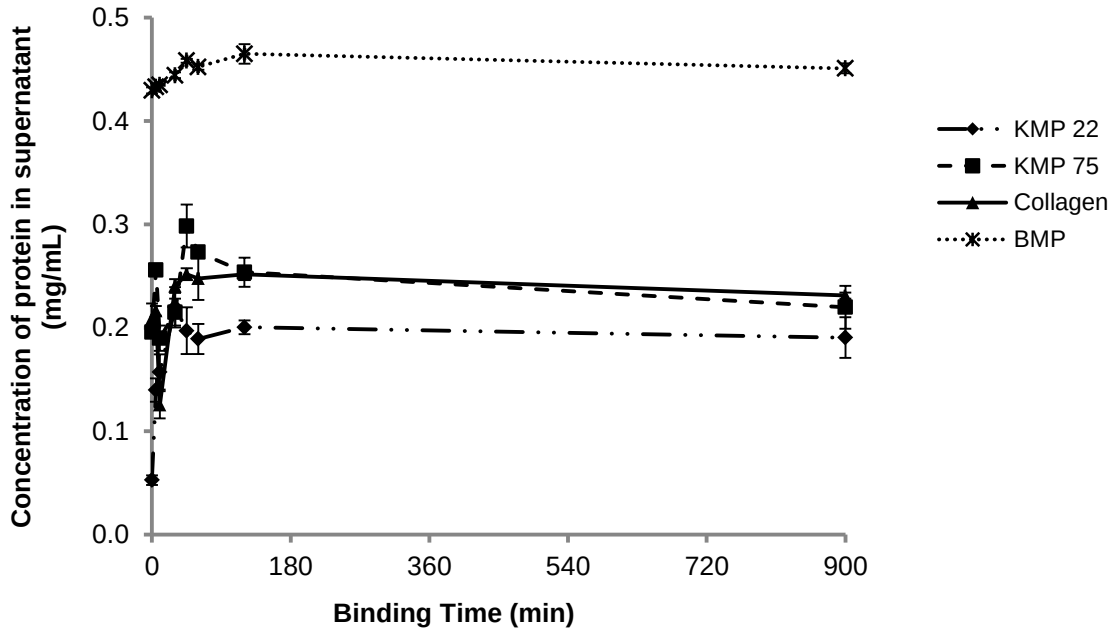

Figure 4.19 Effect of binding of kafirin microparticles (KMP) and collagen standard with BMP on concentration of "BMP complex" in the clear supernatants (free unbound protein), determined by Lowry protein assay. Error bars are standard deviations (n=2). KMP 22– KMP held at ambient temperature (22°C) for 1 h KMP 75– KMP heated at 75°C for 1 h; BMP– bone morphogenetic protein complex without binding material.

SEM showed no changes in the morphology of the kafirin microparticles or collagen particles after binding with BMP (Figure 4.20). These findings are in apparent contrast with the reports in literature such as the work by Balmayor et al. (2009), which showed increase in size of microspheres when bound to BMP-2. It seems the very low concentration of BMP-2 with

respect to the protein in the binding material (kafirin microparticles or collagen), less than one part per million, probably made it impractical to detect any possible changes to the morphology of kafirin microparticles or collagen after binding with BMP.

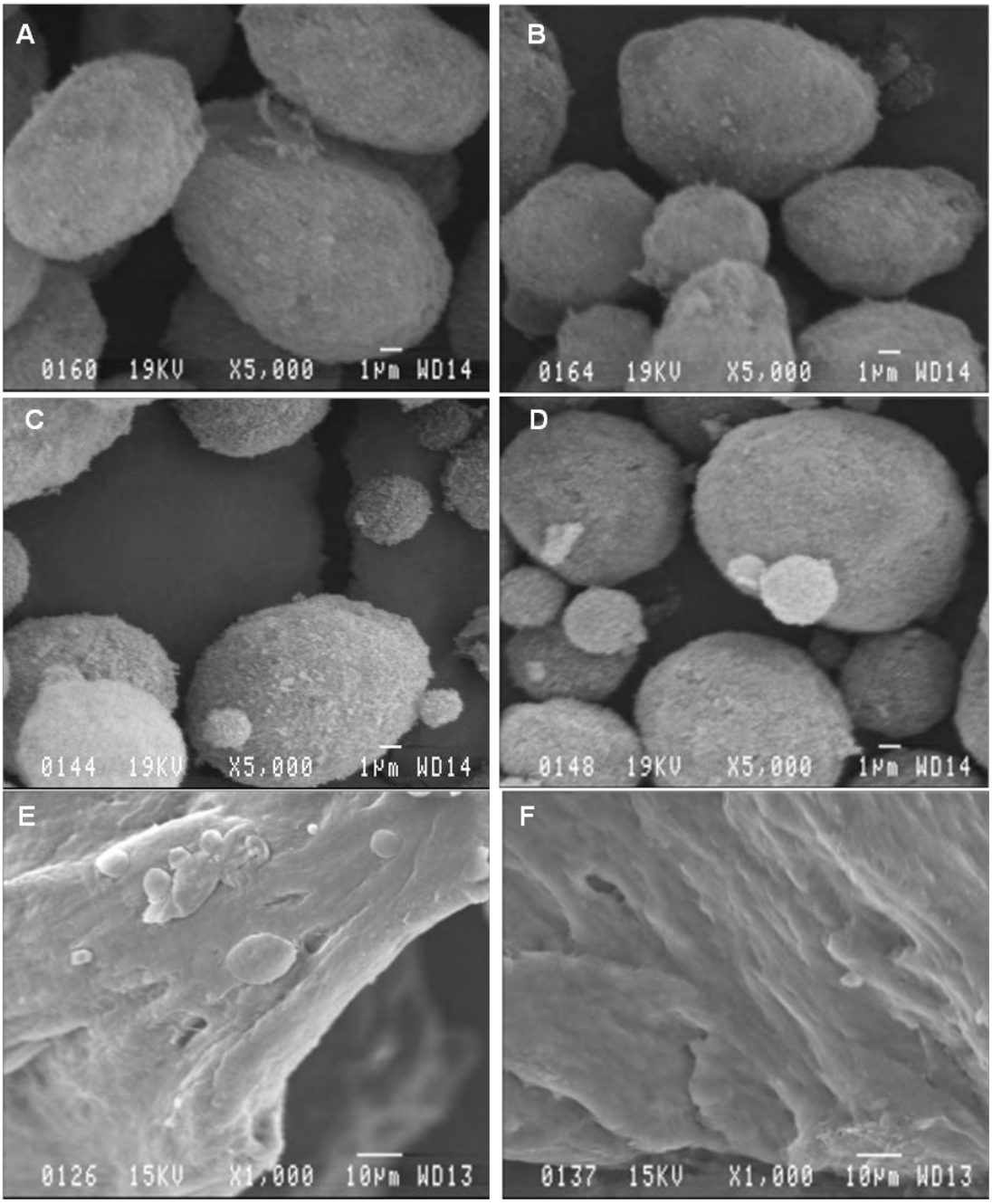

Figure 4.20 SEM of kafirin microparticles (KMP) and collagen standard at the end of binding period with BMP. **A**: KMP 22 (control); **B**: KMP 22 + BMP; **C**: KMP 75; **D**: KMP 75 + BMP; **E**: Collagen; **F**: Collagen + BMP. KMP 22– KMP held at ambient temperature (22°C) for 1 h KMP 75– KMP heated at 75°C for 1 h; BMP– bone morphogenetic protein.

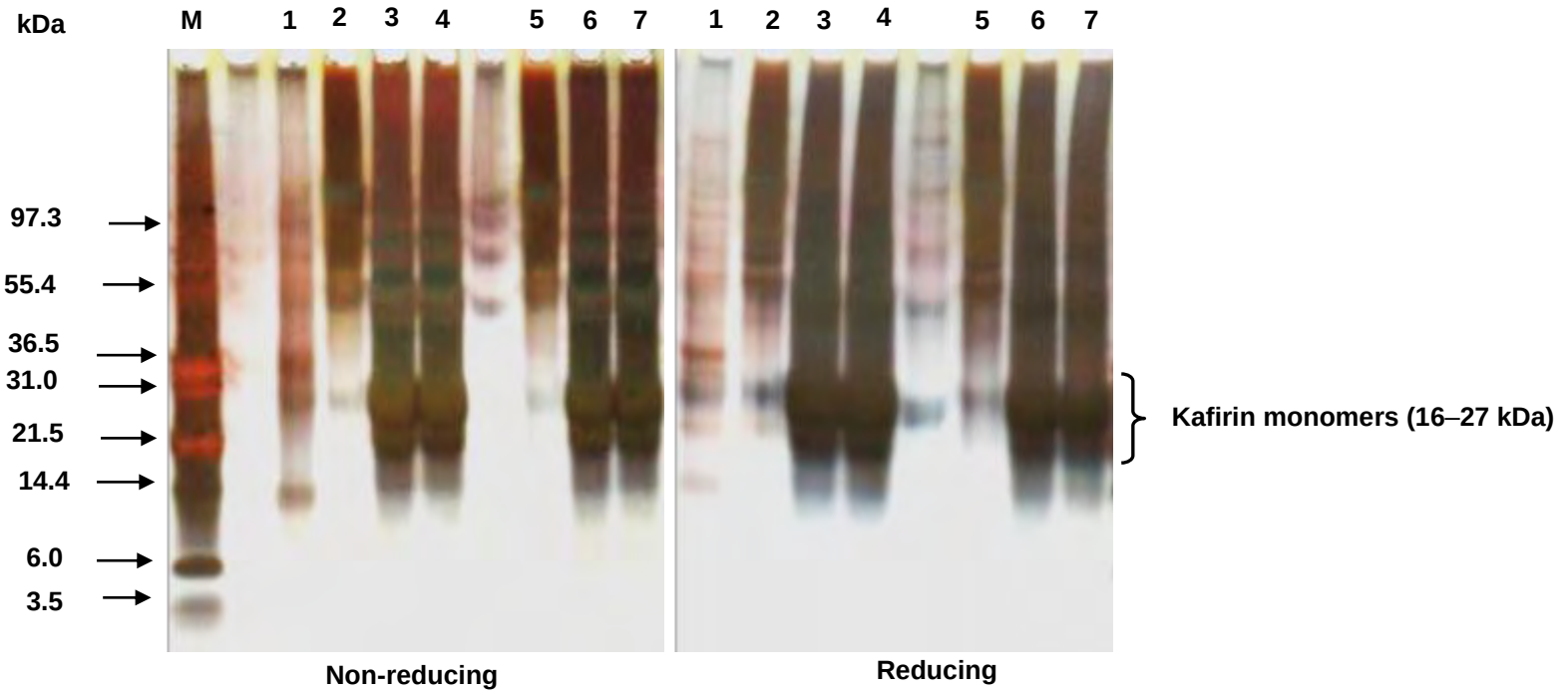

Figure 4.21 SDS-PAGE with silver staining of kafirin microparticles (KMP) and collagen standard after binding with BMP. Protein loading, 10 µg. Lanes M: Molecular markers; 1: BMP; 2: Collagen + BMP; 3: KMP 75 + BMP; 4: KMP 22 + BMP; 5: Collagen; 6: KMP 75; 7: KMP 22.

KMP 22– KMP held at ambient temperature (22°C) for 1 h; KMP 75– KMP heated at 75°C for 1 h; BMP– bone morphogenetic protein.

However, it is important to note that a minimum of 20 ng BMP-2/g binding material is acceptable (Dr Nicolaas Duneas, personal communication), which is a very low concentration. SDS-PAGE with Coomassie Brilliant Blue staining showed no changes in bands after BMP-2 binding (data not shown). Because silver stain has better sensitivity than Coomassie Brilliant Blue (Chevallet, Luche and Rabilloud, 2006), silver staining was used on the same gels previously stained with Coomassie Brilliant Blue after complete destaining in an attempt to detect any possible changes in molecular bands. No clear differences were found in the molecular weight distributions of the kafirin microparticles and collagen standard bound to BMP, compared to their controls using SDS-PAGE with silver staining (Figure 4.21). As with the SEM, it seems that the extremely low BMP complex concentration compared to the kafirin microparticles and collagen, probably made it unfeasible to detect any possible changes in molecular weight. Additionally, the very high sensitivity of silver staining made it difficult to see any differences due to the presence of ghost bands.

BMP-2 ELISA

As indicated, initially kafirin microparticles heat-treated at 75^{o}C was used along with collagen standard to confirm BMP-2 binding. This was because the Lowry protein assay showed closely similar binding profiles for the two binding materials (Figure 4.19). Preliminary ELISA confirmed that kafirin microparticles could bind the BMP-2 (Figure 4.22). Unlike the Lowry assay, ELISA showed reductions in BMP-2 concentration in supernatants with time. After 2 h reaction, the BMP-2 binding capacity of kafirin microparticles was about 15% higher than that of collagen standard. The binding between kafirin microparticles and BMP-2 was probably greater because of the presence of the pores within the kafirin microparticles in which the BMP-2 could diffuse during incubation. Also, as the interaction between BMP-2 and collagen probably involves electrostatic attraction (Patel et al., 2008), a similar but probably stronger interaction may have occurred between kafirin, pI 6 (Csonka et al., 1926) and BMP-2, pI 9 (Geiger, Li and Friess, 2003) given the higher pI of collagen (7.8) (Higberger, 1939). In fact, collagen has a relatively low affinity for BMP-2 (Ishikawa, Terai and Kitajima, 2001; Visser, Arrabal, Becerra, Rinas and Cifuentes, 2009). In addition, kafirin is very hydrophobic for a protein (Duodu et al., 2003). Hence, kafirin may have a better potential to bind to BMP-2, which has been shown to have a stronger attraction to hydrophobic surfaces (Utesch et al., 2011), probably due to the hydrophobic pockets formed by BMP-2 monomer residues (Nickel, Dreyer, Kirsch and

Sebald, 2001). As explained by Scheufler, Sebald and Hülsmeyer (1999), the isolated BMP-2 monomer by itself has no hydrophobic core, whereas a stable BMP-2 structure is achieved by homodimerization. Through interactions of helix α3 in a subunit with the β-sheets of the adjacent subunit, two tightly packed hydrophobic cores are generated, with hydrophobic packing being the most abundant form of subunit interactions in the BMP-2 homodimer.

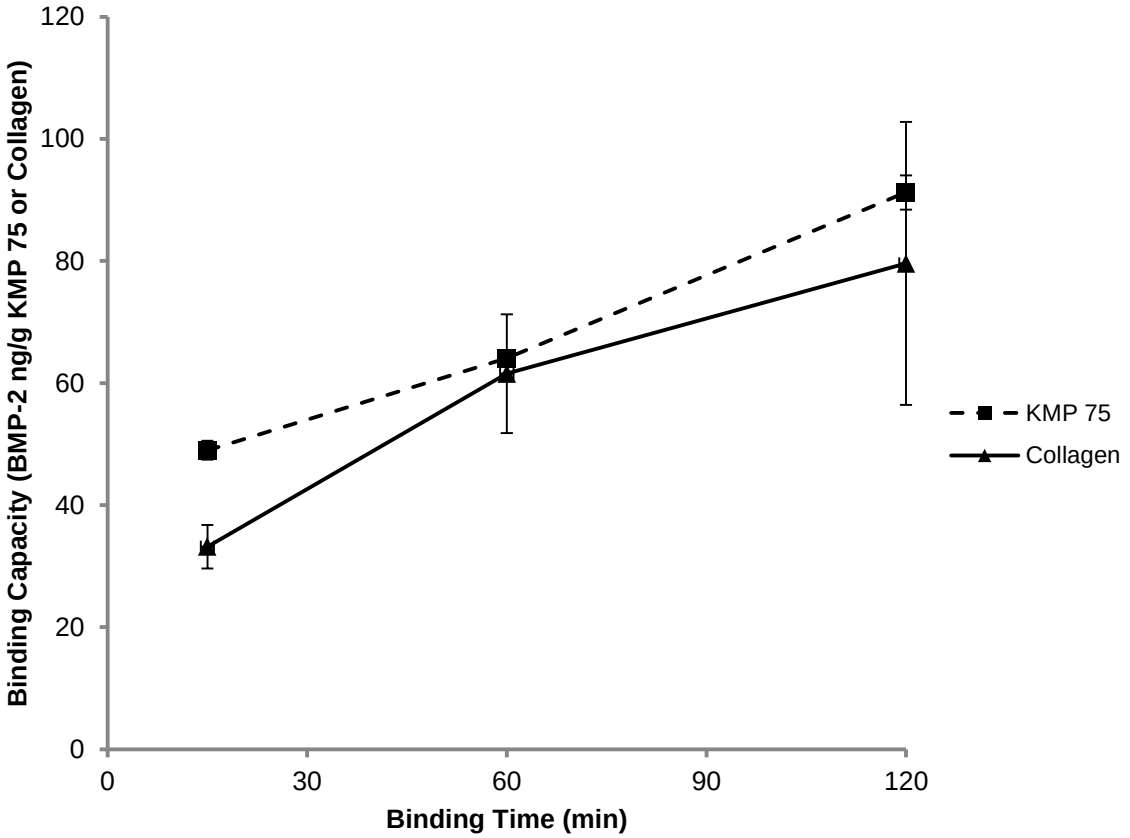

Figure 4.22 Preliminary BMP-2 binding capacity of kafirin microparticles (KMP) heat-treated at 75°C (KMP 75) compared to collagen standard during the first 120 min reaction period, determined by BMP-2 ELISA. The preliminary amounts of bound BMP-2 were calculated by determining the difference in amount of BMP-2 in solution at the beginning (first 2 min as reference point) and after binding for 15, 60 and 120 min time intervals. Error bars are standard deviations (n=2).

Having established from the preliminary binding assay that kafirin microparticles could bind BMP-2 within the first 120 min, a more comprehensive assessment was performed to determine the effects of treating kafirin microparticles with heat, transglutaminase and glutaraldehyde on BMP-2 binding capacity over a longer reaction period (24 h). Heat treatment of kafirin microparticles increased the BMP-2 binding capacity by up to 10%

(Figure 4.23 and Table 4.10), probably as a result of the increase in microparticle and vacuole size in the microparticles (Chapter 1). Ruhé, Boerman, Russel, Spauwen, Mikos and Jansen (2005) working with PLGA also in the form of microparticles reported an increase in BMP-2 entrapment efficiency with increase in particle size. Compared to the collagen standard, control and heat-treated kafirin microparticles had 7% and 18% higher BMP-2 binding capacity, respectively. Transglutaminase treatment of kafirin microparticles resulted in BMP-2 binding capacity 35% higher than collagen standard and an increase of 21% compared to control. As the transglutaminase reaction with kafirin probably occurred through deamidation due to the kafirin's very low lysine content, the excess negative charge may have enhanced electrostatic attraction with BMP-2, thereby resulting in the apparent higher BMP-2 binding capacity. Glutaraldehyde treatment of kafirin microparticles resulted in a BMP-2 binding capacity up to 14% higher than the control. This is probably because of increase in microparticle size, similar to heat treatment. Overall, transglutaminase treatment resulted in microparticles with the highest BMP-2 binding capacity after 1440 min reaction period. This corroborates the suggestion that the interaction between BMP-2 and carrier protein occurs through electrostatic attraction.

The BMP-2 binding obtained were in the range of 86–184 ng BMP-2/g kafirin microparticles and 102–137 ng BMP-2/g collagen depending on the treatment and incubation time. The literature gives both lower and higher BMP-2 binding capacity values compared to the figures in the present study. For example, a study by Friess, Uludag, Foskett, Biron and Sargeant (1999) showed that rhBMP-2 binding to collagen sponge was negligible at pH 3.0 and 4.0, while amounts of rhBMP-2 bound were up to 100000–200000 ng rhBMP-2 per mg collagen at pH 5.2 and pH 6.5. On the other hand, using PLGA microparticles, Ruhé et al. (2005) reported binding capacity values of 6000–7000 ng rhBMP-2 per mg PLGA microparticles. It has been found that apart from pH, many factors may influence the BMP-2 binding capacity, including concentration of the BMP-2 used in the binding process (Schrier and DeLuca, 1999), isoelectric point of the binding protein (Patel et al., 2008), ionic strength of the reaction medium (Geiger et al., 2003) and the method of loading of the BMP-2 to the carrier material (Ruhé et al., 2005). Therefore, these factors may explain the differences seen between BMP-2 binding capacity in the present study and literature values.

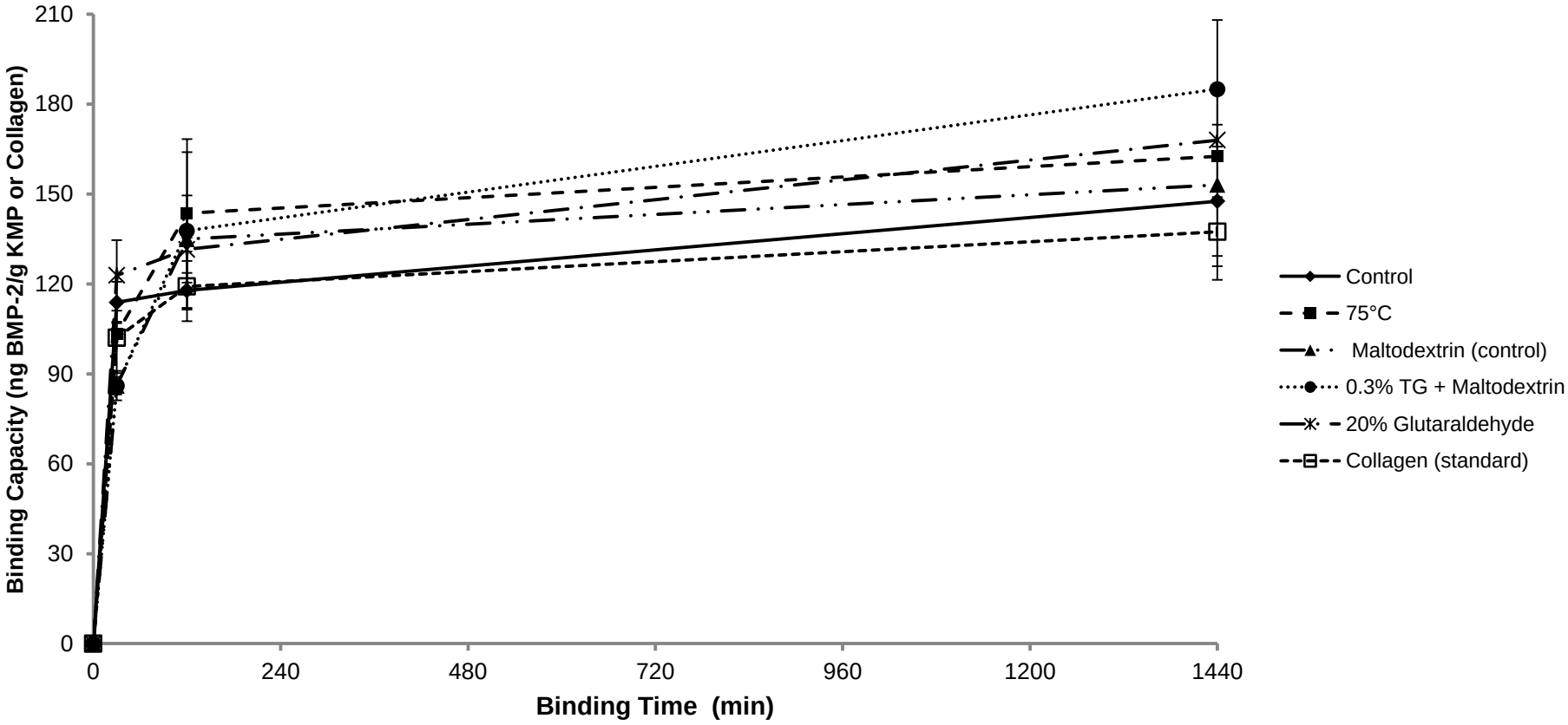

Figure 4.23 BMP-2 binding capacity of kafirin microparticles (KMP) treated with heat, transglutaminase and glutaraldehyde compared with collagen standard over a 24 h reaction period, determined by BMP-2 ELISA. Curves are plotted using mean relative BMP-2 binding capacity at the set time intervals. Error bars are standard deviations (n=2).

Table 4.10 Effects of treating kafirin microparticles with heat, transglutaminase (TG) and glutaraldehyde on their BMP-2 binding capacity (ng BMP-2/g binding material) compared with collagen standard over a 24 h reaction period, determined by BMP-2 ELISA (the data presented here show a statistical analysis of data in Figure 4.23)

Binding material	Treatment		Binding Time (min)		
			30	120	1440
Kafirin microparticles					
	Control	22°C	113.8 bc (6.9) [112]	117.8 a (5.8) [99]	147.6 ab (18.2) [107]
	Heat	75°C	103.4 b (3.9) [101]	143.5 a (24.8) [120]	162.5 ab (10.6) [118]
	Transglutaminase				
		Maltodextrin	86.0 a (2.9) [84]	135.0 a (14.6) [113]	153.0 ab (31.7) [111]
		0.3% TG + Maltodextrin	86.0 a (4.9) [84]	137.7 a (26.2) [116]	184.9 b (23.0) [135]
	Glutaraldehyde	20%	122.8 c (11.8) [120]	131.5 a (3.9) [110]	168.0 ab (16.3) [122]
Collagen standard			102.0 b (11.8)	119.2 a (11.7)	137.4 a (11.5)

Values in a column followed by different letters are significantly different ($p<0.1$). Numbers in ( ) brackets are standard deviations (n=2). Numbers in [ ] brackets are BMP-2 binding capacity of kafirin microparticles as percentage of corresponding binding capacity of collagen standard. Control for heat and glutaraldehyde treatments is the same

Having established that kafirin microparticles could bind BMP-2 in the BMP complex to similar or larger extent compared to collagen standard, the safety, biodegradability and efficacy of kafirin microparticle film-BMP-2 system in bone regeneration was assessed in the animal study. The purified rhBMP-2 was used in the ectopic rat study to preclude possible infection from the porcine BMP complex and to improve the chance of ectopic bone growth as rhBMP-2 appears to be about 10000 times more potent than partially purified BMP-2 for regenerating bone in rats as reviewed by Hollinger et al. (1998). The binding capacities (after 24 h reaction period) of the wet kafirin microparticle films and dry kafirin microparticle films to rhBMP-2 compared to the binding capacity of kafirin microparticles with the BMP-2 in the BMP complex, were approximately three-fold and five-fold lower, respectively (Table 4.11). Similarly, for the same reaction period, the binding capacity of collagen with the rhBMP-2 was about three-fold lower than that obtained with the BMP-2 in the BMP complex. With regard to the kafirin microstructures binding with BMP-2, the formation of kafirin microparticle film from the kafirin microparticles probably changed the morphology of the individual kafirin microparticles, thereby affecting their rhBMP-2 binding capacity. Formation of cast kafirin microparticle films is very similar to an evaporation-induced self-assembly (EISA), which as explained by Wang and Padua (2012), involves binary or tertiary solvents where preferential evaporation of one of the solvents changes the polarity of the solution, which drives the self-assembly of solutes. EISA has been found to result in alteration of the morphology of similar protein microstructures such as zein microspheres (Wang and Padua, 2010). As reported by these authors, the EISA-transformed structures may range from sponges to continuous films, which could have different physical properties compared to the microspheres. For example, Wang et al. (2008) reported a collapse of zein microspheres by EISA as a result of evaporation of methanol trapped within the microspheres. Therefore, in the present study, a similar scenario may have occurred in which the vacuoles within the kafirin microparticles could have collapsed during solvent evaporation to prepare the films, thereby reducing the capacity of the kafirin microparticle films to bind rhBMP-2. This probably resulted in most binding of kafirin microparticle films with rhBMP-2 occurring at the surface as well as in the pores probably created by the soaking and washing out of the plasticizer. In addition, the fact rhBMP-2 and the BMP complex are from different sources suggests that they are innately different. Hence, they may have had different physical and chemical properties, thereby causing differences in their affinity for collagen and kafirin microstructures. The binding data also showed that the wet kafirin

microparticle film had a similar rhBMP-2 binding capacity compared with collagen standard, which was higher than that of the dry kafirin microparticle film. However, these rhBMP-2 binding capacities were not statistically significantly different ($p>0.1$). Therefore, the wet kafirin microparticle film was used as carrier for the rhBMP-2 for ectopic rat bioassay due to its relatively higher mean rhBMP-2 binding capacity compared to dry kafirin microparticle film.

Table 4.11 RhBMP-2 binding capacity of kafirin microparticle films compared with collagen standard after a 24 h reaction period, determined by BMP-2 ELISA

Binding material		rhBMP-2 binding capacity (ng rhBMP-2/g binding material)
Wet kafirin microparticle film	soaked and surface water removed by placing film between paper towels	32.9 a (8.8)
Dry kafirin microparticle film	soaked and dried in a desiccator for 72 h	22.2 a (4.8)
Collagen	standard	31.5 a (1.2)

Values in a column followed by same letter are not significantly different ($p>0.1$). Numbers in the brackets are standard deviations (n=2).

4.3.4.2 *Implant safety assessment*

Evidence of toxicity was sought to assess the safety of the kafirin microparticle film implants when used to deliver BMP-2 to stimulate bone regeneration in a rat. By Day 7 post implantation, there was visible wound healing progress, indicated by the formation of scabs on the implant sites (Figure 4.24). By Day 28 post implantation, there was a complete healing of most of the wounds as evidenced by the faint marks at the external surface of the implant sites. Such observations indicate that the rats reacted normally to the trauma resulting from the skin surgery (Babensee et al., 1998).

The gross appearance of the implants by Day 28 post implantation was also examined. All the implants were surrounded by tissue capsules (Figure 4.25). There was some infiltration of blood vessels within the encapsulated collagen implants**.** There was no difference in gross appearance between collagen control and the rhBMP-2 loaded collagen. There was more prominent infiltration of blood vessels within the encapsulated kafirin microparticle film implants than with collagen.

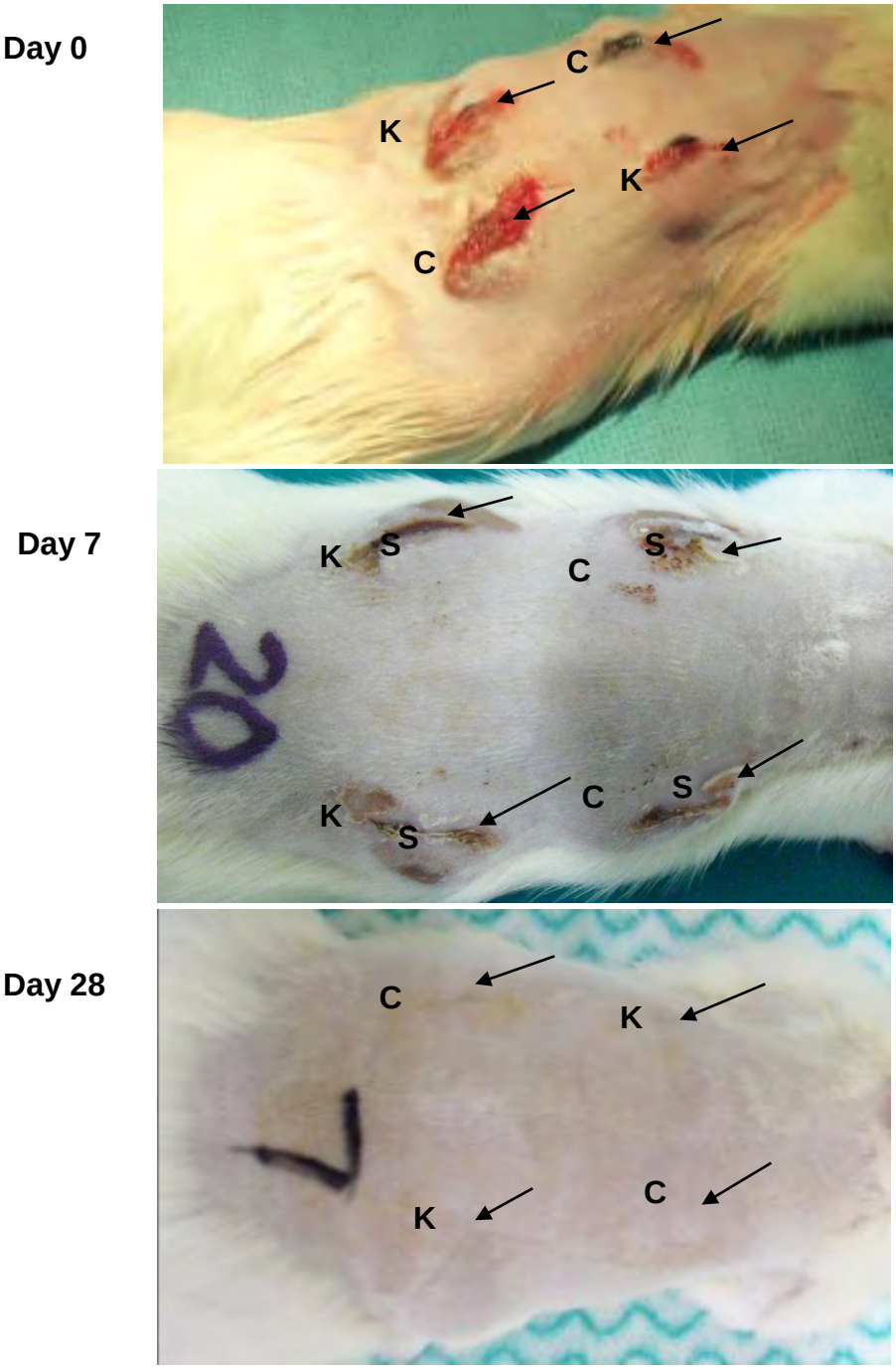

Figure 4.24 Typical appearance of implant sites by Day 0, 7, and 28 post implantation. Arrows point to implant sites. Note the occurrence of scabs denoted by 'S' by Day 7 post implantation and the healing by Day 28 post implantation. C-Collagen implant; K-kafirin microparticle film implant.

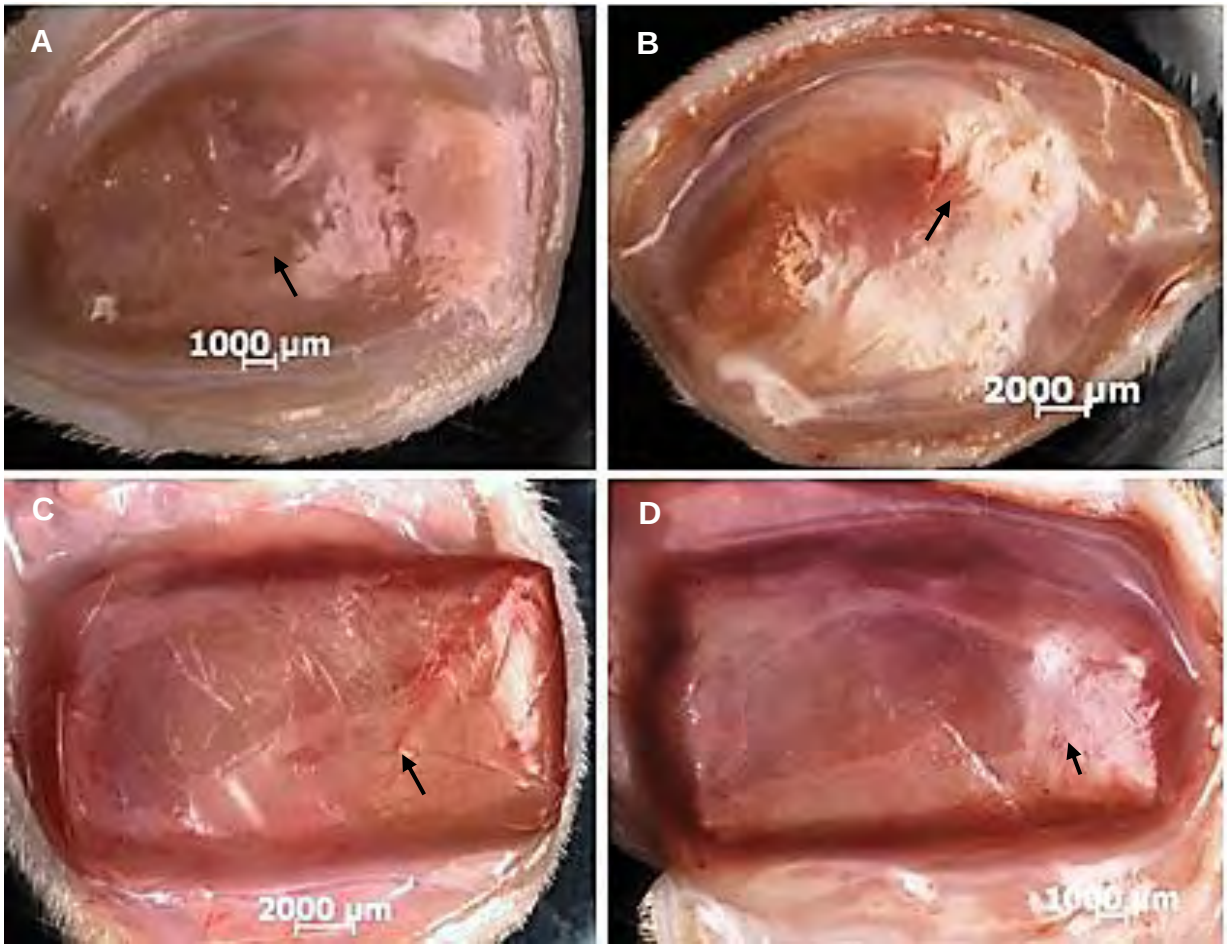

(i)

Figure 4.25 Gross appearance of encapsulated implants by Day 28 post implantation

(i) Plane view. **A**. Collagen control; **B**. Collagen+ rhBMP-2; **C**. Kafirin microparticle film control; **D**. Kafirin microparticle film+ rhBMP-2. Arrows point to blood vessels.

(ii) Cross-sectional view. **A**. Collagen control; **B**. Collagen+ rhBMP-2; **C** Kafirin microparticle film control; **D** Kafirin microparticle film+ rhBMP-2. Arrows are pointing at the encapsulated implant material.

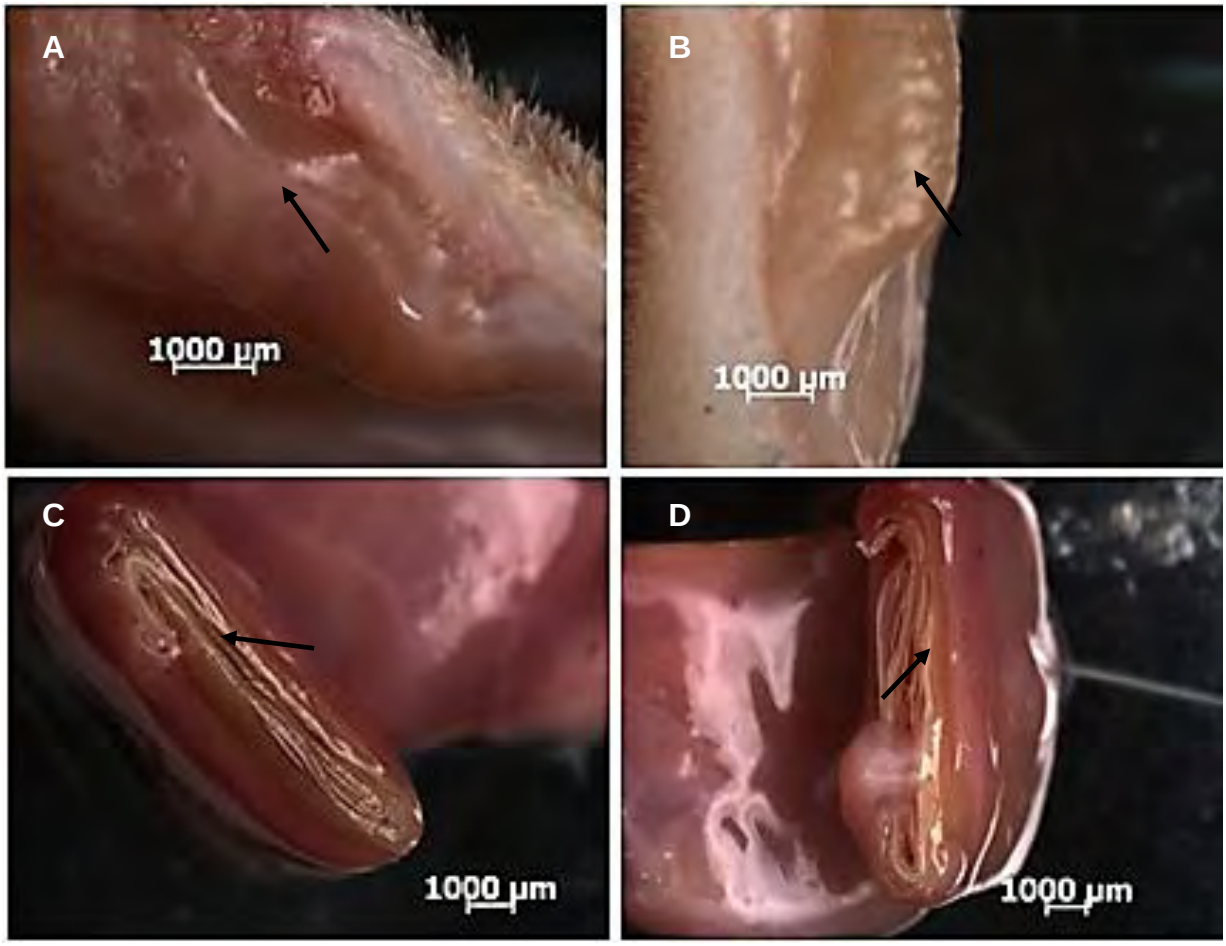

(ii)

As with the collagen standard, no difference in gross appearance was observed between the control and the rhBMP-2 loaded kafirin microparticle film implants. According to Nag and Banerjee (2012) there are four different types of tissue responses to the biomaterial implants concerning toxicity. Firstly, if the implant is toxic the surrounding tissue dies. Secondly, for a nontoxic and biologically inactive biomaterial, a fibrous tissue forms. Thirdly, if the biomaterial is nontoxic and active, the tissue bonds with it. Lastly, for a non-toxic and dissolving biomaterial implant, it is replaced by the surrounding tissue. According to the Idexx Laboratories report (Annex 2), macroscopic and histological evaluation did not show abnormal pathology for both rhBMP-2 loaded and unloaded kafirin microparticle film and collagen implants. As a measure of toxicity, tissue inflammatory response to the implants was examined. According to the Idexx Laboratories report (Annex 2), by Day 7 post implantation small microgranulomas were observed around all the implants, typical for a foreign body inflammatory reaction, with the response being more prominent for the collagen implant

compared to kafirin microparticle film implant (Table 4.12). The greater foreign body inflammatory reaction initially seen for the collagen implants possibly occurred as collagen was in a particulate matrix form while the kafirin microstructure was a film. According to Weiler, Helling, Kirch, Zirbes and Rehn (1996), the level of inflammatory cells present at the implant site is dependent on the amount of particles available for phagocytosis. In the case of the collagen implant with its granular form a large surface area would be available for phagocytosis with the result that more cells would migrate into the area of inflammation. In contrast, for the kafirin microparticle film the slow rate of biomaterial degradation meant that the surface area available to cells was much lower, hence resulting in a smaller degree of cellular attraction to the area. Further support for this theory can be seen by the presence of the multinucleated giant cells (Figure A3 in Annex 2). The presence of the giant cells is specific for the presence of poorly soluble, indigestible material in the tissue, as the smaller macrophages or epithelioid cells fuse (forming the giant cells) to enhance total phagocytic activity (reviewed by Rippey, 1994). By Day 28 post implantation, foreign body reaction was evident in all of the implantation sites. By this point post implantation, foreign body reaction varied from mild to severe with little difference between the collagen implants and the kafirin microparticle film implants.

Skin ulceration was examined as part of safety assessment. According to the Idexx Laboratories report (Annex 2), the areas of ulceration were small and microscopically confirmed at the implantation site on the surface of the skin that showed superficial exudative crusts and some areas of full-thickness epithelial necrosis. Mild inflammation was present in the dermis underneath the ulcerated skin. At Day 7 post implantation, these superficial ulcerations were found at both collagen and kafirin microparticle film implant sites. However, at Day 28 post implantation, superficial ulceration in the epidermis was found in only three collagen implantation sites (Table 4.12). As explained in the Idexx Laboratories report, the superficial skin ulceration was probably due to external irritation from animal scratching. The Idexx Laboratories report also indicated that dermal scarring due to the implantation was present underneath these ulcers and in some of the non-ulcerated sites. This was attributed to be probably part of the normal healing process. The fact that ulceration was found in only a few collagen implantation sites is possibly an indication of interspecies variation, which is an issue in toxicity testing using animal models (reviewed by Smart, Nicholls, Green, Rogers and Cook, 1999).

Table 4.12 Summary of Idexx Laboratories report on the histological scoring for inflammatory and osteogenic response of rat tissue to kafirin microparticle (KMP) film and collagen loaded with BMP-2 and polyphenol and glutaraldehyde treated KMP film implants by Day 7 and Day 28 post implantation

Day 7 post implantation

Carrier material	Treatment	Foreign body reaction	Granulomatous reaction	Ulcerated skin	Osteolysis[#]	Osteogenesis
Collagen						
	Control	+++ (1), ++ (3)	+++ (4)	++ (1), + (2), - (1)	+++ (2), ++ (2)	- (4)
	Low rhBMP-2*	+++ (1), ++ (2)	+++ (3)	+ (2), - (1)	+++ (1), ++ (2)	- (3)
	High rhBMP-2	+++(1), ++ (3)	+++ (4)	+ (3), - (1)	+++ (1), ++ (2), + (1)	- (4)
KMP film						
	Control	+ (1), - (3)	++ (1), + (3)	++ (1), + (2), - (1)	- (4)	- (4)
	Low rhBMP-2	++ (1), + (1), - (2)	+++ (1), ++ (1), + (2)	++ (2), + (1), - (1)	- (4)	- (4)
	High rhBMP-2	+ (1), - (3)	+++ (1), ++ (1), + (2)	+++ (1), - (3)	- (4)	- (4)
	Glutaraldehyde	+ (1), - (3)	+ (4)	+ (3), - (1)	- (4)	- (4)
	Polyphenol	++ (1), + (1), - (2)	+++ (1), ++ (1), + (2)	++ (1), + (2), - (2)	- (4)	- (4)

(Continued over leaf)

Day 28 post implantation

Carrier material	Treatment	Foreign body reaction	Granulomatous reaction	Ulcerated skin	Osteolysis[#]	Osteogenesis
Collagen						
	Control	+++ (3), + (1)	+++ (3), ++ (1)	+ (1), - (3)	+++ (1), ++ (3)	- (4)
	Low rhBMP-2	++ (4)	+++ (2), ++ (1), + (1)	+ (1), - (3)	++ (2), + (2)	- (4)
	High rhBMP-2	+++(2), ++ (2)	+++ (1), ++ (2), + (1)	+ (1), - (3)	+++ (1), ++ (3)	+ (1), - (3)
KMP film						
	Control	++ (2), + (2)	+++ (1), ++ (2), + (1)	- (4)	+++ (1), ++ (2), - (1)	- (4)
	Low rhBMP-2	++ (3), + (1)	+++ (2), ++ (1), + (1)	- (4)	++ (2), + (1), - (1)	- (4)
	High rhBMP-2	++ (3), + (1)	+++ (1), ++ (2), + (1)	- (4)	++ (1), + (2), - (1)	- (4)

Results were graded as follows: negative/none (-), mild (+), moderate (++), severe (+++). The number of implants with the indicated score is in the brackets. Total number of implants per treatment =4. RhBMP-2 Dose: Control=0 µg/g, Low=0.107 µg/g; High=2.14 µg/g

* One implant sample lost

NB: The treatments were coded before evaluation by Idexx Laboratories.

[#] Osteolysis was used as measure of degradation of the implant material (Dr W.S. Botha, Idexx Laboratories, personal communication post submission of the Idexx report).

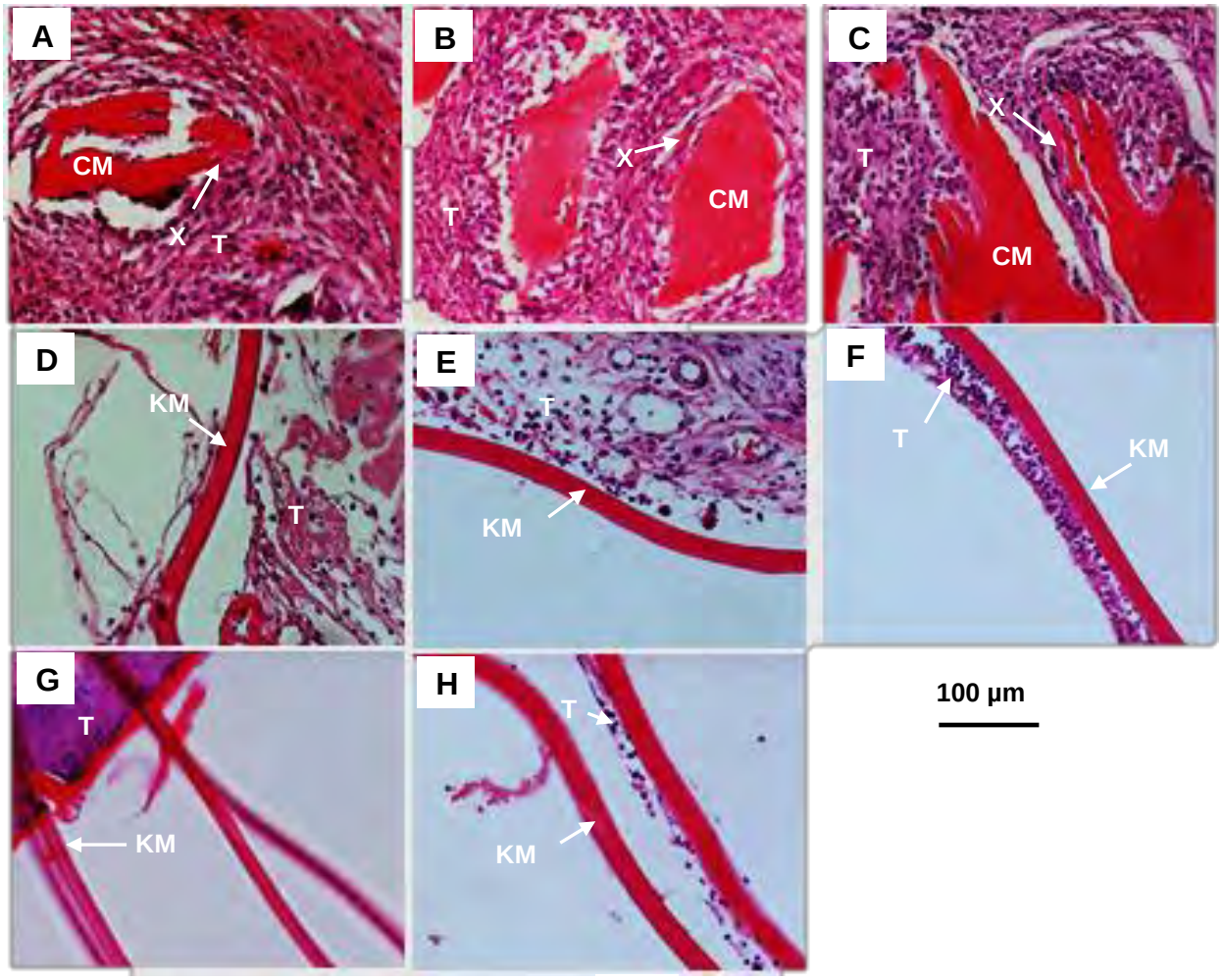

(i)

Figure 4.26 Images of haematoxylin–eosin stained sections of implants showing evidence of degradation of implants. The photographs were taken of slides prepared by Idexx Laboratories for the report (Annex 2).

(i) Day 7 post implantation. **A.** Collagen control. **B.** Collagen + low rhBMP-2 dose. **C.** Collagen + high rhBMP-2 dose. **D.** Kafirin microparticle film control. **E.** Kafirin microparticle film + low rhBMP-2 dose. **F.** Kafirin microparticle film + high rhBMP-2 dose. **G.** Glutaraldehyde-treated kafirin microparticle film. **H.** Polyphenol-treated kafirin microparticle film. KM-Kafirin microparticle film material; CM-Collagen material, T-Tissue. X-Degraded section of implant.

(ii) Day 28 post implantation. **A.** Collagen control. **B.** Collagen + low rhBMP-2 dose. **C.** Collagen + high rhBMP-2 dose. **D.** Kafirin microparticle film control. **E.** Kafirin microparticle film + low rhBMP-2 dose. **F.** Kafirin microparticle film + high rhBMP-2 dose. KM- Kafirin microparticle film material; CM-Collagen material, T-Tissue. NB. Glutaraldehyde-treated and polyphenol-treated kafirin microparticle film implants were only subjected to a 7-day implantation. X-Degraded section of implant.

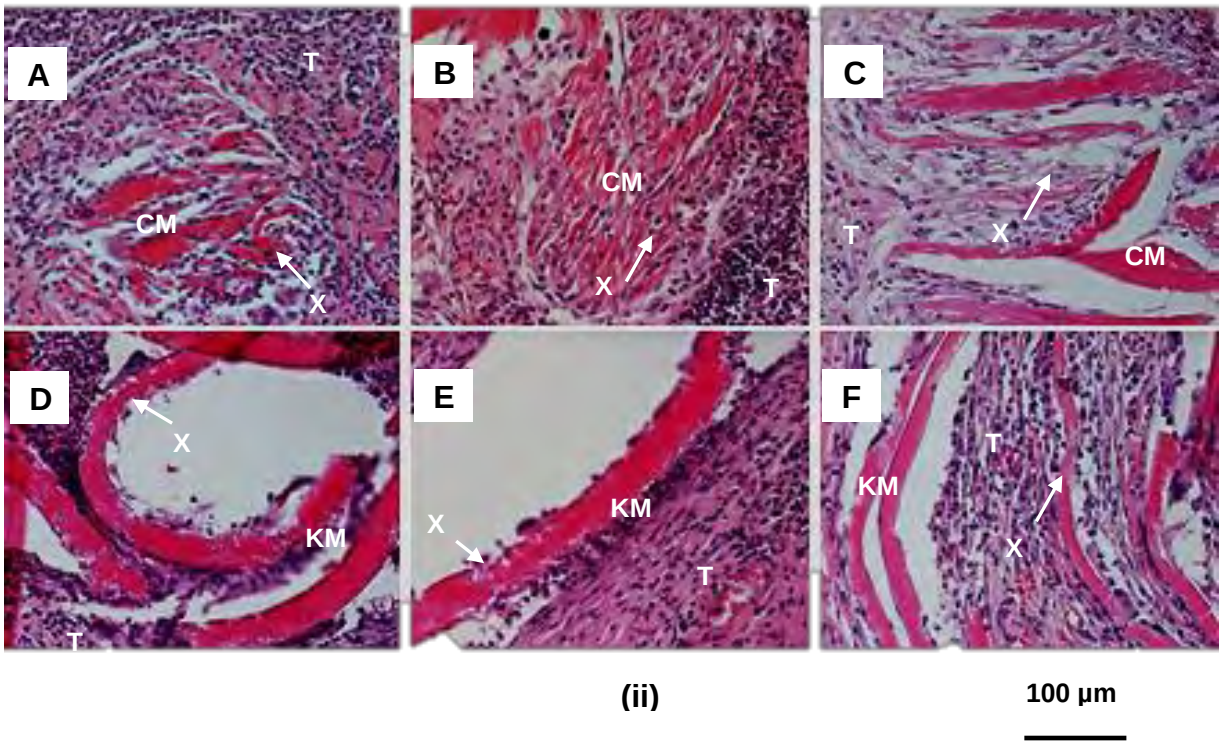

Overall, according to the Idexx report the safety assessment data showed that kafirin microparticle film implants were non-irritant to the animals. This is probably because kafirin is non-allergenic (Ciacci et al., 2007) as it does not contain the amino acid sequences known to be toxic (reviewed by Wieser and Koehler, 2008).

4.3.4.3 *Evidence of implant degradation*

Lysis of the implant was used as a measure of implant degradation (Dr W.S. Botha, Idexx Laboratories, personal communication post submission of the Idexx report). According to Idexx Laboratories report (Annex 2), by Day 7 post implantation, degradation of the collagen implants had started, as indicated by resorption of the implant material, while the kafirin microparticle film implants were all intact (Table 4.12 and Figure 4.26 (i)). By Day 28 post implantation, most of the collagen implants had completely degraded (Figure 4.26 (ii)). In contrast, the kafirin microparticle film implants showed signs of some degradation but a large proportion of these implants was still intact. Studies have found that collagen implants degrade relatively quickly as a result of proteolysis. For example, Brown, Li, Guda, Perrien, Guelcher and Wenke (2011) worked on biodegradable polyurethane microsphere scaffolds compared to collagen sponge delivery system for release of rhBMP-2 in a critical-sized rat segmental defect model. These authors reported in their histological evaluation of the tissues with scaffold implants that after four weeks post implantation the polyurethane scaffolds

were still visible, but the collagen carrier had been degraded. In the present study, the fact that kafirin microparticle film implants were still largely intact by Day 28 post implantation indicated that the kafirin microparticle films were biodegradable but at a slower rate, probably due to the low susceptibility of kafirin to proteolysis (Emmambux and Taylor, 2009), as result of its hydrophobicity, as discussed.

Another factor that may have contributed to the more rapid degradation of the collagen implants compared to kafirin microparticle film implants was probably the differences in size of the implants. Despite the fact that the implants were of the same weight, the collagen implants were smaller but with a large surface area due to its granulated form. On the other hand, kafirin microparticle films were folded which may have changed how they degraded.

4.3.4.4 *Evidence of ectopic bone morphogenesis*

Radiographs of the rats post-mortem showed no indication of new bone for any of the implants by Day 28 post implantation (Figure 4.27). This was confirmed by histological evaluation by Idexx Laboratories (Annex 2). By Day 7 post implantation, osteogenesis appeared to be absent in the implants sites (Table 4.12). Histological evaluation, however, did indicate mild osteogenesis by Day 28 post implantation in one of the collagen implant sites. Alkaline phosphatase (ALP) activity was evaluated as a chemical pathological marker of early osteoblast differentiation, because ALP activity is expected to be elevated in case of an increased osteoblastic activity as bone ALP is localised in the plasma membrane of osteoblastic cells (reviewed by Withhold, Schulte and Reinauer, 1996). No substantial change in the ALP activity was evident for either BMP-2 loaded collagen or the kafirin microparticle films (Table 4.13) in agreement with the findings from the radiographs and the histopathology. The collagen implants nonetheless seemed to have significantly higher ALP than the kafirin microparticle film implants ($p<0.05$), probably because collagenous implants have the ability to induce some bone morphogenesis (Hollinger et al., 1998). However, the results in the present study were confounded by the apparent reduction of physically visible collagen implant material, probably due to digestion by tissue enzymes, while the kafirin microparticle film implants maintained their integrity. Hence, the collagen implant samples used in ALP assay probably had a relatively higher content of animal tissue material obtained from the implant site than the kafirin microparticle film implant material. This greater amount of tissue material in the collagen implants may have resulted in the apparently higher ALP activity value, as a result of contribution from serum ALP.

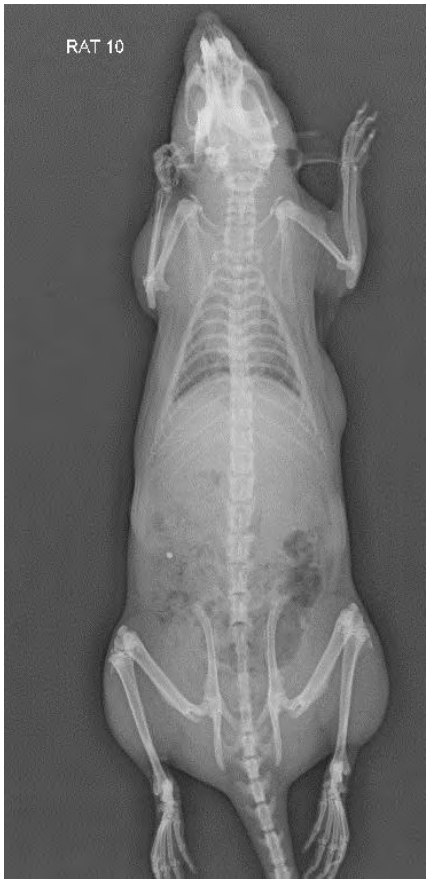

Figure 4.27 Representative radiograph of rat by Day 28 post implantation. All the radiographs of the rats with implantations were similar.

Table 4.13 Alkaline phosphatase (ALP) activity of capsule and kafirin microparticle film or collagen standard implants loaded with rhBMP-2 after 28 days of implantation

Carrier material	rhBMP-2 Dose	ALP concentration (pmol/g capsule + implant)	ALP concentration (pmol/g capsule*)
Collagen			
	Control	174.3 c (11.5)	
	Low	184.3 c (8.6)	
	High	244.3 d (7.4)	
Kafirin microparticle film			
	Control	111.0 b (3.8)	195.4 c (6.6)
	Low	72.4 a (8.2)	95.6 a (10.8)
	High	118.6 b (8.4)	130.1 b (9.2)

Values in a column followed by different letters are significantly different ($p<0.05$). Numbers in the brackets are standard deviations, (n=4)

*Collagen was digested by the tissue enzymes; hence, it was impractical to calculate concentration of the ALP in the tissue without collagen implant

RhBMP-2 Dose: Control=0 µg/g, Low=0.107 µg/g; High=2.14 µg/g

ALP activity is not specific for bone growth as other body organs such as the liver and intestines also form the enzyme (reviewed by Hoffmann et al., 1994). The radiology, histology and ALP data all indicated the absence of ectopic bone morphogenesis induced by kafirin microparticle film-rhBMP-2 or the collagen-rhBMP-2 system.

A patent of Duneas (2010) states that a collagen and BMP complex system can induce bone growth in rats, as measured by ALP activity, as early as 12 days post implantation. While it could not be ascertained why the implant failed to induced to osteogenesis, a number of reasons are plausible. First, the rhMBP-2 dose was possibly too low, particularly in comparison to the BMP complex applied in the work by Duneas (2010), which was 100000 ng per implant. Although low BMP-2 dosage levels in a carrier-BMP-2 system could induce bone growth (Dr Nicolaas Duneas, personal communication), the wide range of BMP-2/rhBMP-2 doses, the different animal models and the different implantation durations used in similar studies made it difficult to determine the appropriate BMP-2 dosage. For example, Bessa et al. (2010) working with silk fibroin microparticles reported bone morphogenesis measured by ALP activity in a rat model when they used 5 µg and 12.5 µg BMP-2 per implantation site. Similarly, Yasko, Lane, Fellinger, Rosen, Wozney and Wang (1992) working with demineralized rat-bone matrix as a carrier applied 1400000 ng and 11000000 ng rhBMP-2 per implant site and reported bone growth determined by radiology, histology and mechanical analysis. The BMP-2 levels used by these workers were greater than the 8 ng and 160 ng rhBMP-2 per implant that was used in the present study or the 1 ng BMP-2 per implant used by Fu, Nie, Ho, Wang and Wang (2008) in their study using a nude mice model. The choice of the relatively low rhBMP-2 dosage in the present study was motivated by the higher potency of rhBMP-2, which has been reported to be about 10000 times more than partially purified BMP-2 for regenerating bone in rats (reviewed by Hollinger et al, 1998).

Secondly, the duration of study was probably too short and therefore insufficient to induce osteogenesis. Although Wang, Rosen, D'Alessandro, Bauduy, Cordes, Harada, Israel, Hewick, Kerns, Lapan, Luxenberg, McQuaid, Moutsatsos, Nove and Wozney (1990) and Bessa et al. (2010) reported BMP-2 induced ectopic bone morphogenesis measured by ALP activity in rats within a month post implantation, many researchers have also found substantial subcutaneous bone morphogenesis induced by BMP-2 loaded biomaterials after a longer time post implantation, usually greater than three months (reviewed by Babensee et al., 1998; Kempen, Lu, Hefferan, Creemers, Maran, Classic, Dhert and Yaszemski, 2008).

Thirdly, immune sensitization may have occurred since the rhBMP-2 could have induced an immune reaction such as osteolysis of regenerated bone as the animals were immunocompetent. Other additional factors that may have also caused the disparity of results in the present study and those in literature include differences in placement site for the implants and differences in age of the animals (Prof Vinny Naidoo, University of Pretoria Biomedical Research Centre, personal communication). Therefore, it was difficult to make a direct comparison between the rat tissue response to kafirin microparticle film-BMP-2 system in the present study and data from the similar systems in the literature.

4.3.5 Conclusions

Kafirin microparticles can bind BMP-2. This binding is enhanced through modification by heat, transglutaminase or glutaraldehyde treatment. Also, kafirin microparticle film is non-toxic showing no abnormal inflammatory reactions when implanted subcutaneously in a rat. In addition, kafirin microparticle film shows a prolonged degradation when implanted in an animal tissue, which is a great advantage as the kafirin microparticle film implants can eventually degrade after their scheduled "task" is complete by the body's own metabolic process. The kafirin microstructures could therefore have application as biomaterials such as bioactive scaffolds for hard or soft tissue repair. However, at the low BMP-2 levels (107–2140 ng/g) and for the short implantation period (28 days), the kafirin microparticle film-BMP-2 does not induce bone morphogenesis in the rat model. Therefore more work needs to be done to optimize BMP-2 loading and release profile with kafirin microstructures.

4.3.6 References

Babensee, J.E., 1990. Morphological assessment of HEMA-MMA microcapsules for liver cell transplantation. PhD Thesis, University of Toronto, Toronto.

Babensee, J.E., Anderson, J.M., McIntire, L.V., Mikos, A.G., 1998. Host response to tissue engineered devices. Advanced Drug Delivery Reviews 33, 111–139.

Balmayor, E.R., Feichtinger, G.A., Azevedo, H.S., Van Griensven, M., Reis, R.L., 2009. Starch-poly-ε-caprolactone microparticles reduce the needed amount of BMP-2. Clinical Orthopaedics and Related Research 467, 3138–3148.

Bensaid, W., Triffitt, J.T., Blanchat, C., Oudina, K., Sedel, L., Petite, H., 2003. A biodegradable fibrin scaffold for mesenchymal stem cell transplantation. Biomaterials 24, 2497–2502.

Bessa, P.C., Balmayor, E.R., Hartinger, J., Zanoni, G., Dopler, D., Meinl, A., Banerjee, A., Casal, M., Redl, H., Reis, R.L., Van Griensven, M., 2010. Silk fibroin microparticles as carriers for delivery of human recombinant bone morphogenetic protein-2: in vitro and in vivo bioactivity. Tissue Engineering: Part C 16, 937–945.

Bessa, P.C., Casal, M., Reis, R.L., 2008. Bone morphogenetic proteins in tissue engineering: the road from laboratory to clinic, Part II (BMP delivery). Journal of Tissue Engineering and Regenerative Medicine 2, 81–96.

Brown, K.V., Li, B., Guda, T., Perrien, D.S., Guelcher, S.A., Wenke, J.C., 2011. Improving bone formation in a rat femur segmental defect by controlling bone morphogenetic protein-2 release. Tissue Engineering: Part A 17, 1735–1746.

Chen, D., Zhao, M., Mundy, G.R., 2004. Bone morphogenetic proteins. Growth Factors 22, 233–241.

Chevallet, M., Luche, S., Rabilloud, T., 2006. Silver staining of proteins in polyacrylamide gels. Nature Protocols 1, 1852–1858.

Ciacci, C., Maiuri, L., Caporaso, N., Bucci, C., Del Giudice, L., Massardo, D.R., Pontieri, P., Di Fonzo, N., Bean, S.R., Ioerger, B., Londei, M., 2007. Celiac disease: in vitro and in vivo safety and palatability of wheat-free sorghum food products. Clinical Nutrition 26, 799–805.

Csonka, F.A., Murphy, J.C., Jones, D.B., 1926. The iso-electric points of various proteins. Journal of the American Chemical Society 48, 763–768.

Cuq, B., Gontard, N., Guilbert, S., 1998. Proteins as agricultural polymers for packaging production. Cereal Chemistry 75, 1–9.

Duneas, N., 2010. Osteoinductive biomaterials. European Patent Office EP 1 539 812 B1.

Duodu, K.G., Taylor, J.R.N., Belton, P.S., Hamaker, B.R., 2003. Factors affecting sorghum protein digestibility. Journal of Cereal Science 38, 117–131.

Emmambux, N.M., Taylor, J.R.N., 2003. Sorghum kafirin interaction with various phenolic compounds. Journal of the Science of Food and Agriculture 83, 402–407.

Emmambux, N.M., Taylor, J.R.N., 2009. Properties of heat-treated sorghum and maize meal and their prolamin proteins. Journal of Agricultural and Food Chemistry 57, 1045–1050.

Friess, W., Uludag, H., Foskett, S., Biron, R., Sargeant, C., 1999. Characterization of absorbable collagen sponges as rhBMP-2 carriers. International Journal of Pharmaceutics 187, 91–99.

Fu, Y.-C., Nie, H., Ho, M.-L., Wang, C.-K., Wang, C.-H., 2008. Optimized bone regeneration based on sustained release from three-dimensional fibrous PLGA/Hap composite scaffolds loaded with BMP-2. Biotechnology and Bioengineering 99, 996–1006.

Gautschi, O.P., Frey, S.P., Zellweger, R., 2007. Bone morphogenetic proteins in clinical applications. ANZ Journal of Surgery 77, 626–631.

Geiger, M., Li, R.H., Friess, W., 2003. Collagen sponges for bone regeneration with rhBMP-2. Advanced Drug Delivery Reviews 55, 1613–1629.

Haidar, Z.S., Hamdy, R.C., Tabrizian, M., 2009. Delivery of recombinant bone morphogenetic proteins for bone regeneration and repair. Part B: Delivery systems for BMPs in orthopaedic and craniofacial tissue engineering. Biotechnology Letters 31, 1825–1835.

Higberger, J.H., 1939. The isoelectric point of collagen. Journal of the American Chemical Society 61, 2302-2303.

Hoffmann, W.E., Everds, N., Pignatello, M., Solter, P.F., 1994. Automated and semiautomated analysis of rat alkaline phosphatase isoenzymes. Toxicologic Pathology 22, 633–638.

Hollinger, J.O., Schmitt, J.M., Buck, D.C., Shannon, R., Joh, S.P., Zegzula, H.D., Wozney, J., 1998. Recombinant human bone morphogenetic protein-2 and collagen for bone regeneration. Journal of Biomedical Materials Research 43, 356–364.

Ishikawa, T., Terai, H., Kitajima, T., 2001. Production of a biologically active epidermal growth factor fusion protein with high collagen affinity. Journal of Biochemistry 129, 627–633.

Kempen, D.H.R., Lu, L., Hefferan, T.E., Creemers, L.B., Maran, A., Classic, K.L., Dhert, W.J.A., Yaszemski, M.J., 2008. Retention of in vitro and in vivo BMP-2 bioactivities in sustained delivery vehicles for bone tissue engineering. Biomaterials 29, 3245–3252.

Kiernan, J.A., 2000. Formaldehyde, formalin, paraformaldehyde and glutaraldehyde: What they are and what they do. Microscopy Today 00-1, 8–12.

Kim, C.-S., Kim, J.-I., Kim, J., Choi, S.-H., Chai, J.-K., Kim, C.-K., Cho, K.-S., 2005. Ectopic bone formation associated with recombinant human bone morphogenetic proteins-2 using absorbable collagen sponge and beta tricalcium phosphate as carriers. Biomaterials 26, 2501–2507.

King, G.N., Cochran, D.L., 2002. Factors that modulate the effects of bone morphogenetic protein-induced periodontal regeneration: a critical review. Journal of Periodontology 73, 925–936.

La, W.-G., Kang, S.-W., Yang, H.S., Bhang, S.H., Lee, S.H., Park, J.-H, Kim, B.-S., 2010. The efficacy of bone morphogenetic protein-2 depends on its mode of delivery. Artificial Organs 34, 1150–1153

Lowry, O.H., Rosebrough, N.J., Farr, A.L., Randall, R.J., 1951. Protein measurement with the Folin phenol reagent. Journal of Biological Chemistry 193, 265–275.

Nag, S., Banerjee, R., 2012. Fundamentals of medical implant materials. In: Narayan, R. (Ed.), ASM Handbook: Materials for Medical Devices. ASM International: Russell Township, OH, Vol. 23, pp. 6–17.

Nickel, J., Dreyer, M.K., Kirsch, T., Sebald, W., 2001. The crystal structure of the BMP-2:BMPR-IA complex and the generation of BMP-2 antagonists. Journal of Bone and Joint Surgery 83-A (Suppl. 1, Part 1), S7–S14.

Patel, Z.S., Yamamoto, M., Ueda, H., Tabata, Y., Mikos, A.G., 2008. Biodegradable gelatin microparticles as delivery systems for the controlled release of bone morphogenetic protein-2. Acta Biomaterialia 4, 1126–1138.

Ripamonti, U., Duneas, N., Van Den Heever, B., Bosch, C., Crooks, J., 1997. Recombinant transforming growth factor-β1 induces endochondral bone in the baboon and synergizes with recombinant osteogenic protein-1 (bone morphogenetic protein-7) to initiate rapid bone formation. Journal of Bone and Mineral Research 12, 1584–1595.

Rippey, J.J., 1994. General Pathology. Illustrated Lecture Notes. (2nd ed.), Wits University Press: Johannesburg, South Africa, pp. 151–152.

Ruhé, P.Q., Boerman, O.C., Russel, F.G.M., Spauwen, P.H.M., Mikos, A.G., Jansen, J.A., 2005. Controlled release of rhBMP-2 loaded poly(DL-lactic-co-glycolic acid)/calcium phosphate cement composites in vivo. Journal of Controlled Release 106, 162–171.

Scheufler, C., Sebald, W., Hülsmeyer, M., 1999. Crystal structure of human bone morphogenetic protein-2 at 2.7 Å resolution. Journal of Molecular Biology 287, 103–115.

Schrier, J.A., DeLuca, P.P., 1999. Recombinant human bone morphogenetic protein-2 binding and incorporation in PLGA microsphere delivery systems. Pharmaceutical Development and Technology 4, 611–621.

Shah, P, Keppler, L., Rutkowski, J., 2011. A review of bone morphogenic protein: an elixir for bone grafting. Journal of Oral Implantology (in press) DOI: http://0-dx.doi.org.innopac.up.ac.za/10.1563/AAID-JOI-D-10-00196.

Silva, G.A., Ducheyne, P., Reis, R.L., 2007. Materials in particulate form for tissue engineering. 1. Basic concepts. Journal of Tissue Engineering and Regenerative Medicine 1, 4–24.

Singleton, V.L., Rossi, J., 1965. Colorimetry of total phenolics with phosphomolybdic-phosphotungstic acid reagents. American Journal of Enology and Viticulture 16, 144–158.

Smart, J.D., Nicholls, T.J., Green, K.L., Rogers, D.J., Cook, J.D., 1999. Lectins in drug delivery: a study of the acute local irritancy of the lectins from *Solanum tuberosum* and *Helix pomatia*. European Journal of Pharmaceutical Sciences 9, 93–98.

Taylor, J., Taylor, J.R.N., Belton, P.S., Minnaar, A., 2009a. Formation of kafirin microparticles by phase separation from an organic acid and their characterisation. Journal of Cereal Science 50, 99–105.

Taylor, J., Taylor, J.R.N., Belton, P.S., Minnaar, A., 2009b. Kafirin microparticle encapsulation of catechin and sorghum condensed tannins. Journal of Agricultural and Food chemistry 57, 7523–7528.

Tu, J., Wang, H., Li, H., Dai, K., Wang, J., Zhang, X., 2009. The in vivo bone formation by mesenchymal stem cells in zein scaffolds. Biomaterials 30, 4369–4376.

Utesch, T., Daminelli, G., Mroginski, M.A., 2011. Molecular dynamics simulations of the adsorption of bone morphogenetic protein-2 on surfaces with medical relevance. Langmuir 27, 13144–13153.

Visser, R., Arrabal, P.M., Becerra, J., Rinas, U., Cifuentes, M., 2009. The effect of an rhBMP-2 absorbable collagen sponge-targeted system on bone formation in vivo. Biomaterials 30, 2032–2037.

Wang, E.A., Rosen, V., D'Alessandro, J.S., Bauduy, M., Cordes, P., Harada, T., Israel, D.I., Hewick, R.M., Kerns, K.M., Lapan, P., Luxenberg, D.P., McQuaid, D., Moutsatsos, I.K., Nove, J., Wozney, J.M., 1990. Recombinant human bone morphogenetic protein induces bone formation. Proceedings of the National Academy of Sciences of the United States of America 87, 2220–2224.

Wang, H.-J., Lin, Z.-X., Liu, X.-M., Sheng, S.-Y., Wang, J.-Y., 2005. Heparin-loaded zein microsphere film and hemocompatibility. Journal of Controlled Release 105, 120–131.

Wang, H.-J., Gong, S.-J., Lin, Z.-X., Fu, J.-X., Xue, S.-T., Huang, J.-C., Wang, J.-Y., 2007. In vivo biocompatibility and mechanical properties of porous zein scaffolds. Biomaterials 28, 3952–3964.

Wang, Q., Yin, L., Padua, G.W., 2008. Effect of hydrophilic and lipophilic compounds on zein microstructures. Food Biophysics 3, 174–181.

Wang, Y., Padua, G.W., 2010. Formation of zein microphases in ethanol-water. Langmuir 26, 12897–12901.

Wang, Y., Padua, G.W., 2012. Nanoscale characterization of zein self-assembly. Langmuir 28, 2429−2435.

Weiler, A., Helling, H.-J., Kirch, U., Zirbes, T.K., Rehn, K.E., 1996. Foreign-body reaction and the course of osteolysis after polyglycolide implants for fracture fixation. Journal of Bone and Joint Surgery [Br] 78-B, 369–376.

Wieser, H., Koehler, P., 2008. The biochemical basis of celiac disease. Cereal Chemistry 85, 1–13.

Yasko, A.W., Lane, J.M., Fellinger, E.J., Rosen, V., Wozney, J.M., Wang, E.A., 1992. The healing of segmental bone defects, induced by recombinant human bone morphogenetic protein (rhBMP-2). A radiographic, histological, and biomechanical study in rats. Journal of Bone and Joint Surgery 74-A, 659–670.